

$$\rho_{app} = \rho_{rock} \cdot (1 - p) + \rho_w \cdot p \cdot S_r \quad (3.3)$$

**NOTE:** The apparent mass density is to be used for design of hydraulic works.

### 3.3.3.3 Degree of saturation in stability calculations

The value of mass density  $\rho_{app}$  that is used when applying armourstone stability formulae, eg Hudson and Van der Meer (see Section 5.2.2.2), has traditionally been assumed to be the *saturated surface dry* mass density as it was considered the most applicable density term for armourstone in the intertidal zone under wave action. When fully saturated, the value of  $\rho_{app}$  is therefore the value determined by testing in a saturated surface dry condition (ie degree of saturation,  $S_r = 100$  per cent). More recently, it has been recognised that different degrees of saturation are appropriate for stones in different zones of the structure. A correction to the density is now recommended for stability calculations to reflect the lower stability of blocks in the intertidal zone when they are not fully saturated. An assumed saturation of 25 per cent is recommended for armourstone that is not in permanent contact with water and for armourstone permanently below water, a saturation of 50 per cent is suggested (Laan, 1999); see also Table 3.17.

#### Box 3.5 Effect of water saturation on apparent mass density

For material with limited water absorption, the water content has a limited influence on the apparent density. However, for rock displaying a larger water absorption or porosity, the additional mass density attributable to the mass of water existing in the pores may be accounted for. Figure 3.9 gives the additional mass density due to the amount of water absorbed in accordance with Equation 3.3.

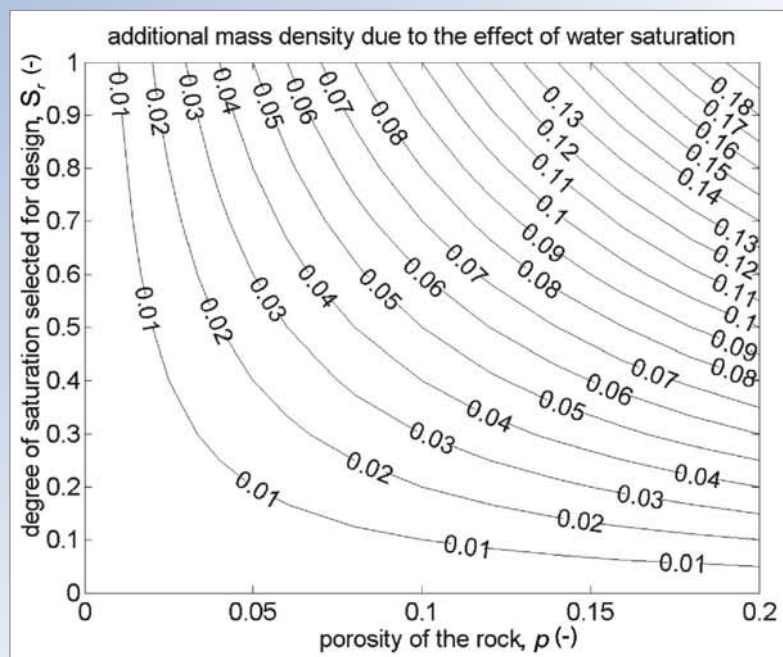


**Figure 3.9** Effect of degree of saturation  $S_r$  (-), on the apparent mass density of porous rock  $\rho_{app}$ . Contours indicate the correction value (in  $t/m^3$ ) to be added to the dry mass density  $\rho_{rock}$

For example, a rock with dry mass density of  $2.4 t/m^3$  and a porosity of 10 per cent ( $p = 0.1$ ) has a correction value of  $0.05 t/m^3$  for degree of saturation,  $S_r = 50$  per cent and  $0.10 t/m^3$  for a fully saturated situation. In other words, the apparent mass density is  $2.45 t/m^3$  or  $2.50 t/m^3$  for 50 per cent or 100 per cent saturation respectively.

**Major breakage** refers to breakage of individual armour stones along pre-existing defects, as shown in Figure 3.10 for armourstone with different geological origins. Any defects are controlled by the geology of the rock source and the production technique. For example, sedimentary rocks may contain bedding planes, stylolites, calcite veins or shaly partings, while igneous rocks may contain mineral veins, contacts between distinct petrographic units or cooling cracks. In addition, macro-flaws may be induced by blasting or fragmentation of the rock mass during extraction. If these defects propagate, a proportion of stones will be transformed into large fragments. If major breakage takes place on a significant number of stones, this may significantly affect the mass distribution of the armourstone and consequently the value of design parameters such as  $M_{50}$  or  $D_{n50}$  (see Section 3.6.6). Resistance to major breakage is known as **integrity**.

**Minor breakage** refers to breakages of asperities. This often occurs when stone edges or corners are knocked off during routine handling, by the traffic of heavy plant during construction, or during initial settlement of the structure (see Figure 3.11). This phenomenon takes place along new fractures created through the mineral fabric of the stone. It is often associated with bruising and crushing, and generally creates fragments of limited size (up to a few tens of kilogrammes) depending on the armourstone grading. This phenomenon has a limited impact on the mass distribution and the  $M_{50}$  value (see Section 3.6.6), but can contribute to edge rounding. Many strength tests exist for measuring the resistance of mineral fabric to breakage and are discussed in Section 3.8.5 but they do not correlate with armourstone integrity tests (Perrier *et al*, 2004).

In simple terms, **armourstone integrity** is the ability of armourstone pieces to withstand excessive breakage during their life cycle. It should not be confused with resistance to breakage through the mineral fabric, ie resistance to minor breakage that might be tested on small laboratory specimens or aggregates. From a survey of feedback from 200 professionals, including designers, contractors, quarry companies, port and waterways authorities, armourstone integrity was identified as an **essential property** (Dupray, 2002). Two aspects of integrity should be distinguished.

- 1 The integrity of armourstone as an individual piece is its ability not to display excessive breakage. The threshold for excessive breakage is discussed in Section 3.8.5.
- 2 The integrity of armourstone as a granular material is the ability of a consignment not to display excessive changes of mass distribution and especially of its characteristic masses.

Integrity is a property of heavy and light armourstone, among others such as shape characteristics, that may be evaluated by initial type tests, ie one-off tests giving information about an armourstone source to promote design optimisation. Such initial type testing is distinct from routine testing of the quality of consignments in association with factory production control.

1

2

3

4

5

6

7

8

9

10



**Figure 3.15** Visual comparison of stone shapes showing roundness quantified using the Fourier asperity roughness. Left: Rounding of gneiss; very round. Right oolitic limestone by shingle attack, 1 m scale bar; semi-round (courtesy J-P Latham)

#### 3.4.1.5 Proportion of crushed or broken surfaces

In some European countries rounded glacial boulders, cobbles and core stones from basalt and dolerite quarries have been used for hydraulic structures. In order to ensure adequate mechanical interlock for these materials, the percentage of crushed or broken surfaces is also specified where appropriate.

#### 3.4.1.6 Shape for specification purposes

Shape is an example of a property that may be used in two distinct ways. It may be specified in order to establish the stone consignment's fitness for purpose. If quantified in more detail, it can provide information useful for design. Integrity is a similar property in this respect.

For specification, it is desirable to limit the proportion of pieces with a length-to-thickness ratio,  $LT$ , of greater than 3:1 to a level that is reasonable for the intended use. Because smaller stones tend to have larger  $LT$ , in Europe (see Section 3.7.1) the following levels are suggested:

- heavy armourstone in cover layers                      typically < 5 per cent
- light armourstone in cover layers                      typically < 20 per cent.

Restricting the proportion of pieces with  $LT > 3$ , ie the flaky or elongated pieces, should ensure reasonable interlock. It will also limit the damage from breaking eg induced by construction plant trafficking over granular surfaces.

It has also been suggested that removal of all stones with cubicity values greater than 3 will target the removal of flaky pieces more effectively than applying an  $LT$  limit at 3. In practice, it remains unclear whether further criteria based on cubicity would have this desired effect.

#### 3.4.1.7 Shape for design and dimensioning purposes

In Section 5.2.2.2 possible stability increases corresponding to lower armour layer porosities achieved by tighter non-random placement methods are tentatively presented. These lower porosities can only be achieved with certain armour shape characteristics. In Section 3.5.1 conversion charts for armour layer porosity of individually placed layers as a function of two shape parameters ( $LT$  and  $BLc$ ) and placement method are given to aid stability and dimensioning calculations.

For CE marking  $LT_A$  is required (ie a specified maximum percentage of stones with  $LT > 3$ ) to ensure shape control (see Section 3.7.1). However, average values for  $LT$  and  $BLc$  should not be specified as a requirement for factory production control as, by doing so, there is a risk of significantly decreasing the production rate, increasing the price of armourstone or even excluding rock sources that have the potential to provide the most economic project

**Table 3.5** Heavy, light and coarse European EN 13383 standard grading requirements

Heavy	Class designation	ELL	NLL	NUL	EUL	$M_{em}$	
	Passing requirements kg	< 5% kg	< 10% kg	> 70% kg	> 97% kg	lower limit kg	upper limit kg
	10 000–15 000	6500	10 000	15 000	22 500	12 000	13 000
	6000–10 000	4000	6000	10 000	15 000	7500	8500
	3000–6000	2000	3000	6000	9000	4200	4800
	1000–3000	700	1000	3000	4500	1700	2100
	300–1000	200	300	1000	1500	540	690

Light	Class designation	ELL	NLL	NUL	EUL	$M_{em}$	
	Passing requirements kg	< 2% kg	< 10% kg	> 70% kg	> 97% kg	lower limit kg	upper limit kg
	60–300	30	60	300	450	130	190
	10–60	2	10	60	120	20	35
	40–200	15	40	200	300	80	120
	5–40	1.5	5	40	80	10	20
	15–300 *	3	15	300	450	45	135

Coarse	Class designation	ELL	NLL	NUL	EUL	
	Passing requirements mm	< 5% mm	< 15% mm	> 90% mm	> 98% mm	< 50% mm
	45/125	22.4	45	125	180	63
	63/180	31.5	63	180	250	90
	90/250	45	90	250	360	125
	45/180 **	22.4	45	180	250	63
	90/180 ***	45	90 ***	180 ***	250	NA

**Notes**

\* = wide light grading, \*\* = wide coarse grading, \*\*\* = gabion grading, NLL = 20% and NUL = 80%. See Table 3.6 in Section 3.4.3.7 for additional information on standard gradings.

For example, to fulfill the mass distribution requirements for an EN standard heavy grading designated “3–6 tonnes” (or 3000–6000 kg), up to 10 per cent (by mass) may be below the nominal lower limit NLL of 3 t, and up to 30 per cent may be above the nominal upper limit NUL of 6 t. These undersize and oversize tolerances make the grading more practical to produce. The grading is allowed a further margin for borderline stones at the extremes using extreme lower (ELL) and extreme upper (EUL) limits. So for the 3–6 t example, ELL restricts the percentage below 2 t to 5 per cent and EUL limits blocks above 9 t to less than 3 per cent, see also Figure 3.21. Similar definitions with slightly different percentage requirements are introduced for light and coarse gradings.

The introduction of a system of standard gradings within EN 13383 has brought several advantages. For the producer, these mostly concern the economics of production, selection, stockpiling and quality control. The system enables engineers and producers to refer to a batch or consignment of stones by its designated bottom NLL and top sizes NUL (using masses or sieve sizes) with a meaning that is consistent to all. Standard gradings are considered essential for coarse and light gradings as these are selected by mechanical means. If non-standard gradings are specified, selection by mechanical means requires changing bar openings, new screen decks or completely new barrels. With only a few grading classes

$3n_{RRM}$ . This relationship between uniformity indices of mass and size is valid for nominal diameter, equivalent sphere diameter and can also be considered valid for sieve sizes. If a graded material is represented by Equation 3.12 using masses, it may also be represented by its equivalent Rosin-Rammler equation using nominal sizes. Masses may be converted into sizes in terms of nominal diameter  $D_n$  or sieve diameter  $D$ , which should not be confused. Conversion of masses to sizes is achieved by dividing by density to give volume, the cube root of which gives the nominal diameter  $D_n$ . To plot particle size obtained as  $D_n$  in terms of sieve diameter  $D$ , divide by 0.84.

#### Relating theory to NUL/NLL

Given any two fixed points on the Rosin-Rammler curve,  $M_{50}$  and  $n_{RRM}$  can be determined. For example, if the nominal lower limit mass of a grading is NLL and the fraction passing at that value is  $y_{NLL}$ , and similarly the nominal upper limit mass is NUL and the fraction passing at that value is  $y_{NUL}$ , then by solving the following two equations:

$$M_{50} = NLL \left( \frac{\ln(1 - y_{NLL})}{-0.693} \right)^{-1/n_{RRM}} \quad M_{50} = NUL \left( \frac{\ln(1 - y_{NUL})}{-0.693} \right)^{-1/n_{RRM}} \quad (3.14)$$

to give

$$n_{RRM} = \log \left( \frac{\ln(1 - y_{NUL})}{\ln(1 - y_{NLL})} \right) / \log(NUL/NLL) \quad (3.15)$$

the full curve described by Equation 3.12 is given.

#### How the idealised standard grading curves are obtained

The position and steepness of each idealised standard grading curve is set up not only to comply with the limit requirements, but also to lie in the middle of the range of compliant specifications for that grading. Standard EN gradings (eg 1000–3000 kg) impose requirements such that  $y$  lies between 0 and 10 per cent passing at NLL (1000 kg) and between 70 and 100 per cent at NUL (3000 kg). To define each idealised grading curve uniquely and keep the system simple, each standard heavy and light grading has been constrained using Equation 3.15 at the same two percentage passing points on the curve for each pair of NLL and NUL values designated in the EN 13383 standards. The values chosen are  $y_{NLL} = 6$  per cent and  $y_{NUL} = 90$  per cent respectively. Theoretically, these values give designers maximum reassurance that the  $M_{50}$  plotted lies near 0.5 (NLL+NUL). The more obvious first choice of 5 per cent and 85 per cent would lead the wider idealised standard grading curves to miss 0.5 (NLL+NUL) by an unacceptable degree. The values chosen minimise these differences to within 10 per cent of the target for the full suite of standard heavy and light gradings. The only exception is the special wide grading of 15–300 kg, where  $M_{50}$  is 26 per cent lower than the average of the nominal limits. For a more typical example such as the 1000–3000 kg grading, the idealised curve gives  $M_{50} = 2.08$  t, ie within 4 per cent of 0.5(NLL+NUL). For further details see Latham *et al* (2006).

#### Plotting grading curves using Rosin-Rammler

Substitute a series of mass values  $M_y$  into Equation 3.12. This will return the series of fraction passing  $y$  values needed to complete the plot. Before doing so, first set the  $n_{RRM}$  and  $M_{50}$  values needed in Equation 3.12. To plot any heavy or light standard grading designated with NUL and NLL, calculate the uniformity index  $n_{RRM}$  using Equation 3.15 with  $y_{NLL} = 0.06$ ,  $y_{NUL} = 0.90$ . To obtain  $M_{50}$ , substitute  $n_{RRM}$  using either the NLL or NUL form of Equation 3.14. The resulting idealised grading curves are presented in Figure 3.20. These summarise the expectations of a purchaser of standard gradings.

**Size distribution similar to standard gradings – detailed approach for coarse gradings**

The first three coarse gradings shown in Table 3.5 have ratios characterised by the following:

$$ELL/D_{50} = 0.28 \quad NLL/D_{50} = 0.56 \quad D_{50min}/D_{50} = 0.79 \quad NUL/D_{50} = 1.57 \quad EUL/D_{50} = 2.24$$

For any user-defined  $D_{50}$ , all appropriate limits can be obtained and rounded to available screen sizes.

**Mass distribution not similar to standard gradings for Category B – graphical method**

If a given design  $M_{50}$  requires specification of a non-standard grading wider (easier to produce) or narrower (more difficult to produce) than the equivalent nearest standard grading, the suggested limit requirements in Table 3.7 should be disregarded in favour of limits governed directly by the grading width chosen. Once the user has set the desired NUL and NLL masses, the following graphical method, which assumes a log-linear form to the grading curve, can be used:

- using a log scale for mass and a linear scale for percentage passing, plot the NUL mass point at 70 per cent passing and the NLL mass point at 10 per cent passing
- join the two points with a straight line and interpolate to find the  $M_{50}$  value
- linearly extrapolate to read off mass values at 2 per cent (if light gradings) or 5 per cent (if heavy gradings) to obtain ELL. Similarly, read off mass values at 97 per cent to obtain EUL.

**Designating a non-standard grading**

The EN 13383 gives specifications for a number of standard gradings with both Category A and Category B status, but a producer may wish to declare other gradings for sale. Provided the grading on offer can be tested for conformance using EN 13383 test methods, this is perfectly acceptable within EN 13383 rules, but it must be declared using a labelling system compatible with terms used for EN 13383 gradings: “ $HM_A$  declared  $NLL-NUL$ ; extreme limits:  $ELL-EUL$ ; effective mean mass:  $M_{emll}-M_{emul}$ ”. For example: a 2–4 t grading would be declared by inserting the correct figures in place of the italics, eg using guidance from Table 3.7:

“ $HM_A$  declared 2000–4000; extreme limits: 1050–5900; effective mean mass: 2500–3000”.

A designer wishing to specify limits different to the standard limits in Table 3.5 (Tables 1 to 5 of EN 13383-1:2002) would designate their requirements in a similar way. Note that the prefix letters  $HM_A$ ,  $HM_B$ ,  $LM_A$ ,  $LM_B$  and  $CP$  are used to distinguish heavy mass, light mass and coarse size gradings respectively, where the subscript A refers to Category A, which imposes the  $M_{em}$  restriction, while for Category B it is omitted.

**3.4.4****Core materials**

Core materials are generally used for volume-filling. As such, they do not have requirements for a characteristic size such as  $M_{50}$ . The top size is generally indicated and bottom sizes may be controlled. The geotechnical properties required for core materials, typically shear strength, placed porosity and permeability are identified in Section 5.4. These geotechnical properties are greatly influenced by the width of the grading and most notably, the content of fines. The fine material content is closely related to the tail of the quarry yield curve and the fines removal technique. An approach for the prediction of porosity suitable for core materials is given in Section 3.4.4.3.

properties, the type of placements assigned to granular materials in the works, are classified as:

- random placement
- standard placement
- dense placement
- specific placement.

These terms are described in detail in Section 9.8.1. All bulk-placed materials are designated random placement, whereas any type may be appropriate for stones placed individually into armour layers. In principle, for armour layers, there are two distinct calculations adopted to obtain bulk volumes (ie rock volume,  $V_r$  (m<sup>3</sup>), plus void volume) in a panel.  $V_{b,d}$  (m<sup>3</sup>) is the design bulk volume assumed before construction and  $V_{b,s}$  (m<sup>3</sup>) the surveyed bulk volume after construction.  $V_b$  (m<sup>3</sup>) is the bulk volume referring to either method. By following guidance in Boxes 3.7 and 3.8 their differences should be minimised. The Equations 3.23–3.28 (see also Figure 3.25) define the geometry and related properties of armour layers.

$$\text{Designed bulk volume (m}^3\text{):} \quad V_{b,d} = A t_d \quad (3.23)$$

$$\text{Surveyed bulk volume (m}^3\text{):} \quad V_{b,s} = A_{cs} L \quad (3.24)$$

$$\text{Theoretical orthogonal thickness (m):} \quad t_d = n k_t D_{n50} \quad (3.25)$$

$$\text{Volume of rock (m}^3\text{):} \quad V_r = V_b (1-n_v) \quad (3.26)$$

$$\text{Total number of stones in panel (-):} \quad N_a = n A k_t (1-n_v)/D_{n50}^2 \quad (3.27)$$

$$\text{Bulk (or placed packing) density (t/m}^3\text{):} \quad \rho_b = (1-n_v) \rho_{app} \quad (3.28)$$

where:

$A$  = total surface area (m<sup>2</sup>) of the armour layer panel parallel to the local slope

$A_{cs}$  = cross-sectional area (m<sup>2</sup>)

$L$  = panel chainage length (m)

$n$  = number of layers (-)

$n_v$  = (volumetric) layer porosity (-)

$k_t$  = layer thickness coefficient (-)

$\rho_{app}$  = apparent density of the armourstone (t/m<sup>3</sup>) (see Section 3.3.3).

**NOTE:** The volume of rock,  $V_r$ , should not be confused with the volume of armourstone, which is  $V_b$ . The only practical possible use of  $V_r$  is as an input to determine the mass of rock,  $M_r = \rho_{app} \times V_r$ , which is also the total mass of armourstone.

The placed packing density or **bulk density**,  $\rho_b$  (t/m<sup>3</sup>), can be predicted from Equation 3.28 or, if the mass of armour placed into a panel is known, it may be determined directly from the surveyed bulk volume. When dealing with wider gradings, a better prediction for the number of blocks,  $N_a$  (-), will result if  $D_{n50}$  in Equation 3.27 is replaced by the nominal size calculated from the average mass,  $M_{em}$ .

**Table 3.13** Example of a completed quality rating assessment worksheet (after Lienhart, 1998)

	a	b				c	d	e
	Criterion	Quality rating				Rating value	Weighting	Weighted rating
		Excellent	Good	Marginal	Poor			
		(=4)	(=3)	(=2)	(=1)	Average	%	{(c) × (d)}/ mean of (d)
Field-based indicators	Lithological classification		√			3	58	2.12
	Regional <i>in situ</i> stress			√		2	73	1.78
	Weathering grade		√			3	73	2.67
	Discontinuity analysis		√			3	95	3.48
	Groundwater condition			√		2	73	1.78
	Production method				√	1	95	1.16
	Rock block quality			√		2	80	1.95
	Set-aside		√			3	73	2.67
	Petrographic evaluation			√		2	95	2.32
1	Block integrity test				√	1.5	90	1.65
	Block integrity visual			√				
2	Mass density		√			3	80	2.93
	Water absorption		√					
	Microporosity/total porosity		√					
	Methylene blue absorption		√					
3	Compressive strength			√		1.67	88	1.79
	Schmidt impact index			√				
	Sonic velocity				√			
4	Point load strength			√		2.67	88	2.87
	Fracture toughness		√					
	Los Angeles		√					
5	Micro-Deval			√		2	88	2.15
6	Freeze-thaw loss		√			3.67	80	3.58
	MgSO <sub>4</sub> soundness	√						
	Wet-dry loss	√						
						Sum	1229	34.9
						n	15	15
						Mean	81.9	<b>2.33</b>

**Notes**

- This sheet includes 15 factors (nine field, six laboratory), hence overall rating or armourstone quality designation (*AQD*) is mean of column (e) based on all 15 factors. If no data are available for one or more factors, *AQD* should be based on the number of included factors. A complete and balanced set of data is ideal.
- In addition to engineering geology indicators, each boxed grouping of tests 1 to 6, generates one average rating value in column (c) from one or more suggested tests. They refer to 1: resistance to major breakage; 2: mineral fabric physical quality; 3: resistance to minor breakage (compressive); 4: resistance to minor breakage (tensile, dynamic); 5: resistance to wear (shear and attrition); 6: resistance to in-service weathering.
- Test results and field assessments can be used to generate continuously varying ratings from 0.5 to 4.5 rather than integer values. Similarly, *AQD* results can vary from 0.5 to 4.5.

### 3.6.4 Principles of degradation modelling

In simple terms, a degradation model is the application of mechanics consisting of:

- material **properties + loadings** (and boundary conditions) = deformation or damage **response**

or:

- evolution of material **properties** + history **of loadings applied** = history of damage **response**

or:

- average material **properties** + average **loading intensity** = average **rate of degradation**.

Degradation models use armourstone **properties** representative of the armourstone consignment at the point of leaving the quarry. This may be measured by a specific material property, such as armourstone integrity or abrasion resistance, or an overall quality index, such as *AQD*.

The model then predicts the **response** to future **loading intensity** of the rock armour with such properties. These may be short-term loads or long-term in-service loads. The model output gives the change in the performance parameter (such as  $M_{50}$ , or the complete mass distribution) for any number of handling events or storm/flood events or, alternatively, for the number of years in service including the design life of the structure.

The **loading intensity** or **project site aggressiveness** can be assessed in terms of:

- **attrition** loading intensity: a function of waterborne attrition agents, rocking, sliding and rolling loads (affected by stone size, wave energy, mobility in design, interlock due to shape and grading)
- **breakage** loading intensity: a function of rocking and rolling loads (affected by stone size, wave energy, mobility in design, interlock due to shape and grading)
- **physiochemical climatic** loading intensity: a function of zone on structure, meteorological climate, slope angle.

For static armour designs, mass loss is by both fast and imperceptibly slow or subcritical opening of cracks, spalling, rounding and by accelerated loss of interlock from wear. A comprehensively averaged model is currently considered most appropriate in such cases where wear is the dominant mechanism (see Section 3.6.5).

For a dynamic design, attrition and breakage loading intensity will be considerably higher than climatic loading intensity – a breakage model calibrated using armourstone integrity, mineral fabric strength and/or resistance to wear properties may be more useful.

Degradation models focusing specifically on wear mechanisms (Tomassichio *et al*, 2003) and breakage mechanisms (Tørum and Krogh, 2000; Dupray *et al*, 2004) have also been proposed. Such models consider progressive mass reduction associated with repeated storm events where storm loading exceeds a threshold energy for start of damage, or where armour movement velocity is above a threshold value. Such models attempt to deal with mass loss by specific wear or breakage mechanisms that ignore climatic weathering intensity effects. The fewer the degradation mechanisms considered in a model, the more rigorous the model calibration approaches can be, but the less widely applicable is the model to long-term service life prediction.

Probabilistic methods have been proposed to assess accumulated structural damage (eroded profile area) due to probability of exceedance of the design condition (see Takahashi *et al*, 2003). Such design approaches also require an estimate of the reduction in  $M_{50}$  of the armourstone due to rock material degradation. The degradation model tools described here may be tentatively applied to estimate changes in  $M_{50}$  for such purposes.

**Table 3.14** Ratings estimates for parameters in armourstone degradation model, for input to Equation 3.38 (after Latham, 1991)

Parameter	Rating estimates						Parameter influence $X_{max}/X_{min}$	Calibration Reliability*	
$k_s$	<b>Rock fabric strength</b> Use $M_{DE}$ test value and relationship: $k_s = 4.12 \times 10^{-5} M_{DE}^{1.485}$ or AQD value and relationship: $k_s = 0.032 AQD^{-2.0}$						~500	Excellent	
$X_1$	<b>Size</b> Effect given by $0.5(M_{50})^{1/3}$ ( $M_{50}$ in tonnes)						~10	Good	
	$M_{50}$	15.0	8.0	1	0.1	0.01			
	Rating	1.23	1.00	0.50	0.23	0.11			
$X_2$	<b>Grading width</b> $(M_{85}/M_{15})^{1/3}$	1.1-1.4		1.5-2.4	2.5-4.0		~2.5	Fair	
	Rating	1.2		1.0	0.5				
$X_3$	<b>Initial shape</b>						~2	Fair	
		Angular/ irregular	Blocky/ equant	Semi- rounded	Rounded				
	Rating	1.00		1.1	1.50	2.00			
$X_4$	<b>Incident wave or current energy (treat as independent of size of stone)</b>						~10	Fair	
		Significant wave height, $H_s$ (m)	> 8.0	4.0-8.0	< 4.0				
	Rating	If $I_{M50} > 15\%$		0.3	1.0	2.0			
		If $I_{M50} = 5.0-15.0\%$		0.5	1.3	2.3			
		If $I_{M50} = 2.0-5.0\%$		0.7	1.6	2.6			
		If $I_{M50} < 2\%$		1.0	2.0	3.0			
Rating	If using AQD method		0.7	1.6	2.6				
$X_5$	<b>Zone of structure</b>						~10	Good	
		Intertidal	Supra-tidal /hot	Supra-tidal /temperate	Always submerged				
	Rating	1.0		2.5	8	10			
$X_6$	<b>Meteorological climate weathering intensity</b> (Use MCWI index of Lienhart – see Table 3.15)						~7	Good	
	MCWI index		< 100	100-300	300-600	> 600			
	Rating	If WA > 2.0%		0.8	0.6	0.4			0.2
		If WA = 0.5-2.0%		1.0	0.8	0.6			0.4
		If WA < 0.5%		1.4	1.2	1.0			0.8
Rating	If using AQD method		1.0	0.8	0.6	0.4			
$X_7$	<b>Waterborne attrition agents</b>						~7.5	Poor	
	Sediment type	shingle	gravel	sand	silt	none			
	Rating	0.2	0.5	1.0	1.2	1.50			

**Box 3.14** Calculation of mass density and water absorption during testing

Masses of the test specimen,  $M_T$ , are determined by weighing, which is generally carried out at two extreme values of water content or degree of saturation,  $S_r$ :

- $S_r = 0$  or oven-dried state, OD; in that case  $M_{T(S_r=0)} = M_M$  where  $M_M$  is the mineral mass (see Figure 3.8)
- $S_r = 100$  per cent or saturated surface dry state, SSD; in that case  $M_{T(S_r=1)} = M_M + \rho_w \times V_p$ , where  $V_p$  is the pore volume (see Figure 3.8).

The volume is either indirectly determined by hydrostatic weighing,  $V_{TH}$ , or directly (geometrically) measured on cores or cubes,  $V_{TG}$ , before carrying out other tests such as the compressive strength test.

**a. Direct measure of the volume of the test specimen:** If the volume is geometrically determined and its value is  $V_{TG}$ , then the apparent mass density is defined as:

$$\rho_{app(S_r=0)} = M_{T(S_r=0)} / V_{TG} \quad (3.51)$$

$$\rho_{app(S_r=1)} = M_{T(S_r=1)} / V_{TG} \quad (3.52)$$

**b. Non-direct measure of the volume of the test specimen,  $V_{TH}$ :** Hydrostatic weighing is a useful method for test specimens or aggregates with irregular shape. Equation 3.53 gives the relationship, based on:

- $V_H$  is the volume of water displaced by the specimen;  $V_H = V_M$
- $M_H$  is the hydrostatic mass of the specimen determined by weighing while suspended in water

$$V_{TH} = [M_{T(S_r=1)} - M_{T(S_r=0)}] / \rho_w + V_H \quad (3.53)$$

**Apparent mass densities are determined as follows:**

$$\rho_{app(S_r=0)} = M_{T(S_r=0)} / V_{TG} \cong M_{T(S_r=0)} / V_{TH} \cong \rho_w \times M_{T(S_r=0)} / [M_{T(S_r=0)} - M_H] \quad (3.54)$$

$$\rho_{app(S_r=1)} = M_{T(S_r=1)} / V_{TG} \cong M_{T(S_r=1)} / V_{TH} \cong \rho_w \times M_{T(S_r=1)} / [M_{T(S_r=0)} - M_H] \quad (3.55)$$

In natural conditions on site, the actual apparent mass density of the rock depends on its actual water content as implied by the symbol  $\rho_{app}(S_r)$ . The designer should make the appropriate substitution of  $S_r$  in Equation 3.56 (see Section 3.3.3.3, and Table 3.17):

$$\rho_{app}(S_r) = \rho_{app(S_r=0)} \times (1 - S_r) + \rho_{app(S_r=1)} \times S_r \quad (3.56)$$

**The water absorption and porosity are given by:**

$$WA = [M_{T(S_r=1)} - M_{T(S_r=0)}] / M_{T(S_r=0)} \quad (3.57)$$

$$p = [M_{T(S_r=1)} - M_{T(S_r=0)}] / [\rho_w \times V_{TG}] \quad \text{for geometric measurement of the volume} \quad (3.58)$$

$$p = [M_{T(S_r=1)} - M_{T(S_r=0)}] / [M_{T(S_r=1)} - M_H] \quad \text{for hydrostatic measurement of the volume} \quad (3.59)$$

### 3.8.3 Testing properties of individual pieces of armourstone

#### 3.8.3.1 Shape

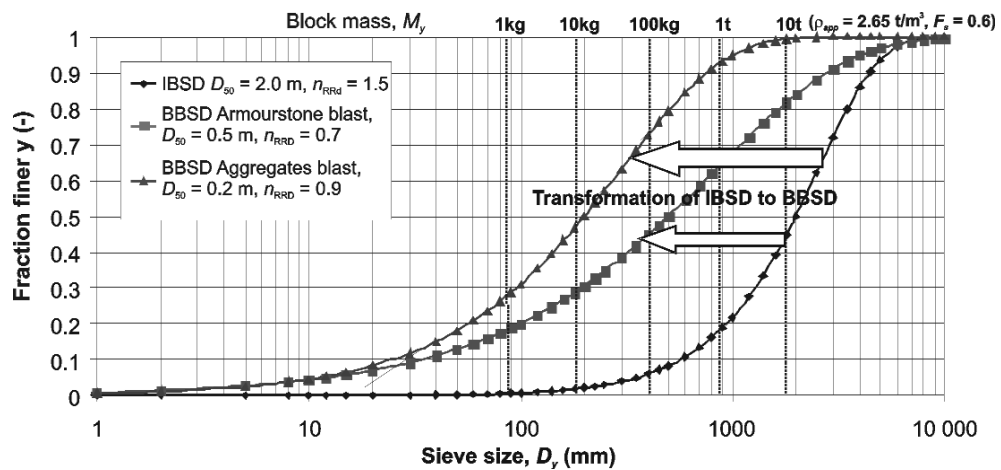
For shape specification compliance, factory production control in EN 13383 uses the test: determination of the percentage of pieces of armourstone with a length-to-thickness ratio  $LT$  greater than 3. The method to determine  $l$  and  $d$  uses two straight laths positioned parallel to each other at right-angles to the longest dimension  $l$  and then to the smallest dimension  $d$ .  $l$  and  $d$  are measured using a carpenter's rule, a tape measure or, to achieve greater accuracy, callipers (see Figure 3.82).

Shape indicators including length-to-thickness ratio,  $LT$ , cubicity,  $(L+G)/2E$ , and blockiness,  $BLC$ , are discussed in Section 3.8.4.

#### 3.8.3.2 Mass and size

The mass of individual armourstone pieces is rarely determined alone but rather to determine:

- the mass distribution by combination of individual masses
- the input and output data for armourstone integrity tests that use destructive testing
- the blockiness index of armourstone pieces (relevant for individually placed armour layers).



#### Notes

$F_s$  is the shape factor, see Section 3.4.2

$n_{RRD}$  is the uniformity coefficient of the size distribution curve, Section 3.4.3.3

**Figure 3.53** Illustration of theoretical scenarios for an aggregates blast and an armourstone blast applied to the same rock mass. IBSD and BBSD are represented by Rosin-Rammler curves

### 3.9.3.4 Suggestions for improving the yields of armourstone

Generally, the proportion of armour stones in the blast increases with increasing tensile strength, increasing Young's Modulus and increasing discontinuity spacing. Normal blasting practice (eg for aggregates and ores) aims to achieve high-fragmentation blasts. By contrast, greater percentages of armour stones can be achieved by adjusting common practice through consideration of the following (see Figure 3.55 for definition of blasting terminology).

- 1 A low **specific charge**. Generally, a specific charge as low as 0.11–0.25 kg/m<sup>3</sup> can be used. If possible, the explosive used should have lower velocity of detonation,  $VOD$  (m/s). For such low specific charges, maintaining high drilling accuracy is critical to avoid insufficient rock break-out.
- 2 The **spacing-to-burden ratio** should generally be less than or equal to 1, with burden larger than the discontinuity spacing in a jointed rock mass.
- 3 If the **bench** is either too high or too low, armourstone production will be poor. For an initial estimate, bench height could be selected as two to three times the burden. In planning bench levels, the rock mass from which most armourstones might be produced, such as thickly bedded layers, should be located nearly at the top of the bench alongside the stemming section of the holes.
- 4 A large **stemming length**, larger than the burden, is usually recommended.
- 5 A small **blasthole diameter**. A diameter of less than 100 mm is recommended.
- 6 One row of holes is found to be better than multiple rows. If permitted, holes should be fired instantaneously rather than using inter-hole delaying (this may cause high ground vibration).
- 7 A **bottom charge** of high energy concentration is needed for the bottom to break clean away.
- 8 A **decoupled column charge** of ANFO (ammonium nitrate/fuel oil) packed in plastic sausages is effective when a 300–3000 kg range is recommended – the explosives are evenly distributed, giving quite even fragmentation.
- 9 A **decked charge**, to break up the continuity of explosives, will be necessary in most situations when armourstone greater than 3 t is recommended. The material for decking can be either air or aggregates.

**Box 3.29** Reselection of armourstone

Reselection of larger stones can sometimes be at higher outputs than selection at the face because the material is much more single-sized. It should be spread out for machinery to access stones easily. The principle of reselection is that a loader fitted with a weighing device and forks instead of a bucket weighs the stones and transports them to stockpiles of standard gradings. If there is doubt about whether the stock complies with requirements, sub-class stockpiles may be used and the stones placed into 1–2 t, 2–3 t, 3–4 t, 4–5 t, 6–8 t, 8–10 t, 10–12 t stocks etc. An excavator may also be used, but specific attention should be paid to the organisation of the stocks to minimise the travelling distances. Table 3.30 provides the appropriate size of machine and experience of outputs.

**Table 3.30** Relationship between the appropriate machine capacity (t) and size of stone to be reselected

Equipment capacity	> 10 t	6–10 t	3–6 t	1–3 t	0.3–1 t	60–300 kg
Front-end wheel loader with fork (bucket not appropriate) (t)	45.0	30.0	22.5	Not recommended		
Excavator (t)	60.0	50.0	37.5	27.5	17.5	10.0
Powerfork (t) (to be fitted to excavator)	3.65	3.05	2.30	1.70	1.10	0.60
Average selection rate (t/h)	250	215	160	95	43	15

**NOTE:** The average output of a front-end wheel loader is difficult to determine since it depends on many parameters, eg the travel distance.

The final grading is produced by recomposition during loading at the quarry and not at the delivery stage. Consequently, the final grading may either be a standard or non-standard grading. The proportion of stones required from each sub-class to create a good fit to the average target grading curve is determined. Mixing at the construction site will ensure that the proper grading is available for construction.

Table 3.31 gives an example of how to prepare a quality control guide table for a 6–10 t grading with  $M_{50}$  between 8.5 t and 7.5 t. The last two columns can be used as a grading plan for 1000 t used by the machine driver when loading the trains, barges or trucks. The operator keeps a record of the number of pieces loaded from each sub-class and once or twice a day a grading curve is plotted. If sizes are drifting off target grading curves, future loads can be adjusted.

**Table 3.31** Heavy grading quality control plan

Sub-class	Cumulative % in sub-class	Percentage in sub-class	Tonnage in sub-class	Average stone mass (t)	Number of stones
< 4.0 t	0.0	0.0	0		
4.0–5.0 t	2.5	2.5	25	4.5	6
5.0–6.0 t	5.0	2.5	25	5.5	5
6.0–7.0 t	27.5	22.5	225	6.5	35
7.0–8.0 t	50.0	22.5	225	7.5	30
8.0–9.0 t	67.5	17.5	175	8.5	21
9.0–10.0 t	85.0	17.5	175	9.5	18
10.0–12.0 t	91.0	6.0	60	11.0	5
12.0–14.0 t	97.0	6.0	60	13.0	5
14.0–16.0 t	100.0	3.0	30	15.0	2
<b>Total:</b>			<b>1000 t</b>		<b>126</b>

**NOTE:** Although permitted according to the standard, at this stage there should not be any piece smaller than the 4 t. This allows for the fragments to be produced during the handling of the materials during transport and placing.

**Quarry run.** This category includes everything from the finest material of the quarry yield up to a maximum size in the blastpile and is best described as 0– $M$  kg. Consequently, the production simply consists of removing the oversize. This can easily be done with a wheel loader or an excavator. When using a wheel loader, the large size of the bucket and the limited visibility of the driver will make it practically impossible to produce a lighter core material than 0–1000 kg. Using an excavator with a smaller bucket and digging towards the cabin could produce a 0–500 kg material. Note that the grading of the *muckpile* gets finer when digging deeper into it.

**Processed core materials.** This material is produced by removing both the oversized and fines, generally by means of a robust static grizzly (see Box 3.33). Due regard should be given to the lower cut-off value since it significantly affects the amount of by-product for which an alternative use should be found. Changing the lower limit from 1 kg to 5 kg may effectively lead to rejection of an extra 10 per cent of quarry yield (see also Section 3.4.4).

### 3.9.7.4 **Technologies for the different selection or processing methods**

This section presents different techniques or tools suitable for armourstone production, illustrated in Boxes 3.30–3.35 as follows:

- crusher (Box 3.30)
- selection hill (Box 3.31)
- trommel screen (Box 3.32)
- bars or static grizzly (Box 3.33)
- barsizer unit (Box 3.34)
- sidekick (Box 3.35).

Vibrating screens and grizzlies may be used for production of coarse grading armourstone provided they are sturdier than traditional aggregates screens. They can be located after the primary crusher with possible adjustment of its characteristics to produced gradings with nominal upper limit up to 100 kg or 200 kg (see Box 3.30). This may be appropriate for production of gabion stone, for instance. The vibrating screen decks will need to be adapted to handle the larger stones. Constraining the maximum feed size and the smallest mesh or hole opening will generally prevent damage. Typical limitations are given in Table 3.32.

**Table 3.32** *Limitation of screening device to limit damages*

	Maximum feed size	Minimum passing size
Grizzly	~ 120 kg	~ 100 mm (1.7 kg)
Holed steel plate	~ 200 mm (13.0 kg)	150 mm (5.6 kg)
Woven wire mesh	~ 125 mm (3.2 kg)	75 mm (0.7 kg)

**NOTE:** It is easier to make round holes in a steel plate in a workshop than to make square ones. The diameter should be increased by 1.23 times the width of a square hole needed for a similar screening result. However, a steel plate with round holes has a lower screening capacity. Bigger screening areas and decks are therefore required for similar production rates.

For existing structures, regular monitoring, at least after storms, should be carried out and broken armour units may need to be replaced. Rather than repairing a Dolos armour layer the US Army Corps of Engineers has developed the Core-loc, which can fulfil this role.

**Tetrapod** (see Figure 3.94)

The tetrapod unit was the first concrete unit with a special shape. This unit has been used extensively and projects with units up to 50 m<sup>3</sup> can be found. The tetrapod has recently been used mostly in Japan in multi-layer systems.

Analysis on the structural resistance of the unit and its hydraulic stability led to comprehensive guidance (Sotramer-Sogreah, 1978) for manufacturing of the formworks, the fabrication of the units, their storage and placement of the units in two layers. The formwork for producing tetrapods is composed of a bottom shell and three lateral shells.

Wear and breakage have been experienced in several structures caused by rocking of the units in the top layer. The placement of the units as per the recommended standards is essential to guarantee the interlocking and the required porosity of the armour layer.



**Figure 3.94**

*Example of Tetrapods used as armour on breakwater with crown wall (courtesy M Scott)*

#### **3.12.2.4 Interlocking units used in a single layer**

**Accropode** (see Figure 3.95)

The Accropode unit was developed from experience of the tetrapod and the observation that double-layer systems may allow unwanted movements of units in the upper layer. This unit has been used extensively and blocks up to 20 m<sup>3</sup> have been employed in some projects.

Analyses of structural resistance of the block and of its hydraulic stability has led to comprehensive standards for manufacturing of formworks, fabrication of blocks, storage and placement of units in one layer (Sogreah, 1988). Formwork is made with two lateral shells, allowing a production of one unit per day per mould.

Accropodes are placed in a single layer in a predefined grid whereby the orientation of the blocks has to be varied; the latter is typically specified. Various sling techniques are recommended for placement. The best interlocking of Accropodes can be achieved on steep slopes (3:4 or 1:1.5). For further details see also Sogreah (2000).

For situations where a natural rock appearance is required, the Ecopode (a unit closely related to the Accropode) has been developed.

other, or from sheathed fibres where the outer coating has the lower melting point. Typical polymers used are polypropylene (PP) or high-density polyethylene (HDPE).

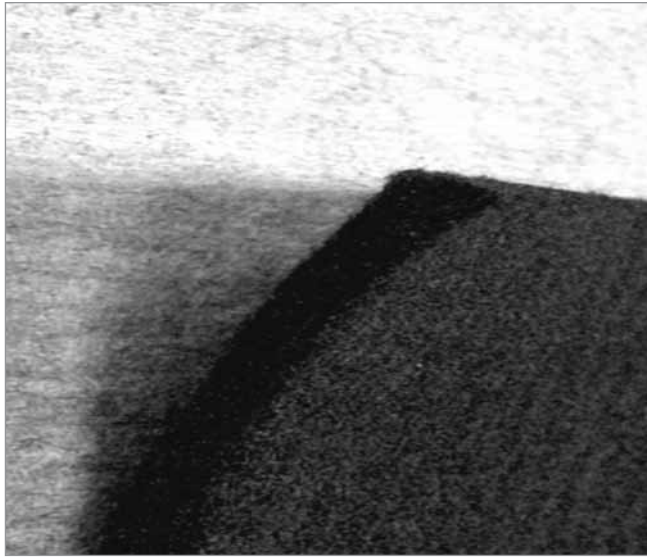


**Figure 3.110** Non-woven geotextile (courtesy Geofabrics)

### 3.16.2.2 Woven geotextiles

Woven geotextiles are flat structures of at least two sets of threads woven at right angles; see Figure 3.111. The sets of threads are referred to as the warp running lengthwise and the weft running across. Woven geotextiles can be categorised by the type of thread and the tightness of the weave.

- **monofilament fabrics** are gauze meshes that offer small resistance to through-flow. The mesh size must be adapted to the grain size of the material to be retained. Monofilament fabrics are principally made from HDPE or PP
- **tape fabrics** are made from very long strips of stretched HDPE or PP film, which are laid untwisted and flat in the fabric. They are laid closely together, resulting in limited openings in the fabric
- **split-film fabrics** are made from fibrillated yarns of PP or HDPE. The size of the openings in the fabric depends on the thickness and form of the cross-section of the yarns and the fabric construction. Split-film fabrics are generally heavy. Tape and split-film fabrics are often called slit-films
- **multifilament fabrics** are often described as cloth because they tend to have a textile appearance and are twisted or untwisted multifilament yarns. These fabrics are usually made from polyamide (PA 6 or PA 6.6) or PETP.

These thread types can also be mixed to form other families of wovens.

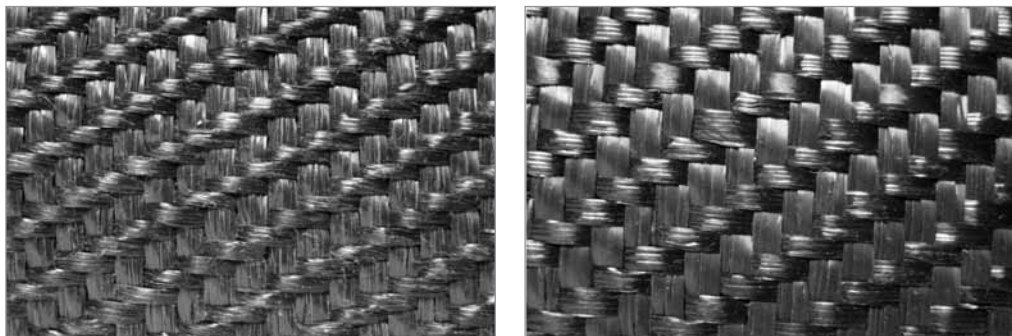


**Figure 3.111** Woven geotextiles (courtesy Ten Cate)

place will be different and the typical **neap tide** (MHWN) timing is about six hours earlier or later than the MHWS timing. When planning work on structures it is useful to know the timing of the most extreme low waters and whether or not they occur during daylight.

For a detailed description of sea level fluctuations and tidal phenomena, see Pugh (1987).

#### 4.2.2.3 Storm surges

Meteorological phenomena, namely atmospheric pressure and wind, may also affect the sea level in particular during storm events. This section focuses on atmospheric pressure effects while wind effects are considered in the next section. Pressure and wind effects are often combined during storms generating long waves, called **storm surges**, with a characteristic time-scale of several hours to one day and a wavelength approximately equal to the width of the centre of the depression, typically 150–800 km. These storm surges produce significant variations of the sea level, up to 2–3 m at the shore depending on the shape of the coastline and the storm intensity. In practice, the term **storm surge level** is sometimes used loosely to include the astronomical tidal component and other meteorological effects.

Local low atmospheric pressures (depressions) cause corresponding rises in water level. Similarly, high pressures cause drops in water levels. This is the so-called **inverse barometer effect**.

For open water domains, Equation 4.9 gives the relationship between the **static** rise in water level  $z_a$  (m) and the corresponding atmospheric pressure:

$$z_a = 0.01(1013 - p_a) \quad (4.9)$$

where  $p_a$  = atmospheric pressure at sea level (hPa) and 1013 hPa is the pressure in normal conditions (see Section 4.2.1.2).

**NOTE:** Equation 4.9 results from simple equilibrium between the atmosphere and the ocean in static conditions. Where the atmospheric pressure is higher than the mean value of 1013 hPa, the sea level decreases, provided that it can increase at another place where the atmospheric pressure is lower than the mean value. This simple relationship does not apply for closed domains of small dimensions such as lakes. Indeed, if the atmospheric pressure is the same over the whole water domain there is no change in static water level.

Dynamic effects can cause a significant amplification of the rise in water level, however. When the depression moves quickly, the water level rise follows the depression. The height of these long waves may increase considerably as a result of shoaling in the nearshore zones. Along the coasts of the southern North Sea, storm surges with a height of 3 m have been recorded.

#### 4.2.2.4 Wind set-up

Shear stress exerted by wind on the water surface causes a slope in the water surface (see Figure 4.11), as a result of which wind set-up and set-down occur at downwind and upwind boundaries, respectively.

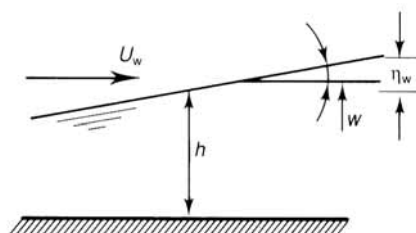


Figure 4.11 Wind set-up

referred to as **infra-gravity waves**. If the waves approach a beach obliquely the long waves can modify the longshore currents and also form **edge waves** that travel along the beach and are often *trapped* within the nearshore zone. Long waves also produce variations in both the set-up and the run-up in the surf zone caused by the primary waves. The long-period oscillations in these effects can cause both greater damage to, and overtopping of coastal structures.

An order of magnitude of the surf-beat amplitude in shallow water and in the surf zone can be obtained by using Equation 4.23, an empirical formula derived by Goda (2000):

$$\frac{\varepsilon_{rms}}{H'_0} = 0.01 \left[ \frac{H'_0}{L_o} \left( 1 + \frac{h}{H'_0} \right) \right]^{-1/2} \quad (4.23)$$

where  $\varepsilon_{rms}$  = root-mean-square amplitude of the surf-beat profile (m). It is a function of the equivalent deep-water (significant) wave height  $H'_0$  defined in Section 4.2.2.5 (m), the deep-water wavelength  $L_o$  (m) computed from the significant wave period  $T_s$  (see Section 4.2.4.4) as  $L_o = g(T_s)^2/(2\pi)$ , and the local water depth,  $h$  (m).

Bowers (1993) also provides formulae to estimate the amplitude of bound long waves for intermediate depths and also for surf beat significant wave height. For the case of coastal structures exposed to long waves, Kamphuis (2001) proposed the use of Equation 4.24 to estimate the zero moment wave height of the long waves,  $(H_{m0})_{LW}$ , at the structure as a function of the breaking significant wave height  $H_{s,b}$  and the peak wave period  $T_p$  (see Section 4.2.4.5).

$$\frac{(H_{m0})_{LW}}{H_{s,b}} = 0.11 \left[ \frac{H_{s,b}}{gT_p^2} \right]^{-0.24} \quad (4.24)$$

Equation 4.24 can be approximated as a rule of thumb by  $(H_{m0})_{LW} = 0.4H_{s,b}$ . Kamphuis (2001) also addresses the problem of reflection of these long waves on coastal structures, showing that the long wave profile (with distance offshore) may be described as the sum of an absorbed wave and a standing wave. The long wave reflection coefficient was about 22 per cent during the set of experiments.

#### 4.2.2.8 Tsunamis

Tsunamis are seismically induced gravity waves characterised by wave periods that are in the order of minutes rather than seconds (typically 10–60 minutes). They often originate from earthquakes below the ocean, where water depths can be more than 1000 m, and may travel long distances without reaching any noticeable wave height. However, when approaching coastlines their height may increase considerably. Because of their large wavelength, these waves are subject to strong shoaling and refraction effects. Approaching from quite large water depths, they can be calculated using shallow-water theory. Wave reflection from the relatively deep slopes of continental shelves may also be an important consideration.

Some theoretical work is available (eg Wilson, 1963), as well as numerical models to describe tsunami generation, propagation and run-up over land areas (eg Shuto, 1991; Yeh *et al*, 1994; Tadepalli and Synolakis, 1996) and also some large-scale experiments (eg Liu *et al*, 1995). More information on tsunamis can be obtained from the Internet, for example at <[www.pmel.noaa.gov/tsunami](http://www.pmel.noaa.gov/tsunami)>.

Tsunamis are as unpredictable as earthquakes. Figure 4.15 presents observations for height and period of tsunamis from Japanese sources observed at coasts within a range of about 750 km from the epicentre of sub-ocean earthquakes.

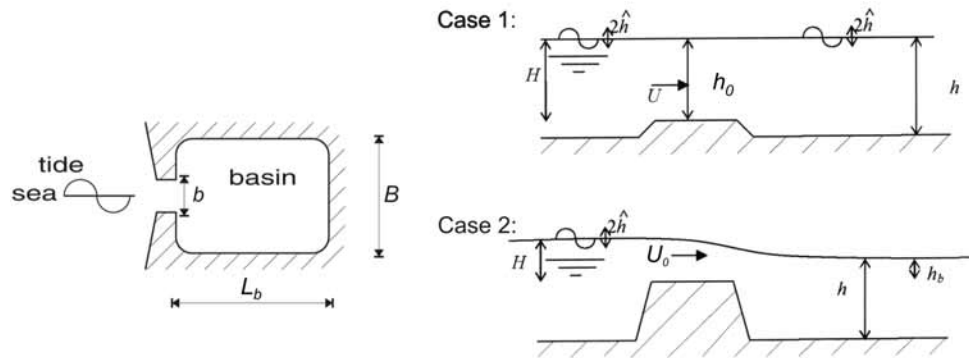
- the upstream discharge.

In the case of tidal motion the physical laws reduce to the so-called **long wave equations**, based on the assumption that vertical velocities and accelerations are negligible. Depending on the type of estuary, the long wave equations may be further simplified.

**Basin storage model for closure dams in estuaries**

When a closure dam is constructed in an estuary the hydraulic resistance changes during the construction phase, which affects the flow velocities and water levels in the estuary. The discharge, water level and maximum flow velocity can be estimated using a basin storage model, provided that the estuary length,  $L_b$  (m), is short relative to the length,  $L$  (m), of the tidal wave (see Equation 4.28).

$$L_b / L < 0.05 \tag{4.28}$$



**Note:**  $b$  is affected by horizontal closure while  $h_0$  is affected by vertical closure.

**Figure 4.18** Definition sketch of basin model

**Case 1 – sill.** As long as there is no appreciable constriction at the estuary mouth, ie when  $b/h_b$  is sufficiently large (see definition sketch in Figure 4.18), the discharge  $Q$  (m<sup>3</sup>/s) through the entrance attributable to the vertical tide inside the basin can be determined by using Equation 4.29:

$$Q(t) = B L_b \frac{dh}{dt} \tag{4.29}$$

where  $Q(t)$  = tidal discharge (m<sup>3</sup>/s) and  $h$  = water level in the estuary or the basin (m).

In the case of a sinusoidal tide of amplitude  $\hat{h}$ , Equation 4.29 becomes Equation 4.30:

$$Q(t) = \frac{2\pi}{T} B L_b \hat{h} \sin\left(\frac{2\pi t}{T}\right) \tag{4.30}$$

where, apart from the definitions shown in Figure 4.18,  $\hat{h}$  = amplitude of tide in the estuary (m),  $t$  = time after the beginning of the tide (s),  $T$  = tidal period (s).

Cross-sectional mean velocity  $U$  (m/s) at the estuary mouth can be evaluated by Equation 4.31:

$$U = \frac{Q}{b h_0} \tag{4.31}$$

where  $h_0$  = water depth in the gap (m) that varies with the tidal time as  $h$  and  $b$  = width of the estuary mouth (m).

**Case 2 – vertical closure.** When the closure dam forms an appreciable vertical constriction, the tidal discharge through the mouth starts to decrease and the mean flow velocity in the closure gap,  $U_0$ , depends on the water levels,  $h$  and  $H$ , inside and outside the basin respectively. When the flow is into the basin,  $U_0$  can as a first estimate be determined by using Equation 4.32:

$$U_g = \sqrt{2g(H - h_b)} \tag{4.32}$$

where  $H$  = sea-side water level above the dam crest (m) and  $h_b$  = water level in the basin above the dam crest (m).

Further discussion of discharge and velocity through the gap is given in Section 5.1.2.3 where discharge coefficients are introduced to improve precision. A simple model to calculate the response water level of the basin,  $h$ , given the tide at the seaward side as the boundary condition,  $H(t)$ , is based upon Equation 4.33, which results from the combination of Equations 4.29, 4.31 and 4.32:

$$BL_b \frac{dh}{dt} = h_0 b \sqrt{2g(H - h_b)} + Q_{river} \tag{4.33}$$

where  $Q_{river}$  = river discharge into the basin ( $m^3/s$ ), if relevant,  $h_0$  = water depth on the crest of the closure dam (m) (see Section 5.1.2.3) and  $H$ ,  $h_b$  and  $b$  are defined according to Figure 4.18.

**Combined closure.** Assuming a sinusoidal tide at sea and  $Q_{river} = 0$  m/s, the maximum flow velocity in the closure gap during the tide,  $U_g$  or  $U_0$  (m/s), can be determined with the design graph given in Figure 4.19. Note that Figure 4.19 plots  $U_g/\sqrt{\hat{h}}$ , which is not a non-dimensional quantity where  $U_g$  is in m/s and  $\hat{h}$  is in m. In this graph  $Y$  serves as an input parameter, the value of which should be calculated with Equation 4.34:

$$Y = 0.001 \frac{T_{M2}}{T} \frac{BL_b}{b/\sqrt{\hat{h}}} \tag{4.34}$$

where  $T$  = tidal period (s) and  $T_{M2}$  = period of semi-diurnal tide (= 44 700 s).

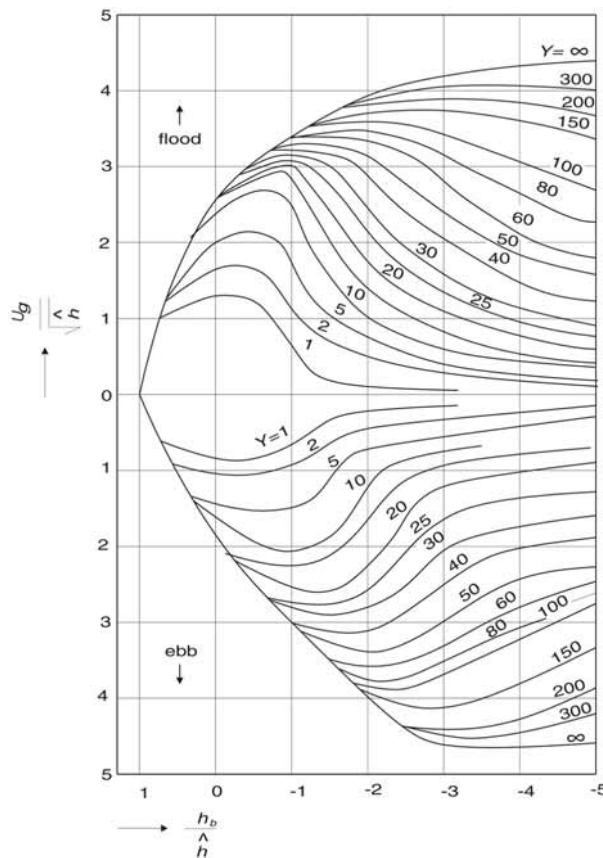


**Figure 4.19**  
Design graph for maximum velocity; note that  $h_b$  should read  $h_0$ , the sill level relative to mean water level in the closure gap

This method is not valid for small closure gaps. If the gap is not wider than about 20 per cent of the original width, it is recommended to use more sophisticated mathematical models.

equation accurately whenever necessary, but explicit approximations, such as given in Box 4.3, can also be used.

The propagation velocity of wave crests (**phase speed**) is  $c = L/T = \omega/k$  (m/s) and the propagation velocity of energy (**group velocity**) is given by  $c_g = \partial\omega/\partial k$  (m/s). In linear wave theory, based on Equation 4.38, the expressions for phase and group velocity are given by Equations 4.39 and 4.40 respectively.

$$c = \frac{g}{\omega} \tanh(kh) = \sqrt{\frac{g}{k} \tanh(kh)} \quad (4.39)$$

$$c_g = nc \quad \text{with} \quad n = \frac{1}{2} \left( 1 + \frac{2kh}{\sinh(2kh)} \right) \quad (4.40)$$

Note that the factor  $n$  has two asymptotic values: (1) when the relative water depth,  $kh$  (-), is small,  $n$  tends towards 1; (2) when  $kh$  is large  $n$  tends towards  $1/2$ ; in this case the wave energy propagates at a speed that is half of that of individual waves. For these asymptotic cases, particular expressions of  $k$ ,  $L$ ,  $c$  and  $c_g$  may be derived analytically and are listed in Table 4.6, together with the non-dimensional criteria for using these approximations. For values in deep water (large value of  $kh$ ), the subscript “0” or “o” was used conventionally (eg  $L_o$  for the deep-water wavelength). Here the latter, “o” (of offshore), is used. From Table 4.6 it should be noted, for example, that in shallow-water conditions,  $c$  and  $c_g$  do not depend any more on the wave period,  $T$ , and that all waves have the same velocity (non-dispersive waves), which, in this case, equals the velocity of energy.

**Box 4.3**      *Explicit approximations of the linear dispersion relation for water waves*

There are numerous approximations of the dispersion relation given by Equation 4.38. Equation 4.41 gives the rational one proposed by Hunt (1979) at order 9, which is very accurate (always less than 0.01 per cent of relative error in  $kh$ ):

$$(kh)^2 = (k_o h)^2 + \frac{k_o h}{1 + \sum_{n=1}^9 a_n (k_o h)^n} \quad (4.41)$$

where  $k_o = 2\pi/L_o = \omega^2/g =$  deep-water wave number (rad/m) and the values of  $a_n$  are as follows:

$$\begin{array}{lllll} a_1 = 0.66667 & a_2 = 0.35550 & a_3 = 0.16084 & a_4 = 0.06320 & a_5 = 0.02174 \\ a_6 = 0.00654 & a_7 = 0.00171 & a_8 = 0.00039 & a_9 = 0.00011. & \end{array}$$

Hunt (1979) also provides a similar formula at order 6, with a relative error in  $kh$  always less than 0.2 per cent.

Alternatively, the simpler explicit formulation by Fenton and McKee (1990) (see Equation 4.42) can be used. Although it is less accurate than the former (1.5 per cent of maximum relative error), it is easier to use on a calculator.

$$k = \frac{\omega^2}{g} \left\{ \coth \left[ \left( \omega \sqrt{\frac{h}{g}} \right)^{3/2} \right] \right\}^{2/3} \quad \text{or equivalent:} \quad L = L_o \left\{ \tanh \left[ (k_o h)^{3/4} \right] \right\}^{2/3} \quad (4.42)$$

Other explicit expressions have been proposed by Eckart (1952), Wu and Thornton (1986), Guo (2002).

**Table 4.6** Asymptotic values of the dispersion relation and related quantities

Variable	Approximations with criteria	
	Shallow-water or long wave approximation ( <i>small kh</i> )	Deep-water or short wave approximation ( <i>large kh</i> )
	$h/L < 1/25$ or $T\sqrt{g/h} > 25$	$h/L > 1/2$ or $T\sqrt{g/h} < 4$
Dispersion relation	$\omega^2 = gh k^2$	$\omega^2 = gk_o$
Wave number $k$ (rad/m)	$k = \omega / \sqrt{gh}$	$k_o = \omega^2 / g$
Wavelength $L$ (m)	$L = T\sqrt{gh}$	$L_o = gT^2 / (2\pi)$
Phase speed $c$ (m/s)	$c = \sqrt{gh}$	$c_o = gT / (2\pi)$
Group velocity $c_g$ (m/s)	$c_g = c = \sqrt{gh}$	$c_{go} = 1/2 c_o = gT / (4\pi)$

**Description and definitions for irregular waves or sea-states**

For a sea-state, composed of waves having different characteristics but belonging to the same random process (ie constant environmental conditions), two approaches are used to describe the wave field.

- 1 **Long-crested random waves** are still unidirectional, but include a range of wave heights and periods. The irregular or **random** wave train is composed of successive waves having different heights and periods. Two approaches are used to describe random waves and are set out below: the statistical (or wave-by-wave) approach, which consists of determining the **statistical distributions** of wave heights, periods, directions etc (see Section 4.2.4.4), and the **spectral approach**, which is based on the determination and use of the spectrum of wave energy (see Section 4.2.4.5). In both cases, representative parameters can be calculated to characterise the sea-state (eg the significant wave height  $H_s$  and the mean wave period  $T_m$ ).
- 2 **Short-crested random waves** additionally include a range of directions, defined in terms of the standard deviation of wave energy propagation direction or some other standard spreading function. A more complete description of the sea-state is given by the directional spectrum ( $S(f, \theta)$ ), which gives the distribution of wave energy as a function of frequency and direction (see Section 4.2.4.5). Short-crested waves provide the best representation of true ocean waves, and this representation of wave conditions has now become the standard way of dealing with wave actions in the engineering practice. The direction of wave incidence and the angular spreading of wave energy have been shown to have some effects on wave-structure interaction processes, such as stability of rubble mound breakwaters, run-up and overtopping (Galland, 1995; Donnars and Benoit, 1997).

**4.2.4.3****Characterisation of wave conditions and wave kinematics****Characterisation of wave conditions by non-dimensional numbers**

In order to characterise wave conditions, to investigate which processes are dominant during wave propagation and transformation, and/or to estimate wave loading on structures, several non-dimensional numbers are used. They can be computed for regular waves or random waves by using representative wave parameters. The most useful parameters are set out below.

- **The relative water depth:  $kh$  or  $h/L$  and the non-dimensional period  $T\sqrt{g/h}$**

They are used to determine the manner in which seabed bathymetry affects waves. For example, the parameters were used in the previous section (see Table 4.6) to derive approximations of phase speed and group velocity in low and large relative water depths respectively.

- *The wave steepness  $s = H/L$  and the relative wave height  $H/h$*

They are measures of non-linearity of the wave (see Figure 4.23). They are used in particular to quantify the importance of non-linear effects and they appear in the formation of criteria for predicting wave breaking. A specific use of the wave steepness is made if the wave height is taken at the toe of the structure and the wavelength in deep water. In fact this is a fictitious wave steepness  $s_o = H/L_o$  and is often used in design formulae for structures. The main goal in this case is not to describe the wave steepness itself, but to include the effect of the wave period on structure response through  $L_o = gT^2/(2\pi)$ , which is only valid offshore.

- *The Ursell number  $U$  (-)*

This is a combination of the former numbers and is presented in Equation 4.43. It is used to characterise the degree of non-linearity of the waves.

$$U = \frac{HL^2}{h^3} = \left(\frac{H}{h}\right) \left/\left(\frac{h}{L}\right)^2\right. \quad (4.43)$$

- *The surf similarity parameter  $\xi$ , also known as the Iribarren number,  $Ir$  (see Equation 4.44)*

This is used for the characterisation of many phenomena related to waves in shallow water, such as wave breaking, run-up and overtopping. It reflects the ratio of bed slope and fictitious wave steepness,  $s_o$ .

$$\xi = \frac{\tan\alpha}{\sqrt{s_o}} = \frac{\tan\alpha}{\sqrt{H/L_o}} = \frac{\tan\alpha}{\sqrt{(2\pi H)/(gT^2)}} \quad (4.44)$$

When the deep-water wave height,  $H_o$ , is used instead of  $H$ , this number is denoted  $\xi_o$  or  $Ir_o$ .

This parameter is often used for beaches, and often for design of structures too. It gives the type of wave breaking and wave load on the structure. Actually, waves can break first on the depth-limited foreshore before reaching the structure and then break once again on to the structure. On the foreshore the breaker type is generally spilling, sometimes plunging. On the structure itself it is never spilling, but plunging (gentle structure slope), surging or collapsing (see Section 4.2.4.7 for the definition of breaker types).

When using these parameters for random waves, it should be stressed and indicated (as a subscript of these parameters, for example) which characteristic wave height and period are being used in their evaluation (eg subscript “ $p$ ” if the peak period  $T_p$  is used, and “ $m$ ” if the mean period  $T_m$  is used).

For further discussion on the use and the notation of  $\xi$ , please also refer to Section 5.1.1.1.

#### Overview of methods for computing wave kinematics

Many wave theories are available to derive other wave parameters and kinematics (velocities, accelerations, pressure etc) from the above-mentioned basic parameters (eg  $H$  and  $T$ , plus possibly a flow speed). The majority of design methods are based on Stokes linear wave theory (ie small amplitude wave theory) derived for a flat bottom (ie constant water depth). A major advantage of linear theory in design procedures is that the principle of superposition can be applied to wave-related data, obtained from a composite wave field. Using linear wave theory, practical engineering approximations can be derived for regular waves propagating in deep and shallow water respectively (see Table 4.6). Expressions for orbital velocities  $u_x$ ,  $u_y$ ,  $u_z$  and pressure  $p$  are presented below as Equations 4.45 to 4.48 for the case of a regular wave with a height  $H$ , period  $T$  (angular frequency  $\omega = 2\pi/T$ ) and direction  $\theta$  with respect to

**Distribution of individual wave heights in a sea-state**

During each sea-state a (short-term) distribution of wave heights applies. Once the distribution function of wave heights is known, all the characteristic wave heights listed in Table 4.7 can be computed. Some basic and important results for wave distributions are summarised below: first for the deep-water case, and then for the shallow-water case. The latter is more important for the design of coastal structures, but also more difficult to model and parameterise.

- *Distribution of deep-water wave heights*

In deep water the water surface elevation usually follows a Gaussian process and thus the individual wave heights closely follow the Rayleigh distribution. Note that the Rayleigh distribution is a particular case of the Weibull distribution, with a fixed shape parameter of 2 (see Box 4.10). This distribution is fully defined by a single parameter, which may be either the mean wave height  $H_m$  or the root mean square (rms) wave height  $H_{rms}$ , or alternatively the variance of the free-surface elevation  $m_0$ . Equation 4.50 gives the equivalent forms of the cumulative distribution function.

$$P(H) = P(\underline{H} < H) = 1 - \exp\left(-\frac{H^2}{8m_0}\right) = 1 - \exp\left(-\frac{\pi}{4}\left(\frac{H}{H_m}\right)^2\right) = 1 - \exp\left(-\left(\frac{H}{H_{rms}}\right)^2\right) \quad (4.50)$$

Equation 4.51 gives the corresponding probability density function.

$$p(H) = \frac{H}{4m_0} \exp\left(-\frac{H^2}{8m_0}\right) = \frac{\pi}{2} \frac{H}{H_m^2} \exp\left(-\frac{\pi}{4}\left(\frac{H}{H_m}\right)^2\right) = \frac{2H}{H_{rms}^2} \exp\left(-\left(\frac{H}{H_{rms}}\right)^2\right) \quad (4.51)$$

The variance  $m_0$  can be computed from the free-surface elevation signal  $\eta(t)$  (see Equation 4.52) or from the wave spectrum  $E(f)$  (it corresponds to the area between spectrum and the  $x$ -axis, see Section 4.2.4.5).

$$m_0 = \eta_{rms}^2 = \frac{1}{T} \int_0^T (\eta(t) - \bar{\eta})^2 dt \quad (4.52)$$

Figure 4.27 shows the Rayleigh distribution.

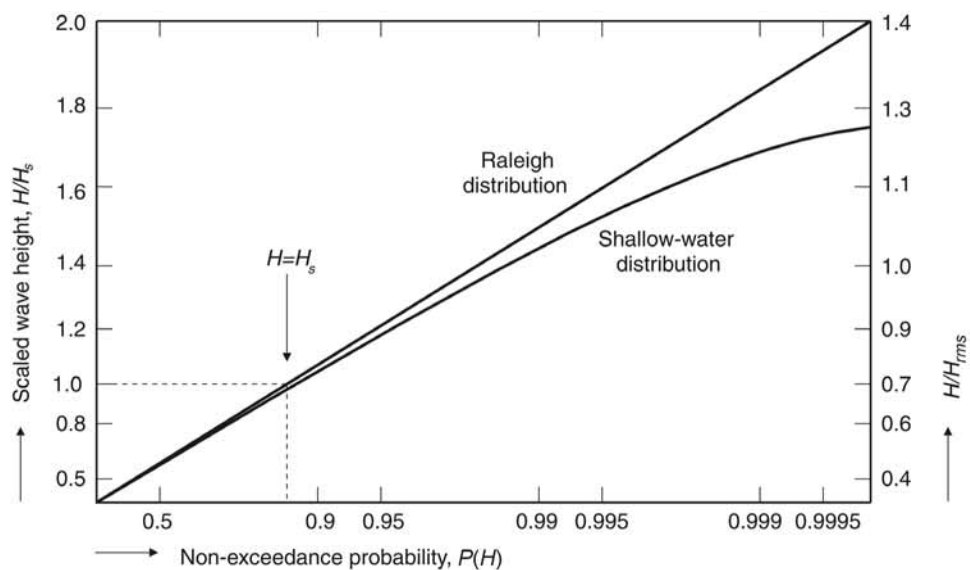


**Figure 4.27** Example of a shallow-water observed distribution of wave heights compared with the Rayleigh distribution

A shortcoming of the Rayleigh distribution is that it is not bounded by an upper maximum value. Thus the maximum wave height can neither be defined nor computed in a deterministic way from this distribution. However, the representative wave heights  $H_{P\%}$  and  $H_{1/Q}$  can be computed analytically (see Equations 4.53 and 4.54) from the Rayleigh distribution (eg Massel, 1996; Goda, 2000).

$$\frac{H_{P\%}}{H_{rms}} = \sqrt{-\ln(P/100)} \tag{4.53}$$

$$\frac{H_{1/Q}}{H_{rms}} = \frac{\sqrt{\pi}}{2} Q \operatorname{erfc}(\sqrt{\ln Q}) + \sqrt{\ln Q}, \quad \text{with } \operatorname{erfc}(x) = \frac{2}{\sqrt{\pi}} \int_x^{+\infty} \exp(-t^2) dt \tag{4.54}$$

The most important and useful results are listed in Table 4.8. An important issue is the estimation of the maximum value of the wave height for the case of sea-states of finite duration. This maximum wave height cannot be determined in a deterministic manner. One can, however, derive a probability density function for the (statistical) ratio  $H_{max}/H_s$  (eg Massel, 1996; Goda, 2000). Two important representative values, namely the mode and the mean values, can be expressed analytically (see Equations 4.55 and 4.56) and computed (see Table 4.9 for some typical results).

**Table 4.8** Characteristic wave height ratios for a sea-state with a Rayleigh distribution of wave heights

Characteristic height $H$	Wave height ratios			
	$H/\sqrt{m_0}$	$H/H_m$	$H/H_{rms}$	$H/H_s$
Standard deviation of free surface $\sigma_\eta = \sqrt{m_0}$	1	0.399	0.353	0.250
Mean wave height $H_m$	2.507	1	0.886	0.626
Root-mean-square wave height $H_{rms}$	2.828	1.128	1	0.706
Significant wave height $H_s = H_{1/3}$	4.004	1.597	1.416	1
Wave height $H_{1/10}$	5.090	2.031	1.800	1.273
Wave height $H_{1/100}$	6.673	2.662	2.359	1.668
Wave height $H_{2\%}$	5.594	2.232	1.978	1.397

• **Mode of the distribution**

The most probable value of the ratio  $H_{max}/H_s$  for a record consisting of  $N$  waves is given by Equation 4.55.

$$\left[ \frac{H_{max}}{H_s} \right]_{mode} \approx \sqrt{\frac{\ln N}{2}} \tag{4.55}$$

• **Mean value of the distribution**

The mean value of the ratio  $H_{max}/H_s$  for a record consisting of  $N$  waves (see Equation 4.56). The mean value is greater than the mode, because of the skewed shape of the distribution:

$$\left[ \frac{H_{max}}{H_s} \right]_{mean} \approx \left( \sqrt{\frac{\ln N}{2}} + \frac{\gamma}{2\sqrt{2\ln N}} \right) \tag{4.56}$$

where  $\gamma$  = Euler constant  $\approx 0.5772$ .



As stated above, a spectral form of the JONSWAP spectrum with a  $f^{-4}$  power law for the high-frequency range is preferable. Modified forms have among others been proposed by Donelan *et al* (1985) and Aono and Goto (1995), which are summarised in Box 4.5.

**Box 4.5** Modified JONSWAP spectra compatible with a  $f^4$  high-frequency tail

Modified JONSWAP spectrum as proposed by Donelan *et al* (1985) with input variables  $U_{10}$  and  $F$  or  $m_0$  and  $T_p$

**Expression of frequency spectrum:**

$$E(f) = \alpha (2\pi)^{-4} g^2 f_p^{-1} f^4 \exp[-(f/f_p)^4] \gamma^\delta$$

with the following relationships:

$$\alpha = 0.006 (U_{10}/c_p)^{0.55} \quad \text{for } 0.83 < U_{10}/c_p < 5$$

$$\gamma = 1.7 \quad \text{for } 0.83 < U_{10}/c_p < 1$$

$$\gamma = 1.7 + 6 \log(U_{10}/c_p) \quad \text{for } 1 < U_{10}/c_p < 5$$

$$\sigma = 0.08 + 0.32 (U_{10}/c_p)^{-3} \quad \text{for } 1 < U_{10}/c_p < 5$$

$$\delta = \exp[-(f/f_p - 1)^2 / (2\sigma^2)]$$

where  $c_p$  = phase speed corresponding to the peak frequency ( $c_p = g / (2\pi f_p)$  in deep water);  $U_{10}/c_p = 0.83$  corresponding to the point of full development; both  $f_p$  and  $c_p$  are a function of the wind-speed  $U_{10}$  and the fetch length  $F$ , through:

$$f_p U_{10} / g = 1.845 (g F / U_{10}^2)^{0.23}$$

Young (1992) derived relationships to calculate the spectrum directly from the variance  $m_0$  and the peak period  $T_p$  through:

$$\alpha = 200 g^{-1.571} (m_0)^{0.786} (T_p)^{-3.143}$$

$$\gamma = 6.489 + 6 \log[(2.649 \cdot 10^7 g^{-2.857} (m_0)^{1.429} (T_p)^{-5.714})]$$

$$\sigma = 0.08 + 6.94 \cdot 10^{-26} g^{8.571} (m_0)^{-4.287} (T_p)^{17.142}$$

Modified JONSWAP spectrum as proposed by Aono and Goto (1995) with input variables  $H_{1/3}$  and  $T_{1/3}$

**Expression of frequency spectrum:**

$$E(f) = \alpha (2\pi)^{-3} g u^* f^{-4} \exp[-(f/f_p)^4] \gamma^\delta$$

with the following relationships:

$$u^* = (H_{1/3})^2 / (g B^2 (T_{1/3})^3) \quad B = 0.067$$

$$f_p = 1 / (1.136 T_{1/3}) \quad f_{p^*} = f_p u^* / g$$

$$\gamma = 6 (f_{p^*})^{0.15} \quad \alpha = 0.17 \gamma^{-1/3}$$

$$\sigma_1 = 0.144 \text{ for } f < f_p \quad \sigma_2 = 0.07 (f_{p^*})^{0.16} \text{ for } f > f_p$$

$$\delta = \exp[-(f/f_p - 1)^2 / (2\sigma^2)]$$

This spectrum conforms to the 3/2 power law of Toba (1973, 1997),  $H^* = B T^{*3/2}$ , with a slight modification of the  $B$  coefficient: 0.067 instead of the original value of 0.062 (Toba, 1973).

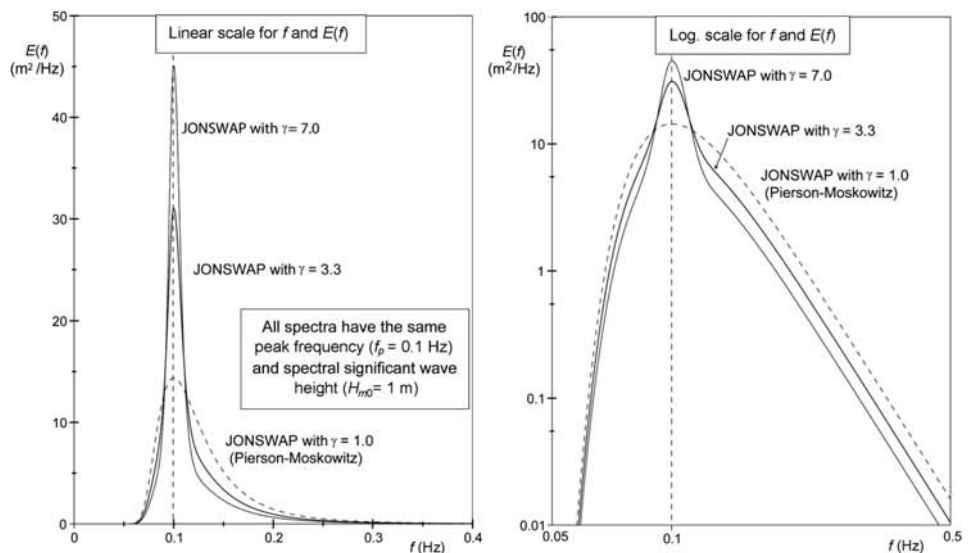


Figure 4.29 Pierson-Moskowitz and JONSWAP spectra

$$\frac{gT_p}{U_{10} \cos(\theta - \phi_w)} = 0.542 \left( \frac{gF_\theta}{(U_{10} \cos(\theta - \phi_w))^2} \right)^{0.23} \quad (4.87)$$

$$\frac{gI_{min}}{U_{10} \cos(\theta - \phi_w)} = 30.1 \left( \frac{gF_\theta}{(U_{10} \cos(\theta - \phi_w))^2} \right)^{0.77} \quad (4.88)$$

The value of the directional fetch,  $F_\theta$ , is limited by the criterion expressed by Equation 4.89 to avoid over-development of wave energy.

$$\frac{gF_\theta}{(U_{10} \cos(\theta - \phi_w))^2} \leq 9.47 \cdot 10^4 \quad (4.89)$$

At this value of non-dimensional directional fetch,  $F_\theta$ , fully development of waves is reached, resulting in Equations 4.90 and 4.91.

$$\frac{gH_s}{(U_{10} \cos(\theta - \phi_w))^2} = 0.285 \quad (4.90)$$

$$\frac{gT_p}{U_{10} \cos(\theta - \phi_w)} = 7.56 \quad (4.91)$$

(c) **Young and Verhagen method**

Young and Verhagen (1996) analysed a large set of wave measurements performed on Lake George (Australia). From this comprehensive dataset they were able to propose wave prediction formulae including both the effect of fetch  $F$  and water depth  $h$  (see Equations 4.92 and 4.93). The formulae are based on the form of the formulae of SPM (1984) for wave generation in finite water depth:

$$\frac{gH_s}{U_{10}^2} = 0.241 \left( \tanh A_1 \tanh \left( \frac{B_1}{\tanh A_1} \right) \right)^{0.87} \quad (4.92)$$

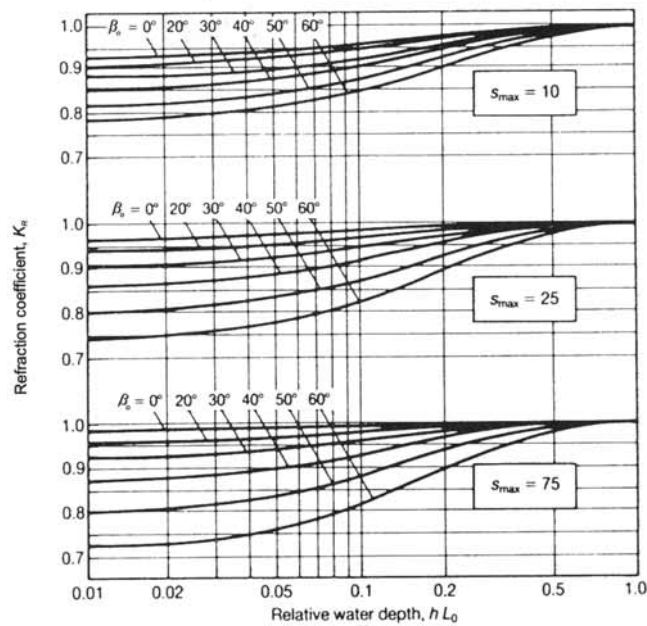
where:  $A_1 = 0.493 \left( \frac{gh}{U_{10}^2} \right)^{0.75}$  and  $B_1 = 0.00313 \left( \frac{gF}{U_{10}^2} \right)^{0.57}$ .

$$\frac{gT_p}{U_{10}^2} = 7.519 \left( \tanh A_2 \tanh \left( \frac{B_2}{\tanh A_2} \right) \right)^{0.37} \quad (4.93)$$

where:  $A_2 = 0.331 \left( \frac{gh}{U_{10}^2} \right)^{1.01}$  and  $B_2 = 0.0005215 \left( \frac{gF}{U_{10}^2} \right)^{0.73}$ .

This latter method offers the advantage of taking account of the actual water depth, which is important for reservoirs. Indeed, the mean water level in a reservoir may change significantly over a year leading to significant variations of fetch length and water depth. Both these parameters are present in the above formulae.

Later Young (1997) observed that these formulae fail to correctly model the wave height for short fetches, which was attributed to the fact that the formulae revert to JONSWAP formulae (Hasselmann *et al.*, 1973) for such cases. For a better treatment of this case, he proposed an equation that has to be integrated numerically to obtain a wave growth curve.



Note:  $s_{max}$  is a parameter used to describe directional spreading. Goda (1985) suggests the following values:

- i) Wind waves:  $s_{max} = 10$
- ii) Swell with short decay distance:  $s_{max} = 25$   
(with relatively large wave steepness)
- iii) Swell with long decay distance:  $s_{max} = 75$   
(with relatively small wave steepness)

Figure 4.34

Retraction coefficient,  $K_R$ , for an irregular directional wave field on a coast with straight, parallel depth contours (Goda, 2000)

### Shoaling

Shoaling is a change in wave height when waves propagate in varying water depths. The shoaling effect is normally expressed in terms of the shoaling coefficient,  $K_S$ , which is defined as the local wave height  $H$  relative to  $H_0$ . Using linear wave theory  $K_S$  can, for a given wave period  $T$ , be written as a function of water depth  $h$  (see Equation 4.98).

$$K_S = \left[ \tanh(kh) \left( 1 + \frac{2kh}{\sinh(2kh)} \right) \right]^{-1/2} \tag{4.98}$$

Under the usual limitations related to the linear wave theory, the above equation gives appropriate estimates for engineering purposes. It can also be applied to irregular sea-states by making use of  $H_{m0}$  and  $T_p$ . In this latter case (distribution of energy over frequency), and as a result of non-linear (finite amplitude) effects, deviations of approximately 10 per cent from Equation 4.98 were reported by Goda (2000). When individual waves are considered, however, the deviation is stronger in the nearshore zone, and in this case the analytical approach of Shuto (1974) may be used.

Of course, the above expression of  $K_S$  has a limitation: it can never grow to very high values, because of wave breaking. This effect is discussed below. If the structure is located in the surf zone, the shoaling has no effect, because waves break first before they reach the structure. Shoaling is only important if the structure is situated in this shoaling area. In this case deep-water wave conditions may **increase** by shoaling before they reach the structure. This is particularly true for low-steepness waves on steep slopes where this increase of wave height can be very significant and may lead to strong (plunging or surging) breakers.

### Dissipation caused by bottom friction

Except for the case of long swell propagating over long distances on continental shelves or in the nearshore zone, energy dissipation caused by bottom friction is usually of less importance compared with the other processes considered in this section (Hamm *et al*, 1993).

## Box 4.7 Brief overview of breaking criteria

- 1 Breaking caused by limiting steepness.** Breaking due to exceedance of the steepness criterion is the main limiting factor in deep and medium water. The steepness criterion is given by Equation 4.100 (Miche, 1944).

$$H/L \leq [H/L]_{max} = 0.14 \tanh(2\pi h/L) \quad (4.100)$$

- 2 Breaking caused by water depth.** The breaking criterion due to water depth is normally given by a useful non-dimensional parameter called the breaker index  $\gamma_{br}$ , defined as the maximum wave height to depth ratio  $H/h$  (see Equation 4.101) where the subscript  $b$  stands for **the value at the breaking point**.

$$H/L \leq \gamma_{br} = [H/h]_{max} = H_b/h_b \quad (4.101)$$

For stable and progressive waves **over a flat bottom**  $\gamma_{br}$  has a theoretical maximum value of 0.78 (McCowan, 1894). Note, however, that  $\gamma_{br}$  is not constant, but ranges roughly between 0.5 and 1.5 depending on the bottom slope and the wave period of the incident waves. Numerous criteria to predict the value of  $\gamma_{br}$  have been proposed. A comprehensive review and comparison of most of them can be found in Rattanapitikon and Shibayama (2000). For regular waves normally incident on a uniform slope,  $m$  (ie  $m = \tan(\alpha)$ ), two criteria (see Equations 4.102 and 4.103) may be recommended for practical use:

$$\text{Goda (1970b)} \quad \gamma_{br} = \frac{H_b}{h_b} = 0.17 \frac{L_o}{h_b} \left\{ 1 - \exp \left[ -1.5\pi \frac{h_b}{L_o} (1 + 15m^{4/3}) \right] \right\} \quad (4.102)$$

$$\text{Weggel (1972)} \quad \gamma_{br} = \frac{H_b}{h_b} = \frac{b(m)}{1 + a(m) \frac{h_b}{L_o}} = b(m) - a(m) \frac{H_b}{L_o} \quad (4.103)$$

where  $a(m) = 6.96 [1 - \exp(-19m)]$  and  $b(m) = 1.56 [1 + \exp(-19.5m)]^{-1}$

Other criteria and a comparison of them on a large set of data can be found in Rattanapitikon and Shibayama (2000) and in Rattanapitikon *et al* (2003), who also proposed a new criterion giving the best fit to the experimental points of the validation database (see Equation 4.104):

$$\frac{H_b}{L_b} = \left[ -1.40m^2 + 0.57m + 0.23 \right] \left( \frac{H_o}{L_o} \right)^{0.35} \quad (4.104)$$

where  $L_b$  = wavelength computed at the breaking point (depth  $h_b$ ) by the linear wave theory.

For irregular waves (represented by the significant wave height  $H_s$ ), typical values are found to be  $\gamma_{br} = 0.5$  to 0.6. The actual limiting wave height ratio  $\gamma_{br}$  depends mainly on such parameters as  $\xi$  and may reach values as large as 1.5 for **individual waves**. Figure 4.39 gives a good impression of the relationship between  $\gamma_{br}$  and  $\xi_o$  (see Section 4.2.4.3) and the related scatter of the data.

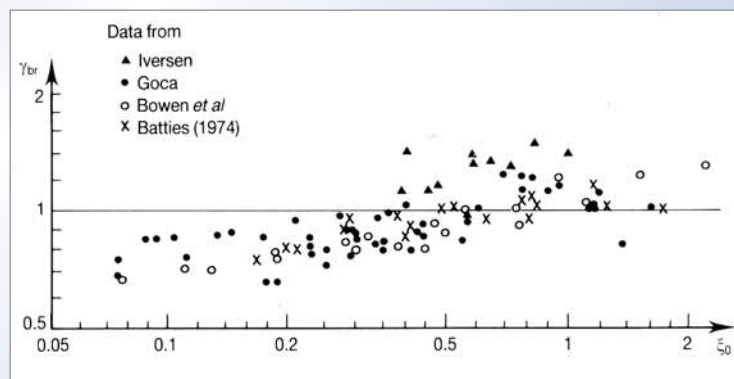


**Figure 4.39**  
Breaker index,  $\gamma_{br}$  as a function of deep-water surf similarity parameter,  $\xi_o$

#### Depth-limited significant wave height for constant bottom slopes

Wave breaking becomes increasingly important in shallow water, and wave models accounting for breaking should be used. The main effect of wave breaking is a lower significant wave height. But there are other changes due to wave breaking which might have an effect on structures. These changes occur both in the time as well as in the frequency domain. The wave height distribution changes as well as the shape of the spectrum. This section describes the decay in significant wave height due to breaking, while the changes of wave height distribution and spectral shape are addressed in Sections 4.2.4.4 and 4.2.4.5 respectively.

**Box 4.10** Extreme value probability distributions

The following extreme value probability distributions (see Equations 4.107 to 4.110) are commonly used to fit the long-term distributions of wave height, water levels etc.

$$\text{Gumbel} \quad P(X) = P(\underline{X} \leq X) = \exp[-\exp(-aX + b)] \quad (4.107)$$

$$\text{Weibull} \quad P(X) = P(\underline{X} \leq X) = 1 - \exp\left[-\left(\frac{X-a}{b}\right)^c\right] \quad (4.108)$$

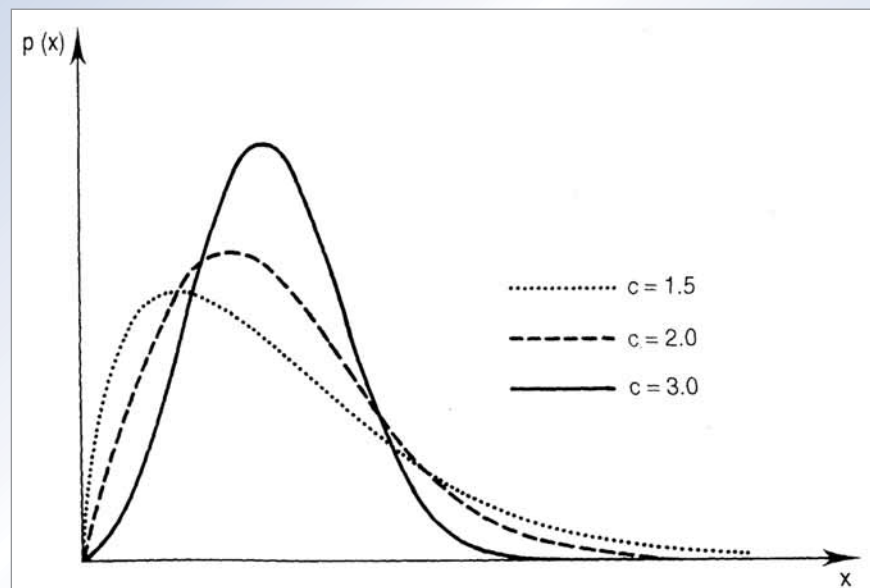
$$\text{Log-normal} \quad p(x) = \frac{1}{a x \sqrt{\pi}} \exp\left[-\left(\frac{\ln(x)-b}{a}\right)^2\right] \quad (4.109)$$

$$\text{Exponential} \quad P(X) = P(\underline{X} \leq X) = 1 - \exp\left[-\frac{X-a}{b}\right] \quad (4.110)$$

where  $P(X)$  is the cumulative probability function, ie the probability that  $\underline{X}$  will not exceed  $X$ , ie  $P(\underline{X} \leq X)$ , and  $p(x)$  is the probability density function of  $x$  and  $p(x) = dP/dx$ .

Note that the three-parameter Weibull distribution reduces to the shifted Rayleigh distribution if  $c = 2$  and  $a \neq 0$  and to the classical shifted Rayleigh distribution if  $c = 2$  and  $a = 0$  (see Figure 4.45).

With  $c = 1$ , the three-parameter Weibull corresponds to the exponential distribution, very often used for extreme wave climate analysis. The more universal nature of the Weibull distribution means that this is often the preferred model.



**Note:** The curve with  $c = 2$  corresponds to the Rayleigh distribution presented in Section 4.2.4.4.

**Figure 4.45** The two-parameter Weibull distribution (third parameter  $a = 0$ )

**Traditional calculation methods**

For a composite cross-section the values of the hydraulic roughness for the various zones usually differ. Early publications on the approach used the Manning-Strickler method for irregular river cross-sections. In such cases, which are very common, the effects of banks and channels on the current distribution have to be considered. An irregular cross-section should be schematised using one of the following approaches.

- 1 A general method is to divide the cross-section into vertical slices parallel to the river axis, each with a more or less constant water depth, as shown in Figure 4.58a.

For the determination of the equivalent roughness, the water area is divided into  $N$  parts with the wetted perimeters  $P_1, P_2, \dots, P_N$  (m) and the Manning coefficients of roughness  $n_1, n_2, \dots, n_N$  (s/m<sup>1/3</sup>) are known.

By assuming that each part of the area has the same mean velocity, the equivalent coefficient of roughness may be obtained by Equation 4.137 (Einstein, 1934; Yassin, 1954; Horton, 1933).

$$n = \left( P_1 n_1^{3/2} + P_2 n_2^{3/2} + \dots + P_N n_N^{3/2} \right)^{2/3} / P^{2/3} \quad (4.137)$$

By assuming that the total force resisting the flow is equal to the sum of the forces resisting the flow developed in the subdivided areas (Pavlovski, 1931; Mülhofer, 1933; Einstein and Banks, 1950), the equivalent roughness coefficient is given by Equation 4.138.

$$n = \left( P_1 n_1^2 + P_2 n_2^2 + \dots + P_N n_N^2 \right)^{1/2} / P^{1/2} \quad (4.138)$$

Lotter (1933) assumed that the total discharge of the flow is equal to the sum of discharges of the subdivided areas (see Figure 4.58a). Thus the equivalent roughness coefficient can be computed from Equation 4.139.

$$n = P R^{5/3} / \left( P_1 R_1^{5/3} / n_1 + P_2 R_2^{5/3} / n_2 + \dots + P_N R_N^{5/3} / n_N \right) \quad (4.139)$$

- 2 Where a main channel and a floodplain can be clearly distinguished, the cross-section should be divided into two separate parts (see Figure 4.58b). Then, using the Chézy formulation, the conditions of equal water surface gradient  $i$  and continuity yield to Equations 4.140 and 4.141.

$$i = U_1^2 / (R_1 C_1^2) = U_2^2 / (R_2 C_2^2) = U^2 / (R C^2) \quad (4.140)$$

$$U A_c = U_1 A_{c1} + U_2 A_{c2} \quad (4.141)$$

This results in Equations 4.142 and 4.143.

$$U A_c = U A_{c1} \left( \sqrt{\frac{R_1}{R}} \frac{C_1}{C} \right) + U A_{c2} \left( \sqrt{\frac{R_2}{R}} \frac{C_2}{C} \right) \quad (4.142)$$

$$\sqrt{R} = \left( A_{c1} \sqrt{R_1} C_1 + A_{c2} \sqrt{R_2} C_2 \right) / (A_c C) \quad (4.143)$$

The overall  $C$ -value can be computed from Equation 4.144.

$$C = (b_1 C_1 + b_2 C_2) / b \quad (4.144)$$

where  $b = b_1 + b_2$  (see Figure 4.58b).

- 3 If the area of the cross-sections ( $A_{c1}$  and  $A_{c2}$ ) cannot be estimated accurately, as in Figure 4.58c, then the application of the hypothesis of Einstein is recommended. Einstein assumed  $U_1 = U_2 = U$ , resulting in Equation 4.145.

$$1/(R_1 C_1^2) = 1/(R_2 C_2^2) = 1/(R C^2) \quad (4.145)$$

maximum. Figure 4.61 illustrates the general pattern of velocity distribution over various vertical and horizontal sections of a rectangular channel section and the curves of equal velocity in the cross-section. The general patterns for velocity distribution in (a) a trapezoidal channel and (b) a natural irregular channel are also shown in Figure 4.61.

In addition to the shape of the section the velocity distribution in a channel section depends on the roughness of the channel and the existence of bends. In a broad, rapid and shallow stream or in a very smooth channel, the maximum velocity may often be found at the free surface. The roughness of the channel causes the curvature of the vertical velocity distribution curve to increase. In a bend the velocity increases greatly at the convex side owing to the centrifugal action of the flow.

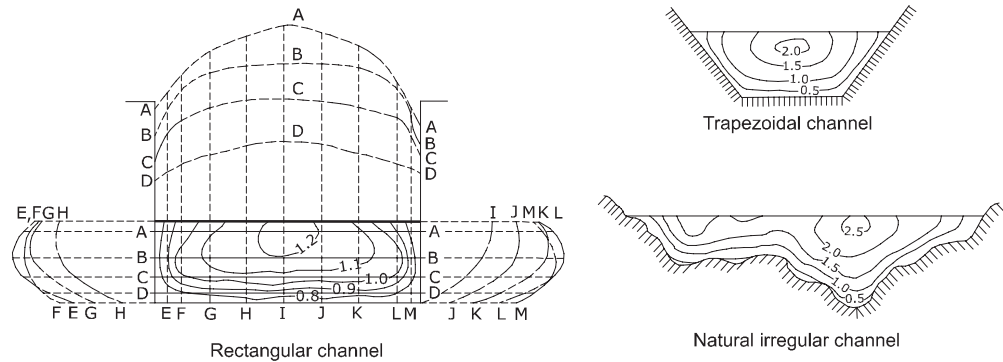


**Figure 4.61** Velocity distribution in a rectangular channel, a trapezoidal and a natural irregular channel (Chow, 1959)

#### Effect of wind

Wind can generate currents in inland waters that are generally limited and thus negligible for the design of rock structures. However, fetch can be significant and wind-generated waves should be taken into account for inland structures. Wind blowing in a sustained way over a large expanse of water such as a reservoir has the potential to generate currents that are strong enough to warrant appropriate assessment. Hedges (1990) suggested that under steady state conditions the current velocity can be taken as about 2–3 per cent of the wind speed. However, for the purpose of protection design it is generally accepted that these currents can be neglected. Further information is given in Section 4.2.

The influence of wind waves on the vertical distribution of velocity is shown in Figure 4.62.

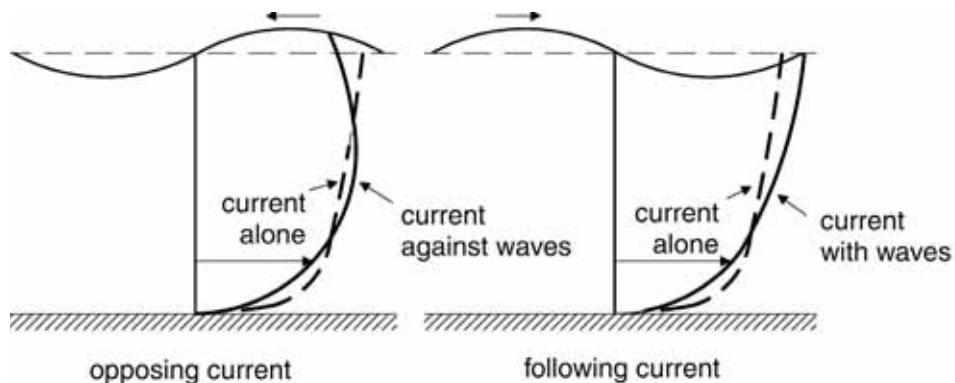


**Figure 4.62** Effect by waves on the velocity profile

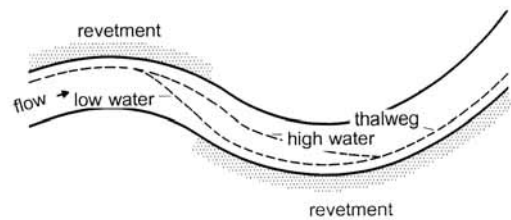


**Figure 4.64** Definition of the thalweg

The effect on the flow velocity patterns is greater for sharper bends. Usually, account is taken of the effect of bends on the flow characteristics and on the stability of the banks by means of the ratio of the centreline radius of the bend  $r$  and the water surface width  $B$ . When  $r/B \geq 26$ , channels are generally considered as straight for the design of erosion protection on banks and beds. Empirical coefficients, such as the velocity distribution coefficient that combine several flow parameters have been introduced in stability equations to account for the effect of bends (see Section 5.2.3.1).

In bends, the curvature of the flow results in a transverse water surface slope  $i_r$  (-), a secondary circulation develops and combines with the main flow into a **spiral flow** (see Figure 4.65). The radial gradient  $i_r$  can be determined with Equation 4.153:

$$i_r = \partial h / \partial r = \alpha U^2 / (gr) \quad (4.153)$$

where  $r$  = (centre) radius of the curved river section (m);  $U$  = depth averaged velocity (m/s) and  $\alpha$  = coefficient defined below (-).

The coefficient  $\alpha$  accounts for the vertical flow velocity distribution, from  $u = 0$  at the bed to  $u = u(h)$  at the water surface, and is about equal to  $\alpha = 1.05$ . The transverse water surface slope is largest near the inner bend because the radius of the inner bend is generally smaller than the radius of the outer bend.

The result of the curved flow is a higher water level in the outer bend than in the inner bend, because of the centrifugal force acting on the water in the upper part of the stream. The streamlines near the bed are directed towards the inner bend. Due to movement of sediment to the inner bend by these near-bed currents, the depth,  $h$  (m), in the outer bend is larger than that in the inner bend. Consequently, the resistance (ie a higher  $C$ -value) is less in the outer bend. As a result, the flow velocity,  $v$  (m/s), in the outer bend is higher than in the inner bend,  $v = C \sqrt{h i}$ .

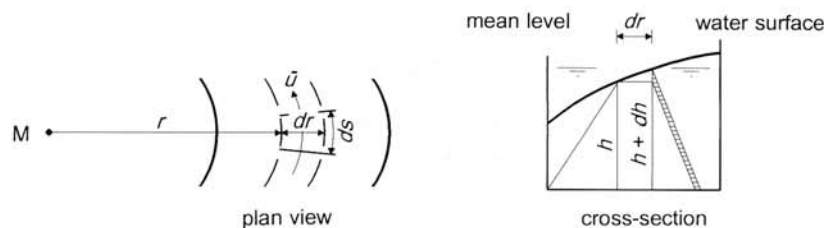


**Figure 4.65** Flow in a river bend

#### Flows affected by structures

Structures in the flow such as bridge piers, abutments, caissons, cofferdams, weirs, gated structures or training works, generate marked changes in:

- the shape of the vertical velocity profile
- the local magnitude of the flow velocity
- the water level
- the level of turbulence of the flow.

$$V_L = (gL_s/2\pi)^{1/2} \quad (4.169)$$

$$V_L = (gh)^{1/2} \quad (4.170)$$

The minimum value should be applied in further calculations.

### 3 Actual speed, $V_s$

The actual speed of the vessel,  $V_s$  (m/s), is evaluated as a factor of the limit speed  $V_L$  (see Equation 4.171):

$$V_s = f_v V_L \quad (4.171)$$

where  $f_v = 0.9$  for unloaded ships and  $f_v = 0.75$  for loaded ships.

For loaded push-tow units and conventional motor freighters the actual speed can also be determined from Equation 4.172.

$$V_s = 2.4 \sqrt{\frac{A_c}{b_w}} \exp\left(-2.9 \frac{A_m}{A_c}\right) \quad (4.172)$$

Note: Equation 4.172 is derived by implicitly assuming that ships sail with a speed of 0.9 times  $V_L$  ( $f_v = 0.9$ ).

### 4 Mean water level depression, $\Delta h$ and mean return flow, $U_r$

The mean water level depression,  $\Delta h$  (m), is calculated by Equation 4.173.

$$\Delta h = \frac{V_s^2}{2g} \left[ \alpha_s \left( A_c / A_c^* \right)^2 - 1 \right] \quad (4.173)$$

where:

$\alpha_s$  = factor to express the effect of the sailing speed  $V_s$  relative to its maximum (-),

$$\alpha_s = 1.4 - 0.4V_s/V_L$$

$A_c^*$  = cross-sectional area of the fairway next to the ship (m<sup>2</sup>),

$$A_c^* = b_b (h - \Delta h) + \cot\alpha (h - \Delta h)^2 - A_m$$

$A_c$  = cross-sectional area of the fairway in the undisturbed situation (m<sup>2</sup>),  $A_c = b_b h + h^2 \cot\alpha$

$\alpha$  = slope angle of the bank (-).

The mean return flow velocity,  $U_r$  (m/s), is calculated by Equation 4.174.

$$U_r = V_s \left( A_c / A_c^* - 1 \right) \quad (4.174)$$

### 5 Maximum water level depression, $\Delta \hat{h}$ and return flow, $\hat{U}_r$

The maximum water level depression,  $\Delta \hat{h}$  (m/s) can be calculated by Equation 4.175:

$$\Delta \hat{h} / \Delta h = \begin{cases} 1 + 2A_w^* & \text{for } b_w/L_s < 1.5 \\ 1 + 4A_w^* & \text{for } b_w/L_s \geq 1.5 \end{cases} \quad (4.175)$$

where  $A_w^* = y h / A_c$  (-).

For ratios of  $A_c/A_m$  smaller than about 5 (ie comparable with  $b_w/B_s < 10$ ) the flow field induced by sailing ships might be considered as one-dimensional. For these situations Equation 4.176 is applicable.

$$\hat{U}_r / U_r = \begin{cases} 1 + A_w^* & \text{for } b_w/L_s < 1.5 \\ 1 + 3A_w^* & \text{for } b_w/L_s \geq 1.5 \end{cases} \quad (4.176)$$

For larger ratios, ie  $A_c/A_m > 5$  or  $b_w/B_s > 10$ , the flow field is two-dimensional. Then, the gradient in the return current and the water level depression between the ship and the bank should be taken into account. In the computer program DIPRO these formulae are incorporated.

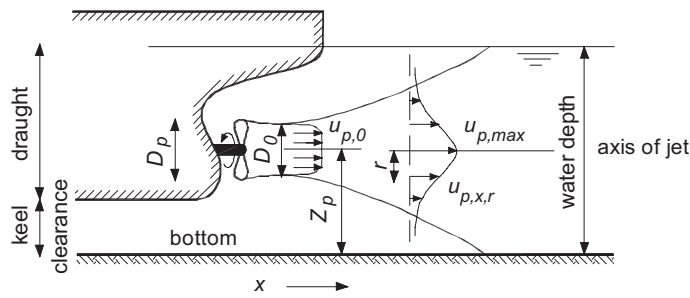


**Figure 4.86** Water movements due to a main propeller

Equations 4.187 to 4.190 can be used to estimate the time-averaged current velocities in propeller jets caused by main propellers (see Figure 4.86, for ship speed  $V_s = 0$  or otherwise relative to the ship when underway) or caused by bow or stern thrusters.

Velocity behind propeller (see Equation 4.187):

$$u_{p,0} = 1.15 \left( P / \rho_w D_0^2 \right)^{1/3} \quad (4.187)$$

Velocity along jet axis (see Equation 4.188):

$$u_{p,axis}(x) = a u_{p,0} (D_0/x)^m \quad (4.188)$$

Velocity distribution (see Equation 4.189):

$$u_p(x,r) = u_{p,axis}(x) \cdot \exp \left[ -br^2/x^2 \right] \quad (4.189)$$

Maximum bed velocity along horizontal bed (see Equation 4.190):

$$u_{p,maxbed} = c u_{p,0} (D_0/z_p)^n \quad (4.190)$$

where  $P$  = applied power (W),  $D_0$  = effective diameter of propeller,  $D_0 = 0.7$  (for free propellers without nozzle) to 1 (for propellers and thrusters in a nozzle) times the real diameter  $D_p$  (m),  $z_p$  = distance between the propeller axis and the bed (m).

A wide range of values for the empirical coefficients  $a$ ,  $b$ ,  $c$ ,  $m$  and  $n$  in Equations 4.188 to 4.190 is available because different researchers have taken into account different influences such as the influence of a quay wall and the influence of a rudder. In addition to the approach presented below, reference is made to Fuehrer *et al* (1987), Römish (1993) and EAU (1996, 2004) where alternative values are presented. For more information, reference is also made to a special publication of the PIANC Working Group 48 (PIANC, in preparation).

In the Netherlands these coefficients are generally used for design, neglecting the influence of rudders and confinements with the following values:  $m = n = 1$ ,  $a = 2.8$  and  $b = 15.4$ , which results in  $c = 0.3$  (Blaauw and Van der Kaa, 1978). In this approach the influence of lateral confinement by a quay wall in some cases is taken into account by increasing the velocity according to Equation 4.190 by 10–40 per cent. Blokland and Smedes (1996) measured a 40 per cent higher bottom velocity in the case of a jet that displays an angle of  $16^\circ$  with the quay wall.

In the case of a propeller jet perpendicular or oblique against a sloping embankment, the velocities above the embankment can be estimated using Equation 4.189. In fact, the velocities in the jet are influenced by the presence of the embankment. In PIANC (1997) this influence is neglected for practical purposes. Hamill *et al* (1996) found that the velocities above the embankment are delayed.

**Table 5.4** Critical overtopping discharges and volumes (Allsop et al, 2005)

	$q$ mean overtopping discharge (m <sup>3</sup> /s per m length)	$V_{max}$ peak overtopping volume (m <sup>3</sup> /per m length)
<b>Pedestrians</b>		
Unsafe for unaware pedestrians, no clear view of the sea, relatively easily upset or frightened, narrow walkway or proximity to edge	$q > 3 \cdot 10^{-5}$	$V_{max} > 2 \cdot 10^{-3} - 5 \cdot 10^{-3}$
Unsafe for aware pedestrians, clear view of the sea, not easily upset or frightened, able to tolerate getting wet, wider walkway	$q > 1 \cdot 10^{-4}$	$V_{max} > 0.02 - 0.05$
Unsafe for trained staff, well shod and protected, expected to get wet, overtopping flows at lower levels only, no falling jet, low danger of fall from walkway	$q > 1 \cdot 10^{-3} - 0.01$	$V_{max} > 0.5$
<b>Vehicles</b>		
Unsafe for driving at moderate or high speed, impulsive overtopping giving falling or high velocity jets	$q > 1 \cdot 10^{-5} - 5 \cdot 10^{-5}$	$V_{max} > 5 \cdot 10^{-3}$
Unsafe for driving at low speed, overtopping by pulsating flows at low levels only, no falling jets	$q > 0.01 - 0.05$	$V_{max} > 0.1$
<b>Marinas</b>		
Sinking of small boats set 5–10 m from wall, damage to larger yachts	$q > 0.01$	$V_{max} > 1 - 10$
Significant damage or sinking of larger yachts	$q > 0.05$	$V_{max} > 5 - 50$
<b>Buildings</b>		
No damage	$q < 1 \cdot 10^{-6}$	
Minor damage to fittings etc	$1 \cdot 10^{-6} < q < 3 \cdot 10^{-5}$	
Structural damage	$q > 3 \cdot 10^{-5}$	
<b>Embankment seawalls</b>		
No damage	$q < 2 \cdot 10^{-3}$	
Damage if crest not protected	$2 \cdot 10^{-3} < q < 0.02$	
Damage if back slope not protected	$0.02 < q < 0.05$	
Damage even if fully protected	$q > 0.05$	
<b>Revetment seawalls</b>		
No damage	$q < 0.05$	
Damage if promenade not paved	$0.05 < q < 0.2$	
Damage even if promenade paved	$q > 0.2$	

1

2

3

4

5

6

7

8

9

10

The **second criterion** is based on the Froude number,  $Fr$  (-). It has a clear physical background and distinguishes whether the flow on the crest is physically governed by upstream ( $Fr > 1$ ) or downstream ( $Fr < 1$ ) boundary conditions. Equation 5.80 gives the Froude number as it is generally defined.

$$Fr = U / \sqrt{gh} \quad (5.80)$$

Using local values for velocity,  $u$  (m/s), and depth,  $h$  (m), the Froude number will show stream wise variations. The actual value of  $Fr$ , or the flow velocity  $u$ , over the crest, decides whether the flow is **subcritical** ( $Fr < 1$ ) or **supercritical** ( $Fr > 1$ ). For  $Fr = 1$  the flow is critical (according to a less strict terminology “critical” is used for  $Fr \geq 1$ ).

Application of the  $Fr$ -criterion however, requires that the value of  $u$  is known beforehand, which results in an iterative procedure. Therefore a less accurate but more practical alternative is to compare the tailwater depth,  $h_b$  (m), with the critical water depth at the crest (both measured relative to the crest level). This critical depth,  $h_{cr}$  (m), can, except for high upstream flow velocities, be approximated with Equation 5.81:

$$h_{cr} = 2/3H \quad (5.81)$$

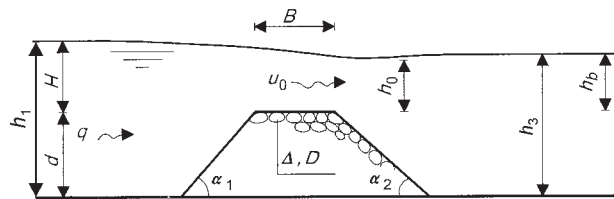
where  $H$  is the upstream water level (m), also measured from the crest level.

The criterion then can be expressed using Equations 5.82 and 5.83 (each using two equivalent formulations):

$$\text{subcritical:} \quad \text{for } h_b > 2/3 H \quad \text{or} \quad H - h_b < 0.5h_b \quad (5.82)$$

$$\text{supercritical:} \quad \text{for } h_b < 2/3 H \quad \text{or} \quad H - h_b > 0.5h_b \quad (5.83)$$

During vertical construction of the dam the crest level is gradually built up and at a certain stage, depending on the up- and downstream water levels, the flow regime might change from a subcritical to supercritical regime. Alternative terminology found in literature for sub- and supercritical flow are *sub-modular*, *submerged* or *drowned flow* and *modular* or *free flow* respectively.



Note:  $D$  should read  $D_{n50}$  in this figure

**Figure 5.21** Definition sketch for vertical closures

The use of the  $Fr$ -criterion becomes particularly important when discharge, velocity or shear concepts are used as design parameters for the armourstone (see Section 5.2.1). Therefore the discharge and/or velocities across the dam have to be determined first.

The **third criterion** to define the type of flow distinguishes between **broad-crested** dams and **short-crested** dams:

Usually, a broad-crested dam is defined by  $H/B < 0.5$ , while for a short-crested dam  $H/B > 0.5$ . Physically the difference should be interpreted as whether bed shear on the crest can be neglected – as is the case for short-crested dams – or not.

- The principles of the **shear concept** are discussed in Section 5.2.1.3, based on the well-known Shields shear-type stability parameter introduced in Section 5.2.1.2. Some specific applications (eg Pilarczyk's formula) are discussed in Section 5.2.3. The method of critical shear is also applicable to oscillatory flow (waves only), as well as to a combination of currents and waves (see Section 5.2.1.3).
- The **critical or permissible velocity method** is discussed in Section 5.2.1.4, based on the well-known Izbash velocity-type stability parameter introduced in Section 5.2.1.2. Some specific applications are shown in Section 5.2.3.
- The use of the  $H/(\Delta D)$  **wave stability criterion** is introduced in Section 5.2.1.5 and discussed for different applications in Section 5.2.2.
- The use of the  $H/(\Delta D)$  parameter to define a stability criterion in terms of a **head difference or height of overtopping** across dams is introduced in Section 5.2.1.6 and discussed in Section 5.2.3.
- In Section 5.2.1.7 the **critical discharge method** is introduced.

The relationships used to transfer some stability parameters into others are described in Section 5.2.1.8. Finally, Section 5.2.1.9 gives an overview of the general design formulae.

### 5.2.1.2 Governing parameters to evaluate stability

Some of the parameters used to evaluate the hydraulic stability of rock structures consist of combinations of hydraulic (loading) parameters and material (resistance) parameters. The parameters that are relevant for the structural stability, can be divided into four categories, discussed below:

- wave and current attack
- characterisation of armourstone
- cross-section of the structure
- response of the structure.

#### Wave attack

In the case of wave attack on a sloping structure the most important parameter, which gives a relationship (see Equation 5.95) between the structure and the wave conditions, is the **stability number**,  $N_s$  (-):

$$N_s = \frac{H}{\Delta D} \quad (5.95)$$

where:

- $H$  = wave height (m). This is usually the significant wave height,  $H_s$ , either defined by the average of the highest one third of the waves in a record,  $H_{1/3}$ , or by  $4\sqrt{m_0}$ , the spectral significant wave height  $H_{m0}$  (see Section 4.2.4). For deep water both definitions give more or less the same wave height. For shallow-water conditions there may be substantial differences up to  $H_{1/3} = 1.3 H_{m0}$  (see Section 4.2.4)
- $\Delta$  = relative buoyant density (-), described by Equation 5.96 (see also Section 3.3.3.2)
- $D$  = characteristic size or diameter (m), depending on the type of structure (see Section 5.2.2.1). The diameter used for armourstone is the median nominal diameter,  $D_{n50}$  (m), defined as the median equivalent cube size (see Section 3.4.2). For concrete armour units the diameter used is  $D_n$  (m), which depends on the block shape (see Section 3.12).

$V$	=	volume of the (concrete) armour unit (m <sup>3</sup> )
$D_n$	=	nominal diameter of the armour unit (m), $D_n = (k_s)^{1/3}D$ , where $k_s$ is shape coefficient and $D$ is characteristic dimension of the concrete armour unit, ie block height (see Section 3.12 for data).

The permeability of the structure is not defined in the standard way, as using Darcy's law (see Section 5.4.4.4), but is rather given as a notional index that represents the global permeability of the structure, or as a ratio of stone sizes. It is an important parameter with respect to the stability of armour layers under wave attack. The permeability depends on the size of the filter layers and core and can for example be given by a *notional permeability* factor,  $P$ . Examples of  $P$  are shown in Figure 5.39 in Section 5.2.2.2, based on the work of Van der Meer (1988b). A simpler approach to account for the influence of the permeability on the stability of rock-armoured slopes under wave or current attack uses the ratio of diameters of core material and armour material.

A practical measure for the permeability of dams (referring to the structure rather than the materials) under current attack is the ratio between armourstone size,  $D_{n50}$  (m), and dam height,  $d$  (m). This ratio,  $D_{n50}/d$  (-), sometimes also called "dam porosity", may be interpreted as a measure for the voids in the rockfill.

The **packing density** is a parameter directly related to the placement pattern of the armour layer. It is a term mainly applied to blocks in armour layers; the influence of the placement pattern on the stability of the structure is discussed in Section 5.2.2.3. Equation 5.99 gives the expression for the estimate of the number of armour units per unit area,  $N$  (1/m<sup>2</sup>), as used in Sections 3.5.1 and 3.12.

$$N = \frac{t_a(1-n_v)}{V} = \frac{nk_t(1-n_v)}{D_{n50}^2} \quad (5.99)$$

where:

$N$	=	$N_a/A$ (1/m <sup>2</sup> ), where $N_a$ is the number of armour units in the area concerned (-); $A$ is the surface area of the armour layer parallel to the local slope (m <sup>2</sup> ); $N$ is sometimes called <i>packing density</i>
$t_a$	=	armour layer thickness (m), defined by $t_a = nk_t D_{n50}$ (see also Section 3.5)
$V$	=	armour unit volume (m <sup>3</sup> ).

**NOTE:** The packing density of concrete armour layers is the same as defined above in Equation 5.99, but then with  $D_n$  instead of  $D_{n50}$ . The packing density is then  $N = \phi/D_n^2$ , where  $\phi$  is the **packing density coefficient** (-), see also Section 3.12.

The term *packing density* is rather widely used in literature, denoted as  $\phi$ , when actually the packing density coefficient, defined in Equation 5.99, is meant.

#### Parameters related to the response of the structure

The behaviour of the structure can be described by a number of parameters, depending on the type of structure. **Statically stable structures** are described by the number of displaced units or by the development of damage, ie differences in the cross-section before and after storms.

The damage to the rock armour layer can be given as a percentage of displaced stones related to a certain area, eg the entire layer or part of it. The **damage percentage**,  $D$  (%), has originally been defined in the *Shore protection manual* (CERC, 1984) as:

**The normalised eroded volume in the active zone, from the middle of the crest down to  $1H_s$  below still water level (SWL).**

The damage percentage (or relative displacement within an area),  $N_d$ , is determined by Equation 5.102, relating the number of displaced units to the total number of units initially in the armour layer.

$$N_d = \frac{\text{number of units displaced out of armour layer}}{\text{total number of units within reference area}} \quad (5.102)$$

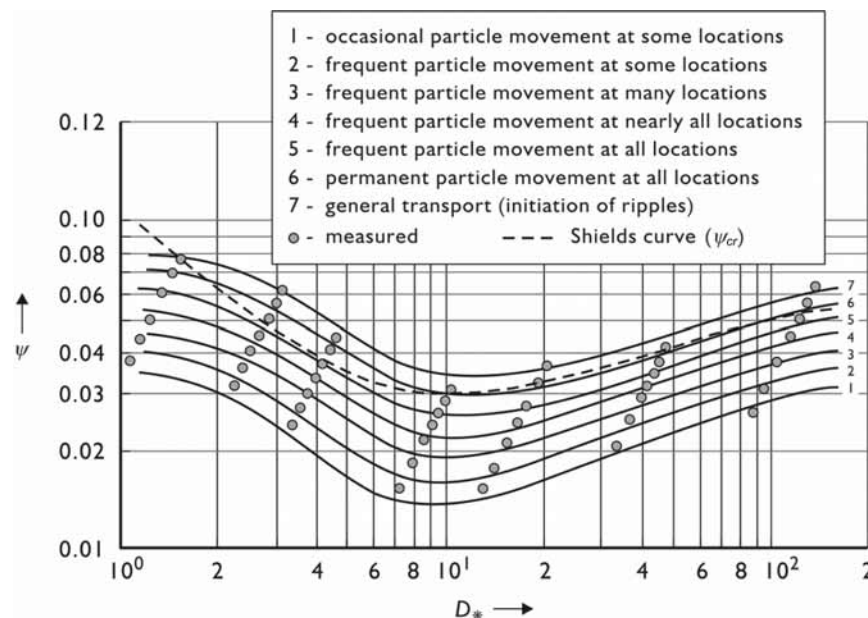
The reference area has to be defined, either as the complete armour area, or as the area between two levels, eg from the crest down to  $1H_s$  below SWL (m), over a certain width (m). For design purposes, both the damage percentage and the number of displaced units for different types of armour units are further discussed in Section 5.2.2.3.

**Dynamically stable structures** allow for a certain initial movement of armour stones until the transport capacity along the profile is reduced to such a low level that an almost stable profile is reached. Dynamically stable structures are characterised by a design profile, to be reached after a certain adaptation period, rather than by the as-built geometry. This type of structure is described in Section 5.2.2.6.

### 5.2.1.3 Critical shear concept

The traditional design method for the hydraulic stability of rockfill is based on the *incipient motion* or *critical shear* concept. For unidirectional steady flow the initial instability of bed material particles on a horizontal, plane bed is described by the Shields criterion (Shields, 1936), based on the general Shields parameter as defined in Equation 5.97.

This criterion essentially expresses the critical value of the ratio of the de-stabilising fluid forces (that tend to move the particle) to the stabilising forces acting on a particle. The forces that tend to move the bed material particle are related to the maximum shear stress exerted on the bed by the moving fluid; the stabilising forces are related to the submerged weight of the particle. When the ratio of the two forces, represented by the Shields parameter,  $\psi$ , exceeds a critical value,  $\psi_{cr}$ , movement is initiated. The Shields criterion for steady uniform flow is expressed in the Equations 5.103 and 5.104. The Shields curve is given in Figure 5.32.



#### Notes

- 1  $\psi$  is the Shields parameter defined in Equation 5.97.
- 2  $D_*$  is the non-dimensional sediment grain or stone diameter, defined in Equation 5.106.

**Figure 5.32** The modified Shields diagram for steady flow

**Table 5.20** Velocity correction factors,  $K_1$ , for water depths ( $h \neq 1$  m) in the range of  $h = 0.3$ – $3$  m

Depth, $h$ (m)	0.3	0.6	1.0	1.5	2.0	2.5	3.0
$K_1$ (-)	0.8	0.9	1.0	1.1	1.15	1.20	1.25

Particularly for structures of limited length in the flow direction such as dams and sills, the vertical velocity profile is not fully developed (as was assumed in Section 4.3.2.4). Thus shear methods can be considered as a means to – but are in fact one step ahead of – the use of velocity correction factors. Use of local velocities by including a velocity factor is discussed in Section 5.2.1.8 and Section 5.2.3.

An example of a velocity-type stability criterion is given in Box 5.10.

**Box 5.10** Velocity-type stability criterion for stones on a sill

A well-known example of a velocity-type stability criterion was presented by Izbash and Khaldre (1970). Their empirically-derived formulae for exposed and embedded stones **on a sill** are given as Equations 5.120 and 5.121 respectively.

**NOTE:** Izbash and Khaldre (1970) defined  $u_b$  as the critical velocity for stone movement (m/s), which can be interpreted as the velocity near the stones and not as the depth-averaged flow velocity,  $U$  (m/s).

$$\text{Exposed stones:} \quad \frac{u_b^2/2g}{\Delta D_{50}} = 0.7 \quad (5.120)$$

$$\text{Embedded stones:} \quad \frac{u_b^2/2g}{\Delta D_{50}} = 1.4 \quad (5.121)$$

where  $D_{50}$  is the median sieve size (m).

**Range of validity:** Equations 5.120 and 5.121 as developed by Izbash and Khaldre (1970) are valid for relative water depths,  $h/D$ , in the range of  $h/D = 5$  to  $10$ .

Another (quasi-) velocity method implies an assumption of a critical shear stress,  $\psi_{cr}$ , and then a transfer of this critical shear stress into a critical velocity. The method is based on logarithmic fully-developed velocity profiles (Section 4.3.2.4) and is discussed in Section 5.2.1.8.

In the complicated case of a non-fully developed velocity profile, the local maximum near-bed velocity has to be measured (or otherwise estimated by assuming a reasonable velocity profile, Section 4.3.2.4). This velocity is then substituted into Equations 5.104 and 5.123.

**Application of correction factors**

All correction factors introduced in this section and in Section 5.2.1.3, except for  $k_t$ , originally refer to shear stresses,  $\tau$  or  $\psi$ . The turbulence factor,  $k_t$ , refers to velocities,  $U$ .

The **resistance** of a bed is represented by shear stress,  $\tau_{cr}$  or  $\psi_{cr}$ , or velocity,  $U_{cr}$ , while the **actual loading** is expressed as  $\tau$  or  $\psi$  (shear stress) or  $U$  (velocity).

The general relationship between shear stress and velocity can be written as:  $U \propto \sqrt{\tau}$  or as:  $\tau \propto U^2$ . Therefore, in some stability formulae (see Section 5.2.3.1), the  $k$ -factors appear in principle in the combinations  $k\tau$ ,  $k\psi$  or  $\sqrt{kU}$ , except for  $k_t$ , which appears as  $k_t^2\tau$ ,  $k_t^2\psi$  or  $k_tU$ .

**NOTE:** With regard to the remaining hydraulic parameters that may be applied in a stability analysis ( $H$  and  $q$ , described at the beginning of this Section 5.2.1), it should be noted that  $H \propto U^2$  and  $q \propto U$ . Consequently, correction factors,  $k$ , should be applied accordingly: for the resistance (slope) reduction factors, eg  $k_{sl}$ , applied to any hydraulic design parameter, for example  $\tau_{cr}$  or  $U_{cr}^2$ , generally  $k_{sl} \leq 1$ , whereas for the load amplification factors ( $k_w$ ,  $k_t$ ),  $k \geq 1$ .

### 5.2.2.1 Structure classification

Coastal structures exposed to direct wave attack can be classified by means of the stability number,  $N_s = H/(\Delta D)$  (see Section 5.2.1.2). Small values of  $N_s$  represent structures with large armour units and large values of  $N_s$  represent for example dynamic slopes consisting of coarse armourstone, both exposed to the same wave height.

With respect to static and dynamic stability the structures can be classified as statically stable structures and dynamically stable (reshaping) structures:

**Statically stable structures** are structures where no or minor damage to the armour layer is allowed under design conditions. Damage to the armour layer is defined as displacement of the armour units. The mass of individual units must be large enough to withstand the wave forces during design conditions. Traditionally designed breakwaters belong to the group of statically stable structures. Statically stable structures have stability numbers  $N_s$  in the range of 1 to 4.

**Dynamically stable (reshaping) structures** are structures that are allowed to be reshaped by wave attack, resulting in a development of their profile. Individual pieces (stones or gravel) are displaced by wave action until the transport capacity along the profile is reduced to such a low level that an almost static profile is reached. Even if material around the still water level is continuously moving during each run-up and run-down of the waves, the net transport capacity may be zero as the profile has reached its equilibrium. The dynamic stability of a structure is characterised by a design profile. Dynamically stable structures have stability numbers  $N_s$  greater than 6. For these structures, which cover a wide range of  $H_s/(\Delta D_{n50})$  – values, the dynamic profile can be described using a parameter that combines the effects of both wave height and wave period. This parameter, defined in Equation 5.132, is the dynamic stability number,  $HoTo$ , with  $Ho$  being an alternative notation of the (static) stability number  $N_s = H_s/(\Delta D_{n50})$  and  $To$  being the wave period factor:  $T_m \sqrt{(g/D_{n50})}$  (-).

$$HoTo = N_s \cdot T_m \sqrt{(g/D_{n50})} \quad (5.132)$$

where  $T_m$  is the mean wave period (s).

The relationship between  $H_s/(\Delta D_{n50})$  and the dynamic stability number  $HoTo$  (sometimes “ $N_{sd}$ ” is used as notation) is listed in Table 5.21.

**Table 5.21** Relationship between static and dynamic stability number

Structure type	$N_s = H_s/(\Delta D_{n50})$	$HoTo$
Statically stable breakwaters	1-4	< 100
Dynamically stable reshaping structures	3-6	100-200
Dynamic rock slopes	6-20	200-1500
Gravel beaches	15-500	1000-200 000

**Note**

Gravel beaches are not discussed in this manual, but the data are given here for information.

This manual focuses on rock-armoured breakwaters and slopes, and berm-type breakwaters, with stability numbers in the range of  $N_s = 1$  to 20. For a final stability analysis to distinguish, for example, the static and dynamic stability, explicit definitions of (acceptable) movement have to be made.

A classification of these structures based on the value of the stability parameter is proposed below.

- $N_s = H/(\Delta D) < 1$ : **Caissons or seawalls**

No damage is allowed for these fixed structures. The characteristic size,  $D$ , can be the height or width of the structure.

- $N_s = H/(\Delta D) = 1$  to 4: **Statically stable breakwaters**

Generally uniform slopes are covered with heavy concrete armour units or natural armour stones. Only limited damage (ie stone displacement) is allowed under severe design conditions. The size,  $D$ , is a characteristic diameter of the unit or the median nominal diameter of stones  $D_{n50}$  (m). A special type of statically stable breakwater is the Icelandic berm breakwater, with typical values of the stability number of:  $H_s/(\Delta D_{n50}) = 2$  to 2.5 (see Section 5.2.2.6).

- $N_s = H/(\Delta D) = 3$  to 6: **Dynamically stable reshaping structures**

These structures are characterised by steeper slopes above and below the still water level and a gentler slope in between. This gently sloping part reduces the wave forces on the armour units. Reshaping structures are often designed with a very steep seaward slope and a horizontal berm just above the (design) still water level. The first storms develop a more gentle profile which remains stable at later stages. The profile changes to be expected are important. Oblique waves may cause incipient longshore transport.

- $N_s = H/(\Delta D) = 6$  to 20: **Dynamic rock slopes and beaches**

The diameter of the armour stones is relatively small and cannot withstand severe wave attack without displacement. The design parameter is the profile that is being developed under different wave boundary conditions. Oblique waves may cause longshore transport.

An overview of the types of structures described above together with the different values of  $H/(\Delta D)$  is given in Figure 5.36. A summary of the static and dynamic stability numbers for these structures was given in Table 5.21.

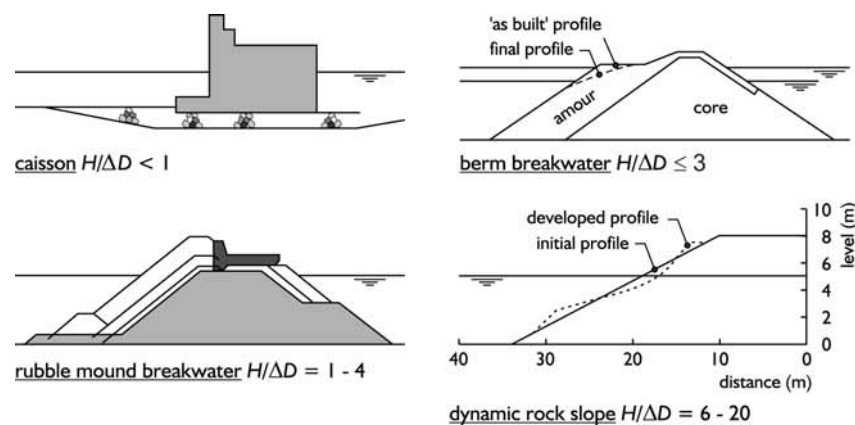


**Figure 5.36** Type of structure as a function of  $H/(\Delta D)$

This manual focuses on the latter three types of structures presented in Figure 5.36: statically stable breakwaters and slopes, dynamic/reshaping breakwaters, and dynamic rock slopes. Of the caisson breakwaters, only the armourstone foundations are considered.

**NOTE:** The given conversion factors to transform  $H_s$  to  $H_{2\%}$  and to transform  $T_m$  to  $T_{m-1,0}$  (see notes to Figure 5.42) are only valid for deep water and standard wave energy spectra. When applying Equations 5.139 and 5.140, the locally determined values of  $H_{2\%}$  and  $T_{m-1,0}$  should be used; a numerical wave propagation model, like SWAN or Boussinesq-type wave models (see Section 4.2.4.10) may be used for this purpose.

Table 5.26 shows the range of validity of the various parameters used in Equations 5.139 and 5.140.

**Table 5.26** Range of validity of parameters in Van der Meer formulae for shallow water conditions

Parameter	Symbol	Range
Slope angle	$\tan \alpha$	1:4–1:2
Number of waves	$N$	< 3000
Fictitious wave steepness based on $T_m$	$s_{om}$	0.01–0.06
Surf similarity parameter using $T_m$	$\xi_m$	1–5
Surf similarity parameter using $T_{m-1,0}$	$\xi_{s-1,0}$	1.3–6.5
Wave height ratio	$H_{2\%}/H_s$	1.2–1.4
Deep-water wave height over water depth at toe	$H_{so}/h$	0.25–1.5
Armourstone gradation	$D_{n85}/D_{n15}$	1.4–2.0
Core material – armour ratio	$D_{n50-core}/D_{n50}$	0–0.3
Stability number	$H_s/(\Delta D_{n50})$	0.5–4.5
Damage level parameter	$S_d$	< 30

**Note**

For further details on the field of application in terms of water depths, see overview in Tables 5.28 and 5.29.

To illustrate the use of the Van der Meer formulae for shallow water, an example is worked out in Box 5.15. To show the typical differences between deep- and shallow-water conditions the example situation as given in Box 5.13 has been taken as starting point.

**Box 5.15** Design methodology for Van der Meer formulae for very shallow water conditions

To design armourstone for the example situation as given in Box 5.13, but now in water of limited depth, the procedure is as follows:

- define design wave conditions at the toe of the structure; with a numerical wave propagation model the value(s) of  $T_{m-1,0}$  and with the Battjes and Groenendijk method (see Section 4.2.4.4) the values of  $H_{2\%}$  at the toe of the structure are determined based on the deep water design condition(s).
- follow in general the procedure as described in Box 5.13, but read Equation 5.139 for 5.136 and Equation 5.140 for 5.137; further, the surf similarity parameter,  $\xi_{s-1,0}$ , is to be used instead of  $\xi_m$ .

**Example**

The water depth at the toe of the structure is given as:  $h = 8$  m. Using a spectral wave propagation model (in this case starting with the deep water values  $H_{so} = 5$  m and  $T_m = 10$  s from the example in Box 5.13) with given bathymetry, this may lead to the following nearshore data:  $H_s = 4$  m;  $T_m = 9.5$  s and  $T_{m-1,0} = 11.5$  s. This gives:  $\xi_{s-1,0} = 2.39$ . The method of Battjes and Groenendijk leads to a value of  $H_{2\%} = 4.95$  m. The values of the other parameters are:  $P = 0.4$ ,  $\tan \alpha = 0.33$ ,  $\Delta = 1.6$  and  $S_d = 2$ .

Application of the deep-water formula (Equation 5.136), using  $T_m$ , will lead in this situation (a 6 h storm, ie  $N = 6 \times 3600/9.5 = 2273$ ) to:  $D_{n50} = 1.27$  m and  $M_{50} = 5.4$  tonnes.

Using the shallow water formula (Equation 5.139), with again  $N = 6 \times 3600/9.5 = 2273$ , leads to:  $H_s/(\Delta D_{n50}) = 1.7$ , which results in a armourstone size of:  $D_{n50} = 1.4$  m and a median mass of:  $M_{50} = 7.2$  tonnes.

**Conclusion:** The stability of rock-armoured slopes in very shallow water conditions requires special attention; in this example the minimum mass of the armourstone is 30 per cent larger than expected based on the deep-water formula.

**NOTE:** In this example the computed values of  $H_s = 4$  m and  $T_{m-1,0} = 11.5$  s are rather extreme values. For most coastal profiles a numerical computation of the wave conditions at  $h = 8$  m will lead to somewhat lower values.

- **Single layer cubes**

The application of cubes in a single layer has been the subject of research by d'Angremond *et al* (1999), Van Gent *et al* (2000 and 2002). The results thereof suggest that there may be some advantages compared with double layer armouring for some cases. The hydraulic **stability as found in model tests** can be described by the Equations 5.161 and 5.162 for *start of damage* and *failure*, respectively.

$$\frac{H_s}{\Delta D_n} = 2.9 - 3.0 \quad \text{start of damage, } N_{od} = 0 \quad (5.161)$$

$$\frac{H_s}{\Delta D_n} = 3.5 - 3.75 \quad \text{failure, } N_{od} = 0.2 \quad (5.162)$$

Design experience with single layer cubes is very limited. It is recommended by Van Gent *et al* (2000 and 2002) to use a packing density corresponding to a porosity  $n_v = 0.25-0.3$  and to place one side of the cube flat on the underlayer. Acceptable damage levels for cubes in a single layer are significantly less than for double layers:  $N_{od} = 2$  for double-layer cubes corresponds to about  $N_{od} = 0.2$  for single-layer cubes. This is because the difference between *start of damage* and *failure* is very small. Moreover, as there is no reserve in the form of a second layer, damage to the armour layer will immediately result in exposure of the underlayer to direct wave attack. **It is therefore recommended to use a safety factor on Equations 5.161 and 5.162** (as for other single-layer armour units), which leads to values for the stability number of single-layer cubes to be used for preliminary design that are close to those for double layer cubes (see Table 5.35).

**NOTE:** The use of **single-layer cubes on the crest requires special attention**, as stability seems to be poor when using the same size as on the front slope. At the time of writing this manual this subject was not yet resolved to such a sufficient level that any design guidance could be included here.

Figure 5.47 illustrates the hydraulic stability as found in model tests, expressed by the stability number  $H_s/(\Delta D_n)$ , for three concrete armour units by presenting the *start of damage* and *failure* limits (for cubes,  $N_{od} = 0.5$  and  $2.0$ ; tetrapods,  $N_{od} = 0.5$  and  $1.5$  and Accropodes,  $N_{od} = 0$  and  $0.5$ , respectively – see Table 5.33) against the fictitious wave steepness,  $s_{om}$  (-), for a storm duration of  $N = 1000$  waves.

**NOTE:** This graph presented in Figure 5.47, is not a design graph; values of the stability number with a safety factor for the single-layer units that are suggested for use in preliminary design, are given in Table 5.35.

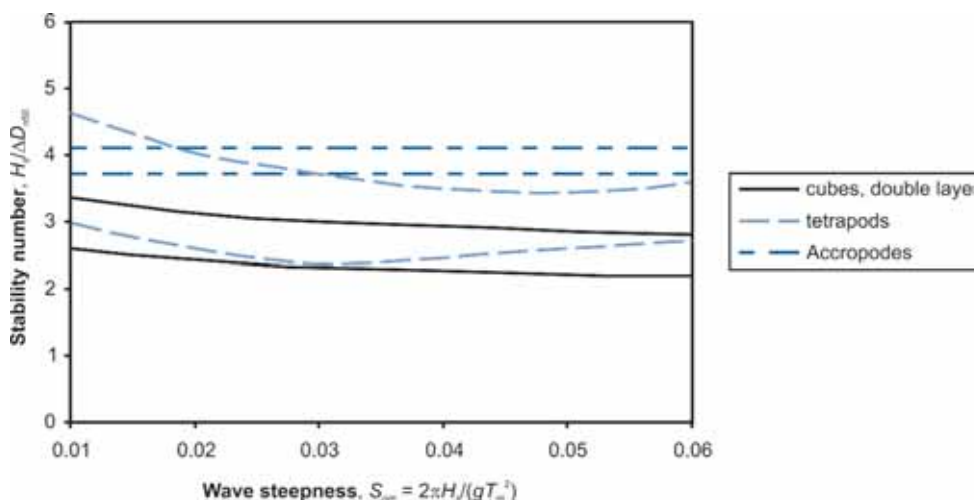


**Figure 5.47** Stability number versus fictitious wave steepness based on results of model tests for start of damage and failure limits ( $N = 1000$  waves; side slope 1:1.5)

The stability of the armourstone on the front slope of a low-crested emergent structure can be related to the stability of a non-overtopped structure. This can be achieved by first calculating the required nominal diameter of the armour unit with one of the design formulae presented in Section 5.2.2.2 for rock armour layers and then applying a reduction factor on this nominal diameter,  $D_{n50}$ . It is, however, advised to take great care when reducing the armour size of a low-crested breakwater.

This approach has been adopted by Van der Meer (1990a). He suggested that the armourstone cover layer stability formulae (Van der Meer, 1988b) (see Section 5.2.2.2) can be used with  $D_{n50}$  replaced by  $r_D D_{n50}$ . The reduction factor,  $r_D$  (-), on the stone size required, is given as Equation 5.164:

$$r_D = \left( 1.25 - 4.8 \frac{R_c}{H_s} \sqrt{\frac{s_{op}}{2\pi}} \right)^{-1} \quad (5.164)$$

where  $R_c$  is the crest freeboard (m), and  $s_{op}$  the fictitious wave steepness (-), based on the peak wave period,  $T_p$  (s).

**NOTE:** The factor  $R_c/H_s \cdot \sqrt{(s_{op}/2\pi)}$  is equal to Owen's dimensionless freeboard,  $R^*$  (see Section 5.1.1.3, Equation 5.28).

Design curves are given in Box 5.20. The limits of Equation 5.164 are given by Equation 5.165 as:

$$0 < \frac{R_c}{H_s} \sqrt{\frac{s_{op}}{2\pi}} < 0.052 \quad (5.165)$$

**NOTE:** Equation 5.164 gives an estimate for the required stone diameter on the front slope. For the crest and the rear side a similar size of material or larger material may be required.

#### Rule of thumb for emergent structures

As a rule of thumb Equation 5.166 can be used to obtain a first estimate of the stone size,  $D_{n50}$  (m), in a conceptual design phase for **emergent structures** (Kramer and Burcharth, 2004) in **depth-limited wave conditions**, ie with breaking waves on the foreshore.

$$D_{n50} \geq 0.3h \quad \text{for } \frac{H_s}{h} = 0.6, \cot\alpha_s \geq 100 \text{ and } \Delta \cong 1.6 \quad (5.166)$$

where  $H_s$  is the significant wave height at the toe of the structure (m);  $h$  is the water depth at the toe of the structure (m);  $\alpha_s$  is the slope angle of the foreshore ( $^\circ$ ).

**NOTE:** Other values for  $H_s/h$ ,  $\cot\alpha_s$  and  $\Delta$  might lead to very different values for the stone size required.

### Berm breakwater profile model derived by Hall and Kao (1991)

Hall and Kao (1991) have presented guidelines for the design of berm breakwaters based on the results of an extensive series of model tests at Queen's University, Canada. The guidelines are specific to a particular initial profile shown in Figure 5.63, but are considered to be useful as the profile is a widely adopted one, matching both typical quarry yields from dedicated quarries and natural side slopes. A clear exception is the upper slope: nowadays this is typically 1:1.5 to 1:2. The results are valid in the range:  $2 < H_s/(\Delta D_{n50}) < 5$ .

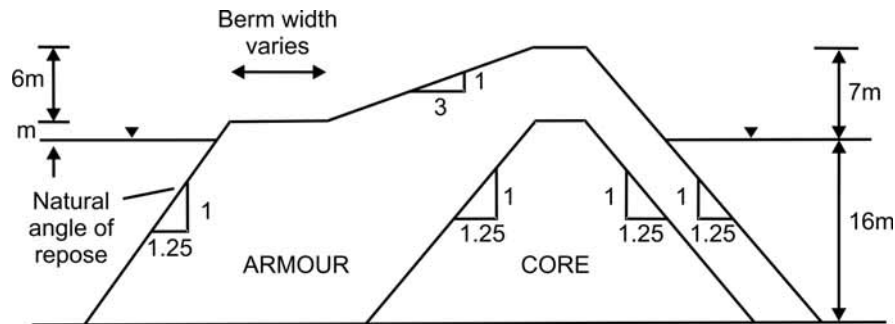


**Figure 5.63** Basic berm breakwater outline

Hall and Kao (1991) defined four basic parameters (see Figure 5.64):

- $A$  = cross-sectional area of armour stones required for stable reshaping ( $\text{m}^2$ )
- $L$  = width of toe after reshaping (m)
- $B_B$  = width of berm eroded (m),  $B_B = Rec$
- $R_P$  = fraction of rounded stones in the armour (-).

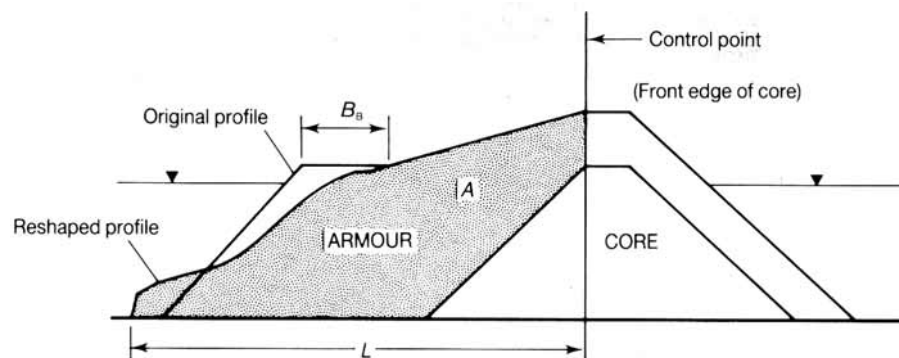


**Figure 5.64** Definition sketch for berm breakwater outer profile parameters

Equation 5.176 (Hall and Kao, 1991) relates the principal design parameter,  $B_B = Rec$  (m), to the wave climate, armourstone size, grading width and shape of the armourstone. The values for  $A$  and  $L$  (see Figure 5.64) should be determined by applying the original work of Hall and Kao (1991); these values should be considered as the minima to be provided in the design. The peak period,  $T_p$ , the groupiness factor,  $GF$  (defined as the degree of occurrence of short series of higher waves followed by short series of lower waves, see Section 4.2.4.4), and the wave steepness,  $s$ , were found to have no significant influence on the stable profile for berm breakwaters.

$$\frac{Rec}{D_{50}} = -10.4 + 0.51 \left( \frac{H_s}{\Delta D_{50}} \right)^{2.5} + 7.52 \left( \frac{D_{85}}{D_{15}} \right) - 1.07 \left( \frac{D_{85}}{D_{15}} \right)^2 + 6.12 R_P \quad (5.176)$$

This original Equation 5.176 is converted to Equation 5.177 so as to express the parameter,  $Rec$  (m), in terms of nominal diameters,  $D_n$  (m), rather than sieve sizes  $D$  (m). The conversion is based on the ratio  $D_n/D \cong 0.84$  as discussed in Section 3.4. The value based on 3000 waves is presented, followed by a correction, in Equation 5.178, for other storm durations, expressed as  $N$  = number of waves.

$$\frac{Rec}{D_{n50}} = -12.4 + 0.39 \left( \frac{H_s}{\Delta D_{n50}} \right)^{2.5} + 8.95 \left( \frac{D_{n85}}{D_{n15}} \right) - 1.27 \left( \frac{D_{n85}}{D_{n15}} \right)^2 + 7.3 R_P \quad (5.177)$$

The time correction factor, Equation 5.178, for duration (number of waves,  $N$ ) is defined as a function of the relative number of waves ( $N/3000$ ) and reads:

$$\frac{Rec_N}{Rec_{3000}} = 1 + 0.111 \ln \left( \frac{N}{3000} \right) \quad (5.178)$$

Hall and Kao (1991) found good agreement between predictions based on these equations and data obtained from prototype berm breakwaters.

### Reshaping method developed by Tørum *et al* (2003)

Tørum (1999), Tørum *et al* (2000) and Tørum *et al* (2003) followed to some extent the approach of Hall and Kao (1991). With reference to Figure 5.65 the recession,  $Rec$  (m), was analysed based on model tests. It was noticed that for a given berm breakwater all the reshaped profiles intersected with the original berm at an almost fixed point A, at a distance  $h_f$  (m) below SWL; see Figure 5.65.

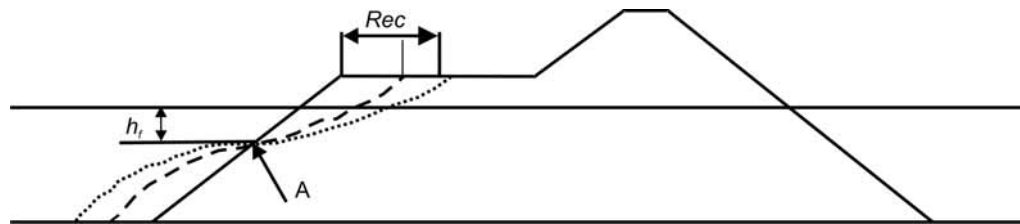


**Figure 5.65** Recession on a reshaping berm breakwater

As an approximation, the *fixed depth*,  $h_f$  (m), can be obtained from Equation 5.179, which gives the relationship between that depth and the structural parameters (Tørum *et al*, 2003):

$$\frac{h_f}{D_{n50}} = 0.2 \frac{h}{D_{n50}} + 0.5 \quad \text{for the range: } 12.5 < h/D_{n50} < 25 \quad (5.179)$$

where  $h$  = water depth in front of the berm breakwater (m)

The relationship between the dimensionless recession,  $Rec/D_{n50}$  (-), and the period stability number  $HoTo$  (-), the gradation of the armourstone,  $f_g$  (-), and the water depth,  $h$  (m), has been derived by a group of researchers, among others Menze (2000) and Tørum *et al* (2003)). This relationship is given here as Equation 5.180 (see also Figure 5.66):

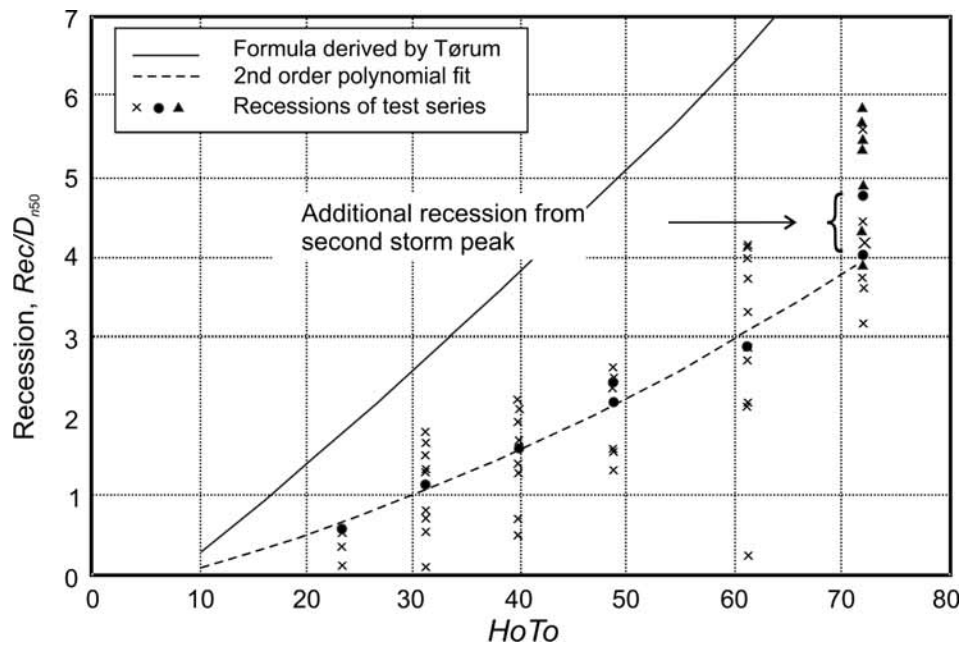
$$\frac{Rec}{D_{n50}} = 0.0000027(HoTo)^3 + 0.000009(HoTo)^2 + 0.11(HoTo) - f(f_g) - f(h/D_{n50}) \quad (5.180)$$

where  $HoTo$  is the wave period stability number,  $= N_s \cdot T_m \sqrt{g/D_{n50}}$  (-),  $f(f_g)$  is gradation factor function given in Equation 5.181;  $f_g = D_{n85}/D_{n15}$  (with  $1.3 < f_g < 1.8$ ):

$$f(f_g) = -9.9 f_g^2 + 23.9 f_g - 10.5 \quad (5.181)$$

and  $f(h/D_{n50})$  = depth factor function, given in Equation 5.182:

$$f(h/D_{n50}) = -0.16 \left( \frac{h}{D_{n50}} \right) + 4.0 \quad \text{for the range: } 12.5 < h/D_{n50} < 25 \quad (5.182)$$



## Notes

- 1 “Formula” derived by Tørum (1999), this is Equation 5.180 without depth correction and with  $f_g = 1.8$ .
- 2 For the preliminary design of non-reshaping statically stable or reshaped statically stable berm breakwaters, further reference is made to PIANC MarCom report of WG40 (PIANC, 2003a).

**Figure 5.66** Dimensionless recession versus period stability number  $HoTo$  for the Sirevåg berm breakwater,  $D_{n50} = 2.09$  m,  $\rho_r = 2.7$  t/m<sup>3</sup>

## Statically stable multi-layer berm breakwaters

Most of the research into the stability and reshaping of berm breakwaters has been done for structures with homogenous berms. But lately some work has also been done on the stability and reshaping of multi-layer berm breakwaters. The principle of this type of berm breakwaters in terms of hydraulic stability is that for design wave conditions the structure is statically stable; only under more extreme conditions reshaping or recession is allowed to a certain extent. The multi-layer berm breakwater allows for a better and more economical utilisation of the quarry yield than a conventional rubble mound breakwater. An example of a berm breakwater with a multi-layer armour around still water level is shown in Figure 5.67. The general design guidance for this type of statically stable non-reshaping berm breakwaters is as follows: the recession data and the dynamic stability number,  $HoTo$ , are based on the value of  $D_{n50}$  belonging to the largest armourstone size.

This special type of rubble mound berm breakwaters is further discussed in Section 6.1.4.3.

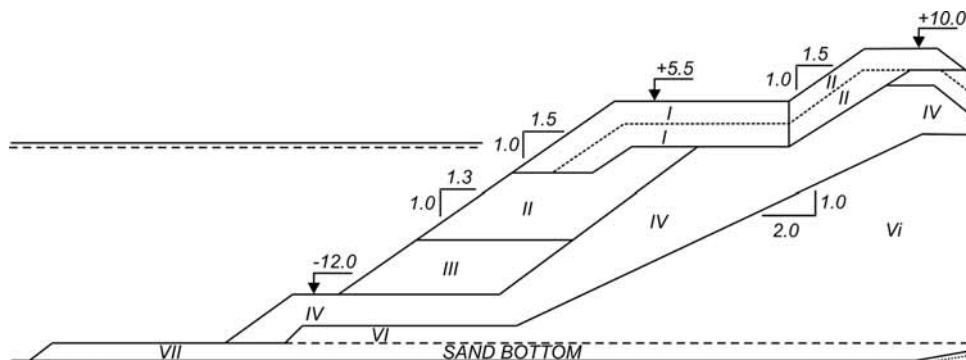


**Figure 5.67** Multi-layer or non-homogenous berm breakwater (Sirevåg in Norway); I = heavy armourstone 20-30 t; II = armourstone 10-20 t (after Tørum, 2003)

**Note:** The stability of the rear-side of a berm breakwater is very important for its overall stability. In the case of moderate to severe damage to the rear-side, the risk of total failure of the crest and front side of a berm breakwater is very large. Van der Meer and Veldman (1992) suggested using the following values for the overall design factor (see also PIANC, 2003a):

$$\frac{R_c}{H_s} s_{op}^{1/3} = 0.25 \quad \text{for start of damage}$$

$$\frac{R_c}{H_s} s_{op}^{1/3} = 0.21 \quad \text{for moderate damage}$$

$$\frac{R_c}{H_s} s_{op}^{1/3} = 0.17 \quad \text{for severe damage}$$

where  $R_c$  is the crest freeboard (m) and  $s_{op}$  is the fictitious wave steepness (-) based on the peak wave period,  $T_p$ (s)

### 5.2.2.7 Composite systems – gabion and grouted stone revetments

The stability of randomly dumped quarried rock can sometimes be improved by using stones in gabions (see Section 3.14) or by binding the stones through grouting with cement- or bitumen-based materials (see Section 3.15). In this section a rough (indicative) stability criterion is presented, which allows the designer to make a comparison for these systems with randomly placed armourstone.

A preliminary comparison of the hydraulic stability can be made using a general empirical formula given by Pilarczyk (1990) for plunging waves: Equation 5.183. For conditions with  $\xi_p > 3$  it is assumed that this equation may be used with  $\xi_p$  set constant at  $\xi_p = 3$ .

$$\frac{H_s}{\Delta D} = \phi_u \phi_{sw} \frac{\cos \alpha}{\xi_p^b} \quad \text{for } \xi_p < 3 \text{ and } \cot \alpha \geq 2 \quad (5.183)$$

where:

- $\phi_u$  = system-determined (empirical) stability upgrading parameter (-);  $\phi_u = 1$  for rip-rap and  $\phi_u > 1$  for other systems
- $\phi_{sw}$  = stability factor for waves (-), defined at  $\xi_p = 1$ , with limiting values  $\phi_{sw} = 2.25$  and 3 for initial and maximum acceptable stone movement respectively
- $b$  = empirical exponent ( $0.5 \leq b < 1$ ; armourstone:  $b = 0.5$ , other systems:  $b = 2/3$ )
- $D$  = system-specific, characteristic size or thickness of protection unit (m)
- $\Delta$  = relative buoyant density of a system unit (-)
- $\alpha$  = slope angle of the protection (°).

#### Box gabions and gabion mattresses

The primary requirement for a gabion or mattress of a given thickness is that it will be stable as a unit. The thickness of the mattress,  $D'$  (m), can be related to the size of the armourstone fill,  $D_n$  (m). In most cases it is sufficient to use two layers of stones in a mattress ( $D' \geq 1.8D_n$ ). Thus the unit thickness  $D'$  (m) is obtained from a stability analysis, using a stability upgrading factor in the range of  $2 \leq \phi_u < 3$ .

The secondary requirement is that the (dynamic) movement of individual stones within the basket should not be too strong, because of the possible deformation of the basket and the abrasion of the mesh-wires. Therefore, the second requirement aims to avoid the situation that the basket of a required thickness  $D'$  will be filled by too small material, and is only related to  $D_n$ , implying that only movements in the lower range of dynamic stability are allowed. By the choice of a stability upgrading factor for wave-exposed stones in the range of

$2 \leq \phi_u < 2.5$ , the accepted associated level of loading of the individual stones is roughly twice that at incipient motion.

The two requirements are summarised as follows:

- 1 **Static stability of the unit** of thickness  $D'$ .
- 2 **Dynamic stability of stones** of characteristic size  $D_{n50}$  inside the basket.

For preliminary design purposes these requirements can be assessed with Equations 5.184 and 5.185 (Pilarczyk, 1998). These equations are adapted from Equation 5.183 and are considered valid for  $H_s \leq 1.5$  m (or  $H_s \leq 2$  m for less frequent waves).

- 1 **Static stability of the units** with a thickness,  $D'$ : Check static stability (stability number  $H_s/(\Delta'D') = 1$  to 4) with Equation 5.184, using  $F = \phi_u \phi_{sw} \leq 7$ , the relative buoyant density of a unit,  $\Delta' \cong 1$  (-), and  $D' \geq 1.8D_{n50}$  (m):

$$\frac{H_s}{\Delta'D'} = \phi_u \phi_{sw} \frac{\cos \alpha}{\xi_p^{2/3}} \quad (5.184)$$

- 2 **Dynamic stability of stones** of characteristic size,  $D_{n50}$ : Check dynamic stability inside the basket with Equation 5.185, using for the stability factor,  $F = \phi_u \phi_{sw} \leq 5$  (-) and with  $\Delta$  equal to the relative buoyant density of the armourstone, usually  $\Delta \cong 1.65$  (-):

$$\frac{H_s}{\Delta D_{n50}} = F \frac{1}{\xi_p^{1/2}} \quad (5.185)$$

In all situations the stone size must be larger than the size of the wire mesh in the basket; this defines the minimum size.

In multi-layer gabions or mattresses (more than two layers) it is preferable to use a finer stone below the armour layers (ie up to  $0.2D_{n50}$ ) to create a better filter function and to diminish the hydraulic gradients at the surface of the underlying subsoil (Section 5.2.2.10 and Section 5.4.5.3). In either case it is important that both the subsoil and the stone filling inside the gabion basket or mattress are adequately compacted. For design conditions with  $H_s > 1$  m, a fine granular sub-layer (about 0.2 m thick) should be provided between the gabion basket or mattress and the subsoil. For other conditions it is sufficient to place the mattress directly onto the geotextile and compacted subsoil. For practical reasons, the minimum thickness of mattresses is about 0.15 m.

#### Bound or grouted stone

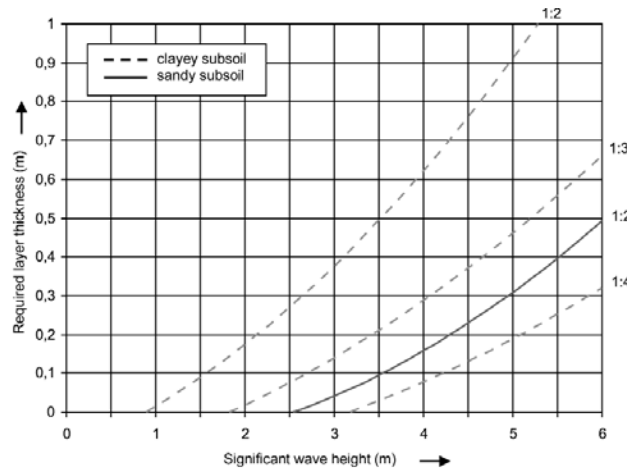
Fully penetrated rock revetments need to be designed for wave impacts. The graph shown in Figure 5.68 can be used to design the required layer thickness. This design graph has been compiled for hydraulic and climate conditions as found in the Netherlands and presents the required layer thickness for different slope angles and types of core material (sand and clay) as a function of the significant wave height,  $H_s$ .

The minimum layer thickness needed in the wave impact zone is also determined by the stone diameter,  $D_{n50}$ . To obtain a well penetrated revetment, the thickness needs to be more than  $1.5D_{n50}$ . For a fully penetrated rock revetment, the stone grading 5–40 kg is usually suitable although, if required, a stone grading of 10–60 kg can be used. Based on an apparent rock mass density of  $\rho_r = 2650$  kg/m<sup>3</sup>, this leads to a layer thickness of 0.30 m for the grading 5–40 kg and 0.35 m for the grading 10–60 kg.

When stone gradings larger than 10–60 kg are used, the voids between the stones will be too big which will result in the asphalt grout flowing away through the revetment. This can be limited by using a less viscous mixture or by adding a coarser grading of gravel or crushed

stone to the asphalt grout. If a smaller grading of stone is used (50/150 mm or 80/200 mm), for example as a new layer over an existing revetment, asphalt mastic must be used as the penetration grout instead of asphalt grout, as this is more viscous and will penetrate the voids more easily (see also Section 3.15).

If fully penetrated revetments are applied in the tidal zone, the revetment needs to be designed for water pressure. For more information on this, reference is made to the *Technical report on the use of asphalt in water defences* (TAW, 2002a).



#### Note

The minimum layer thickness is  $1.5 D_{n50}$  (see page 617)

**Figure 5.68** Layer thickness for fully penetrated rock revetments

For pattern penetrated rock revetments or armourstone cover layers (for example following a pattern of dots or strips) the same design method as for loose armourstone is used and the layer thickness is determined by the size of the armourstone. However, a reduction factor can be applied depending on the degree of penetration, based on Equation 5.183. If the voids are filled up to approximately 60 per cent a value for the upgrading factor  $\phi_u = 1.5$  can be used. With a narrow grading, and if monitored carefully during construction, this value can be increased up to  $\phi_u = 2.0$ . For the stability parameter the value  $\phi_{sw} = 2.25$  can be used, however depending on the number of waves and the safety factor required this value may need to be modified. The parameter  $b$  in Equation 5.183 depends on the interaction between the waves and the revetment. For revetments with pattern penetration the value  $b = 0.5$  is recommended, for surface penetration  $b = 2/3$  is a typical value. With pattern penetrated rock revetments (or armourstone cover layer) good results have been obtained for values of the significant wave height up to 3 to 4 m. More information about penetrated rock revetments can be found in TAW, 2002a.

### 5.2.2.8

#### Stepped and composite slopes

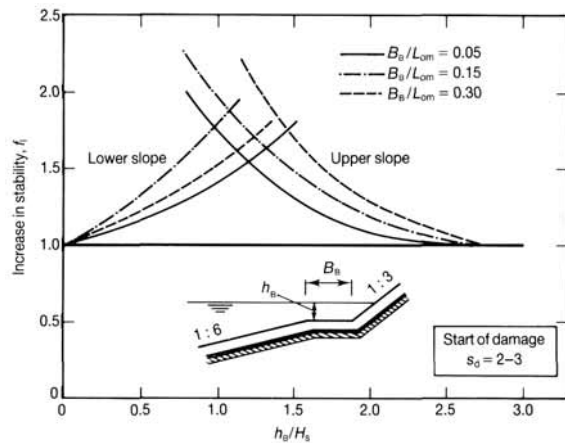
The stability formulae as described in Section 5.2.2.2 are applicable to straight slopes. Sometimes structures are a combination of slopes (composite slopes) and/or have a horizontal berm below the water level (stepped slopes). Design curves are given in this section for three types of structures. Stepped slopes were investigated by Vermeer (1986) and composite slopes by Van der Meer (1990a). The results are shown in Figures 5.69–5.71. The reference for stepped or composite slopes is always the stability of a straight slope, described in Section 5.2.2.2. The stability of the stepped or composite slope is then described by an increase in stability relative to a similar, but straight rock-armoured layer with the same slope angle. This increase in stability, described with a factor  $f_i$ , has a value  $f_i = 1.0$ , if the stepped or composite slope has the same stability as a straight slope. The factor has a value  $f_i > 1.0$ , as the step or transition of the slope has a positive effect on the stability. The curves in Figures 5.69–5.71 are given for start of damage,  $S_d = 2-3$ .

The design procedure is as follows:

- calculate the required  $D_{n50}$  for the part of the stepped or composite slope according to a straight slope, as described in Section 5.2.2.2, and then
- determine the reduced value of  $D_{n50}$  by dividing the  $D_{n50}$  value found above by the increase in stability factor,  $f_i$  (-), obtained from Figures 5.69 to 5.71.

Three types of structures were investigated by Vermeer (1986) and Van der Meer (1990a).

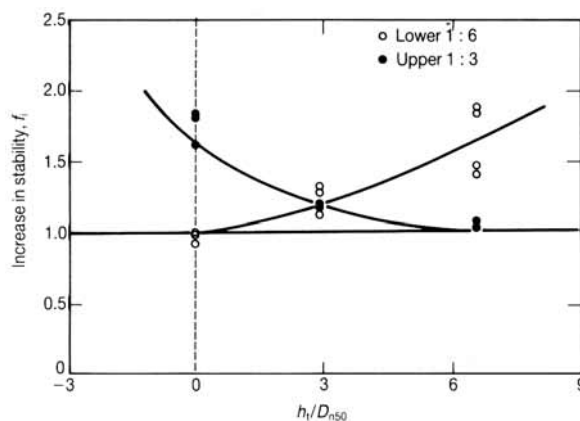
- 1 **A stepped slope with a horizontal berm** at or below the still water level with an upper slope of 1:3 and the lower slope of 1:6. The possible range of application of the design curves given in Figure 5.69 is therefore: 1:2 to 1:4 for the upper slope and 1:5 to 1:7 for the lower one.
- 2 **A composite armourstone slope** with an upper slope of 1:3, a lower slope of 1:6 and the still water level at or above the transition. The possible range of application of the design curves shown in Figure 5.70 is therefore: 1:2 to 1:4 for the upper slope and 1:5 to 1:7 for the lower one.
- 3 **A composite slope** with a lower slope of 1:3 or 1:6 of armourstone, and a smooth upper slope of 1:3 (eg asphalt or placed block revetment). The possible range of application of the design curves shown in Figure 5.71 is therefore: 1:2 to 1:4 for the upper slope and 1:2 to 1:7 for the lower one.



**Note**

$h_b$  (m) is the height of the berm relative to the still water level;  $h_b$  is positive if the berm is below the water level.

**Figure 5.69** Stability increase factors,  $f_i$ , for stepped or bermed armourstone slopes



**Note**

$h_t$  (m) is the height of the transition relative to the still water level;  $h_t$  is positive if the transition is below the water level.

**Figure 5.70** Stability increase factors,  $f_i$ , for composite armourstone slopes

The improved formulae for the stability of the toe (see also Figure 5.74), in which the relative toe depth is given in two ways – as  $h_t/D_{n50}$  and as  $h_t/h$  – are given here as Equations 5.187 and 5.188 respectively (see also Pilarczyk, 1998).

$$\frac{H_s}{\Delta D_{n50}} = \left( 1.6 + 0.24 \left( \frac{h_t}{D_{n50}} \right) \right) N_{od}^{0.15} \quad (5.187)$$

and:

$$\frac{H_s}{\Delta D_{n50}} = \left( 2 + 6.2 \left( \frac{h_t}{h} \right)^{2.7} \right) N_{od}^{0.15} \quad (5.188)$$

A toe with a relatively high level, say  $h_t/h < 0.4$ , comes close to a berm and therefore, close to the stability of the armour layer on the sloping front face of the structure see Section 5.2.2.2. These armourstone cover layers have stability numbers close to  $H_s/(\Delta D_{n50}) = 2$ . This is the reason that Equation 5.187 as shown in Figure 5.74, would if extended not start in the origin, but at  $H_s/(\Delta D_{n50}) = 2$  for  $h_t/h = 0$ . The Equations 5.187 and 5.188 may be applied in the ranges of:  $0.4 < h_t/h < 0.9$  and  $3 < h_t/D_{n50} < 25$ .

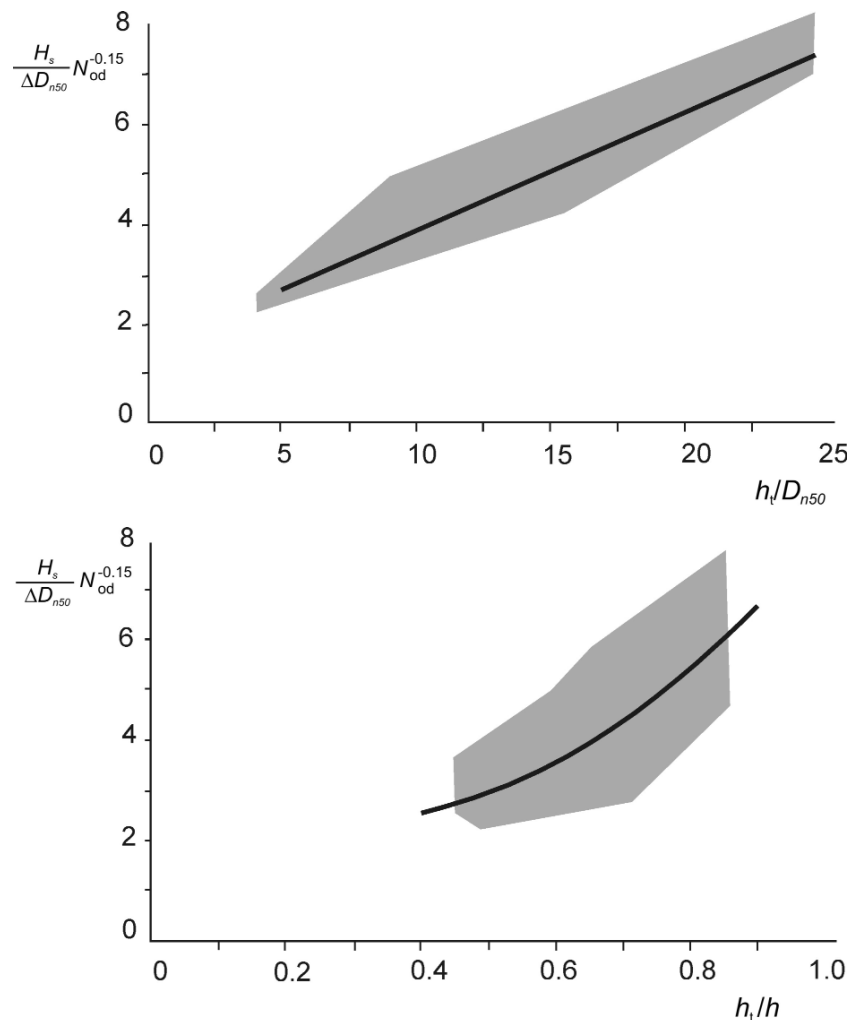


**Figure 5.74** Toe stability as function of  $h_t/D_{n50}$  and  $h_t/h$ ; the grey areas indicates the range of measured data

**NOTE:** The reader should realise that Equation 5.187 is only based on tests with a  $h_t/h$  ratio of 0.7–0.9. **Equation 5.187 should not be extrapolated.** When the water depth becomes more than approximately three times the wave height this formula gives unrealistic (even negative) results for the required size of the toe armourstone. A safe boundary for this equation is:  $h_t/H_s < 2$ .

on structures for which the stability of the rear slope is not influenced by the stability of the front slope or the crest. Guidance is given to determine the size of the armourstone needed at the crest and rear side of marginally overtopped rock structures to ensure stability.

A design guideline is provided to estimate the amount of damage to the rear slopes of rock armoured structures, taking into account several hydraulic and structural parameters, shown in Figure 5.78.

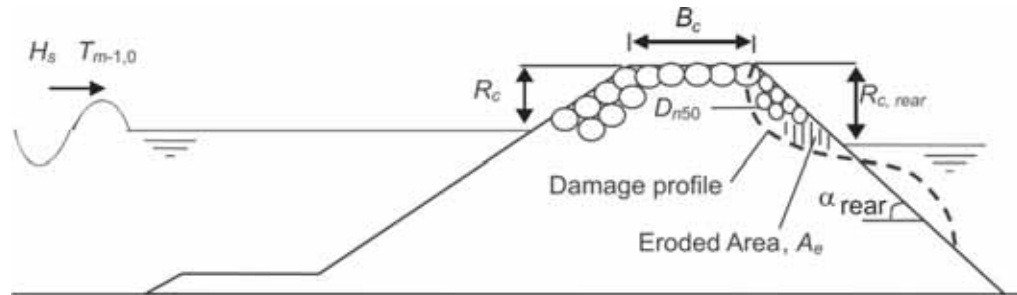


**Figure 5.78** Definition sketch for rear side stability evaluation

The required stone size,  $D_{n50}$  (m), at the rear side of coastal and marine structures for a given amount of acceptable damage,  $S_d$ , can be estimated with Equation 5.194, derived by Van Gent and Pozueta (2005):

$$D_{n50} = 0.008 \left( \frac{S_d}{\sqrt{N}} \right)^{-1/6} \left( \frac{u_{1\%} T_{m-1,0}}{\sqrt{\Delta}} \right) (\cot \alpha_{rear})^{-2.5/6} \left( 1 + 10 \exp(-R_{c,rear}/H_s) \right)^{1/6} \quad (5.194)$$

where:

- $S_d$  = damage level parameter (-);  $S_d = A_e / D_{n50}^2$ , with  $A_e$  = eroded area (m<sup>2</sup>) (see Figure 5.31)
- $N$  = number of waves (-)
- $H_s$  = significant wave height (ie  $H_{1/3}$ ) of the incident waves at the toe of the structure (m)
- $T_{m-1,0}$  = the energy wave period (s) (see Section 4.2.4 for details)
- $\alpha_{rear}$  = angle of the rear side slope (°)
- $R_{c,rear}$  = crest freeboard relative to the water level at rear side of the crest (m)
- $u_{1\%}$  = maximum velocity (depth-averaged) at the rear side of the crest (m/s) during a wave overtopping event, exceeded by 1% of the incident waves (Van Gent, 2003), given by Equation 5.195:

$$u_{1\%} = 1.7 (g \gamma_{f-c})^{0.5} \left( \frac{R_{u1\%} - R_c}{\gamma_f} \right)^{0.5} / \left( 1 + 0.1 \frac{B}{H_s} \right) \quad (5.195)$$

where:

- $B$  = crest width (m)
- $R_c$  = crest level relative to still water at the seaward side of the crest (m)
- $\gamma_f$  = roughness of the seaward slope (-);  $\gamma_f = 0.55$  for rough armourstone slopes and  $\gamma_f = 1$  for smooth impermeable slopes
- $\gamma_{f-c}$  = roughness at the crest (-);  $\gamma_{f-c} = 0.55$  for armourstone crests and  $\gamma_{f-c} = 1$  for smooth impermeable crests
- $R_{u1\%}$  = fictitious run-up level exceeded by 1 per cent of the incident waves (m).

The velocity,  $u_{1\%}$  (m/s), is related to the rear-side of the crest for situations with  $R_{u1\%} \geq R_c$ , in which the (fictitious) run-up level,  $R_{u1\%}$  (m), is obtained using either Equation 5.196 or 5.197 (Van Gent, 2003). Further details are also given in Section 5.1.1.3 – Box 5.5.

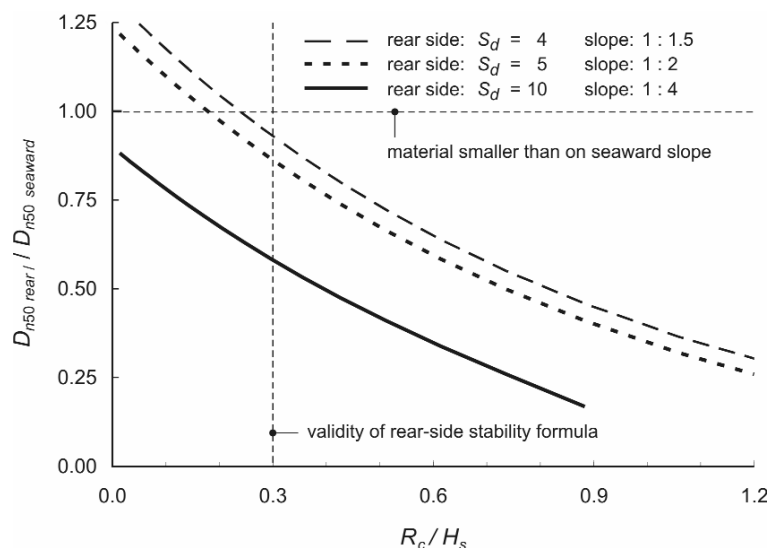
### Ranges of validity

The range of conditions for the various parameters included in Equation 5.194 is summarised in Table 5.48. In the model tests on which this expression is based, the relative buoyant density,  $\Delta$  (-), has not been varied, ie  $\Delta = 1.65$ .

**Table 5.48** Ranges of validity of parameters in Equation 5.194

Parameter	Range
Fictitious wave steepness at toe: $s_{s-1,0} = 2\pi H_s / (gT_{m-1,0}^2)$	0.019–0.036
Number of waves, $N$	< 4000
Relative freeboard at the seaward side, $R_c/H_s$	0.3–2.0
Relative freeboard at the rear side, $R_{c,rear}/H_s$	0.3–6.0
Relative crest width, $B/H_s$	1.3–1.6
Relative crest level with respect to run-up level, $(R_{u1\%}-R_c)/(\gamma H_s)$	0–1.4
Stability number, $H_s/(\Delta D_{n50})$	5.5–8.5
Rear-side slope, (V:H)	1:4–1:2
Damage level parameter, $S_d$	2–3.0

Figure 5.80 shows the reduction in size of armourstone at the rear-side of the structure compared with that at the seaward side. In this graph the material at the seaward side is calculated based on the formula described in Box 5.16 in Section 5.2.2.2. Values of the damage level parameter,  $S_d$ , for different slopes correspond to *intermediate damage*. Figure 5.80 shows that for relatively high crest elevations the required size of armourstone at the rear side is smaller; this reduction is higher for more gentle slopes at the rear side. Figure 5.80 shows a curve for a slope of 1:1.5 although this is not within the range of validity of the formula; nevertheless, this curve shows that the formula provides relatively small differences compared with slopes of 1:2.



#### Notes

- 1 This figure is for **one particular structure type** (rubble mound with **permeable core**) and for a fictitious wave steepness of  $s_{m-1,0} = 0.03$ ; other wave conditions or structure geometries result in different curves.
- 2 This figure is based on best estimates without taking uncertainty into account.

**Figure 5.80** Reduction in armourstone size at the rear side compared with armourstone size at the seaward side

New parameters specific to Maynard's formula, Equation 5.224, are outlined below and guidance on the use of the different parameters is given in Table 5.56. For more information on this equation, see Maynard (1993).

**Velocity distribution factor,  $C_v$ :**

The velocity distribution factor is an empirical coefficient to take into account velocity profile effects.

**Blanket thickness coefficient,  $C_T$ :**

The blanket thickness coefficient takes account of the increase in stability that occurs when stone is placed thicker than the minimum thickness ( $1D_{100}$  or  $1.5D_{50}$ ) for which  $C_T = 1.0$  (see Table 5.56).

**Side slope factor,  $k_{sl}$ :**

The side slope correction factor is normally defined by the relationship given in Section 5.2.1.3 (this definition is for example used in the Pilarczyk formula, Equation 5.219). As results indicate that the use of this side slope is conservative for Equation 5.224, an alternative relationship is recommended by Maynard, given here as Equation 5.225.

**Table 5.56** Design guidance for parameters in Maynard formula (Equation 5.224)

<b>Safety factor, <math>S_f</math></b>	minimum value:	$S_f = 1.1$
<b>Stability coefficient, <math>C_{st}</math></b>	<ul style="list-style-type: none"> <li>angular armourstone:</li> <li>rounded armourstone:</li> </ul>	$C_{st} = 0.3$ $C_{st} = 0.375$
<b>Velocity distribution coefficient, <math>C_v</math></b>	<ul style="list-style-type: none"> <li>straight channels, inner bends:</li> <li>outer bends:</li> </ul> <p>where <math>r_b</math> = centre radius of bend (m) and <math>B</math> = water surface width just upstream of the bend (m)</p> <ul style="list-style-type: none"> <li>downstream of concrete structures or at the end of dikes:</li> </ul>	$C_v = 1.0$ $C_v = 1.283 - 0.2 \log(r_b/B)$ $C_v = 1.25$
<b>Blanket thickness coefficient, <math>C_T</math></b>	<ul style="list-style-type: none"> <li>standard design:</li> <li>otherwise: see Maynard (1993)</li> </ul>	$C_T = 1.0$
<b>Side slope factor, <math>k_{sl}</math></b>	$k_{sl} = -0.67 + 1.49 \cot\alpha - 0.45 \cot^2\alpha + 0.045 \cot^3\alpha$ (5.225) where $\alpha$ = slope angle of the bank to the horizontal (°)	

**Comparison of methods of Pilarczyk, Maynard and Escarameia and May**

A comparison of the three stability equations discussed above is given in Box 5.24 for a fixed water depth of 4 m. For normal turbulence levels, the differences between the results of the three design formulae are rather small. For higher turbulence levels the method proposed by Escarameia and May (Equation 5.223) tends to result in larger armourstone sizes than the other two methods, Pilarczyk and Maynard, Equations 5.219 and 5.224, respectively. For further discussion, see Box 5.24.

For the stability of the armourstone on a near-bed structure under currents only, the start of movement of stones is an important design criterion. Because the load of currents on the structure is present at a more or less constant level, especially compared with wave loads, a certain critical velocity should not be exceeded. The formulae by Hoffmans and Akkerman (1999) are based on the Shields parameter using such a velocity,  $U$  (see Equation 5.227). Equation 5.228 gives the relationship between the required stone sieve size,  $D_{50}$  (m), and the relevant hydraulic and structural parameters:

$$D_{50} = 0.7 \frac{(r_0 U)^2}{g \Delta \psi_{cr}} \quad (5.228)$$

where  $\psi_{cr}$  is the Shields parameter (-) and  $r_0$  is the turbulence intensity (-);  $r_0 = \sigma/u$ , where  $\sigma$  is the standard deviation of the time-averaged flow velocity  $u$  (m/s), more precisely defined in Equation 5.229:

$$r_0 = \sqrt{c_s + 1.45 \frac{g}{C^2}} \quad (5.229)$$

where  $C$  = Chézy coefficient ( $\text{m}^{1/2}/\text{s}$ ) (see Equations 4.131 to 4.133 in Section 4.3.2 and see also Section 5.2.1.8 with transfer relationships), and  $c_s$  is a structure factor (-), defined by Equation 5.230:

$$c_s = c_k \left(1 - \frac{d}{h}\right)^{-2} \quad (5.230)$$

where  $c_k$  is a turbulence factor related to the structure (-) and  $d$  is the near-bed structure height (m). For values of  $c_k$  (and hence  $c_s$ ) see below.

The Equations 5.228 to 5.230 as derived by Hoffmans and Akkerman (1999), take the turbulence into account. These empirical formulae fit very well for uniform, as well as for non-uniform flow conditions, although the factor 0.7 in Equation 5.228 can only be derived theoretically for uniform flow conditions.

In uniform flow the parameter ( $1.45 g/C^2$ ) is about 0.01, resulting in  $r_0 = 0.1$ , which is a well-known value. In the vicinity of structures non-uniform flow conditions are present and the turbulence is higher. Therefore the parameter  $c_s$  has been introduced, which depends on the relative structure height and  $c_k$ . The value of  $c_k$  depends on the structure type. Based on tests a value of  $c_k = 0.025$  is recommended. For  $d/h = 0.33$  (maximum structure height) the value of  $c_s$  becomes about 0.056 and consequently, the value of  $r_0$  becomes about 0.26. For design purposes it is recommended not to exceed a value of  $\psi = 0.035$  for the Shields parameter.

### 5.2.3.3 Toe and scour protection

Adequate protection of the toe of a slope or bank is essential for its stability as many of the failure mechanisms result from reduced strength at the base of the slope (see Section 5.4). In situations where there is no continuous lining of the bed and banks there are two main ways of ensuring toe protection: by providing sufficient material at a sufficient depth to account for the maximum scour depth predicted; or by provision of a flexible revetment (such as rip-rap) that will continue to protect the toe as the scour hole develops. From the above it is clear that the estimation of scour can be an important step in the design of stable rock structures.

The stability equations used for the design of bed and slope protection works are still applicable to the design of the toe protection, any differences are mainly due to construction aspects such as the thickness of the armourstone layer provided at the toe, the depth at which it is built and the way in which it is constructed (underwater or dry construction). Therefore, Equations 5.219, 5.223 and 5.224 in Section 5.2.3.1 and Equation 5.228 in Section 5.2.3.2 can be used for toe design. The choice of materials can however be wider than that available for slopes, since the toe will in many cases be underwater (eg river banks) and partly buried. Materials that are less aesthetically pleasing or that have limited scope for providing amenity improvement, can be adequate choices for that part of the structure.

provision for the discharge of the flow through sufficiently large openings of the cover layer or by means of weepholes in impermeable cover layers.

Design information for granular filters and geotextiles is given in Section 5.4.3.6.

### 5.2.3.5 Stability of rockfill closure dams

#### Overview, definitions and design parameters

This section discusses the hydraulic stability of rockfill closure dams against **current attack**. The hydraulics of these structures is outlined in Section 5.1.2.3.

Both the vertical and the horizontal closure method are evaluated hereafter. The set-up and content of this section is summarised as follows: after the summary of the relevant hydraulic and structural design parameters, design guidance is given for various aspects and features related to the stability of rockfill closure dams:

- vertical closure method subdivided in the various relevant flow regimes, varying from low-dam flow to high dam flow and through-flow
- a comparison of the various design formulae discussed for the vertical closure method
- horizontal closure method with emphasis on relation between stability and loss of material
- closure-related issues, such as down-stream protection, three-dimensional effects etc.

The hydraulic stability of rockfill under current attack is evaluated by means of critical values of design parameters (see Section 5.2.1). For convenience, the corresponding non-dimensional numbers are repeated here.

**NOTE:** In this section  $D$  should read as  $D_{n50}$  throughout unless other definitions are given explicitly (see also Figure 5.96).

Design parameter	Non-dimensional number
• critical discharge	$q/\sqrt{[g(\Delta D_{n50})^3]}$
• critical shear stress	$\psi$
• critical velocity	$U^2/(2g\Delta D_{n50})$
• critical hydraulic head	$H/(\Delta D_{n50})$

In principle, shear stress  $\psi$ , and velocity  $U$ , are, when calculated properly, the best parameters to represent the actual loading on the stones. To a lesser extent, this still holds for discharge  $q$ , but hydraulic height ( $H$ - or  $H - h_b$ ) parameters are only an overall representation for the loading. In principle, therefore better results from  $\psi$  and  $U$  methods may be expected (again, provided that reliable calculation methods for  $\psi$  and  $U$  are available). Moreover, the data describing the influence of geometry and *porosity* are represented by such structural parameters as (see Figure 5.96):

Design parameter	Non-dimensional number
• relative crest width	$B/H$
• relative stone size	$D_{n50}/d$
• structure slope angle	$\tan\alpha$

### The occurrence of internal set-up

The presence of a slope causes a certain set-up of the internal phreatic level, so called *internal set-up*. This is due to the fact that the inflow surface along the slope at the moment of high water level is larger than the outflow surface at the moment of a low water level and that the average path for inflow is shorter than for outflow. Hence, during cyclic water level changes, more water will enter the structure than can leave. Eventually, a compensating outflow of the surplus of water is achieved by an average internal set-up and the consequent outward gradients. Examples are given in Box 5.39. Equations 5.299 and 5.300 may be used to find the maximum internal set-up,  $z_{s,max}$  (m), as given in ICE (1988):

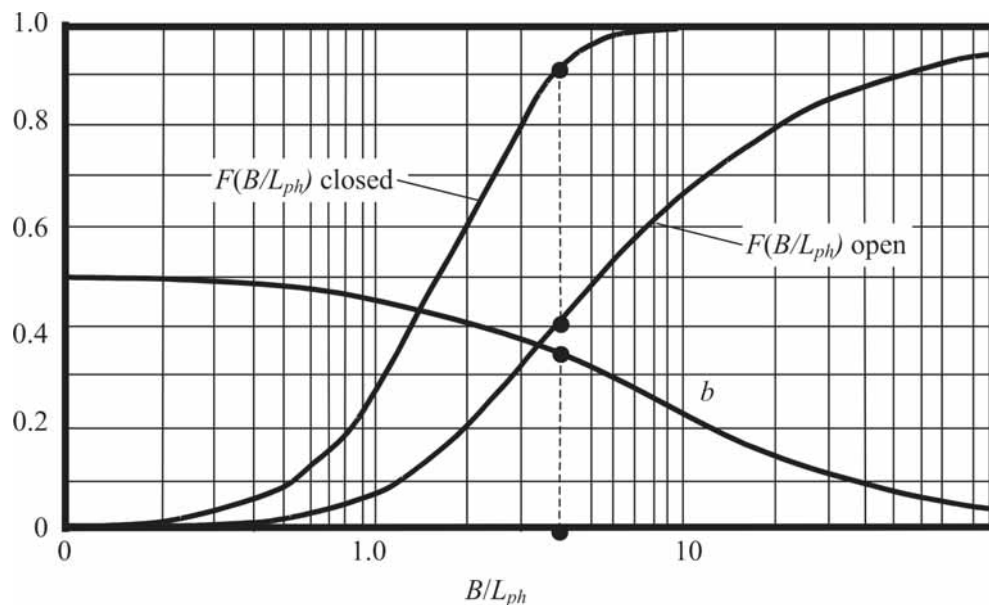
$$\frac{z_{s,max}}{h} = \sqrt{1 + \delta_w F(B/L_{ph})} - 1 \quad (5.299)$$

$$\delta_w = 0.1 \frac{c H_s^2}{n_v L_{ph} h \tan \alpha} \quad (5.300)$$

where:

- $h$  = water depth (m)
- $\delta_w$  = wave height parameter (-)
- $c$  = constant depending on air entrainment and run-up/run-down ( $c > 1$ ) (-)
- $H_s$  = significant wave height at the slope (m)
- $L_{ph}$  = phreatic storage length (see Equation 5.297) (m)
- $\alpha$  = slope angle ( $^\circ$ )
- $F(B/L_{ph})$  = function shown in Figure 5.152 (vertical axis) for two cases.

The two cases of the function  $F(B/L_{ph})$  are: (1) closed (filled) lee side of the rockfill dam (as in Figure 5.153) and (2) open lee side, as occurs with a breakwater protecting a harbour basin (see eg Box 5.39).



#### Note

For open lee side situations maximum set-up is localised at  $b \cdot B$  (m) from sea side, where the value of  $b$  (-) can be seen in this figure.

**Figure 5.152** Diagram for internal set-up due to slope

The set-up is particularly high (up to 0.5 times the wave height), if only reverse drainage (outflow) is possible, back towards the sea. This may be because  $L_{ph} \ll B$  or because the lee side of the rockfill structure is hydraulically closed, eg when a sand backfill behind a breakwater or seawall (see Figure 5.153).

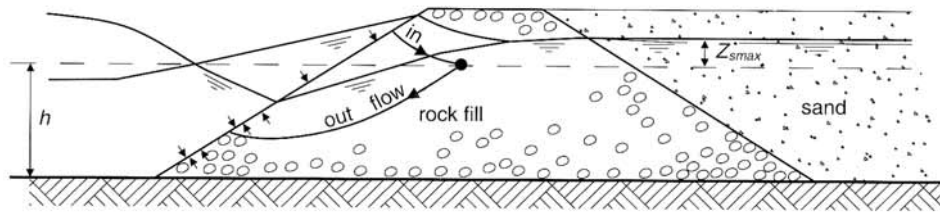


Figure 5.153 Internal phreatic set-up due to backfill

**Box 5.39** Typical examples of internal phreatic set-up

Two examples of internal set-up are given:

**1. Rockfill dike (coarse armourstone) around a lake or harbour basin**

Cross-sectional and structural data are:  $\tan \alpha = 1:3$ ,  $B = 30$  m,  $h = 10$  m,  $n_v = 0.4$  and  $k = 0.1$  m/s. The loading by (short) wind waves is characterised by  $H_s = 4$  m and  $T = 4.5$  s.

Using these data in the Equations 5.296 and 5.297 gives:  $T_{ph} = 1100$  s,  $L_{ph} = 1.9$  m and consequently,  $B/L_{ph} = 16$ ,  $F(B/L_{ph}) = 0.75$  and  $b = 0.19$  (Figure 5.152). Further, substituting  $c = 1$  in Equation 5.300 gives:  $\delta_w = 0.63$ , finally resulting in:  $z_{s,max} = 2$  m (by applying Equation 5.299), occurring at an approximate distance of 6 m from the waterfront.

**2. The same dike and loading as under 1 above, but with a backfill of sand**

In this case:  $T_{ph} = 1100$  s,  $L_{ph} = 1.9$  m,  $F(B/L_{ph}) = 1$  (Figure 5.152) and  $\delta_w = 0.63$ . Consequently,  $z_{s,max} = 2.7$  m, occurring approximately at the boundary with the backfill.

**Pore pressures dominated by elastic storage**

In this section, attention is given to the effects of the elastic compressibility of both the pore fluid and the skeleton. Varying pore pressures cause some variations of the volume of the pore fluid. This variation is very small if the pore fluid is pure water without any air in it, because water is practically incompressible. However, in the region of varying water level, the pore water does contain air and the resulting compressibility may be large enough to contribute to a sequential flow of water in and out the soil mass, according to the following mechanism:

- varying effective stresses,  $\sigma'$ , result in variation of the pore volume caused by compression of the skeleton, which in turn forces pore water to flow in and out of the soil (or rockfill) mass. This flow in and out because of compression of air-containing pore water and/or grain skeleton is called *consolidation*.

When the rate of pressure changes along the external boundary becomes so quick that consolidation in the soil cannot take place completely, then elastic storage plays a role. It means that the change of pore pressure and/or effective stress is retarded by the fact that the required outflow of pore water is not possible. The soil (water/air) system has too long a permeability (low  $k$ -value of soil) and/or possesses too low a stiffness; the modulus of compression of the water/air,  $K_{wa}$  ( $= \Delta p / (\Delta V / V)$ ) and the  $m_{ve}$ -value of the soil, being the elastic coefficient of volume change) in relation to the rate of boundary pressure changes (for definitions and descriptions, see Section 5.4.4.4).

Yamamoto, T, Koning, H L, Sellmeijer, H and van Hijum, E (1978). "On the response of a poro-elastic bed to water waves". *J Fluid Mech*, vol 87, Jul, pp 193–206

Youd, T L, Idriss, I M, Andrus, R D, Arango, I, Castro, G, Christian, J T, Dobry, R, Liam Finn, W D L, Harder, L F, Hynes, M E, Ishihara, K, Koester, J P, Liao, S S C, Marcuson III, W F, Martin, G R, Mitchell, J K, Moriwaki, Y, Power, M S, Robertson, P K, Seed, R B and Stokoe II, K H (2001). "Liquefaction resistance of soils: summary report from the 1996 NCEER and 1998 NCEER/NSF workshops on evaluation of liquefaction resistance of soils". *J Geotech and Geo-env Engg*, vol 127, no 10, pp 817–833

### 5.5.1

#### Standards

##### British standards

British Standards Institution, London

BS 6349-7:1991. *Maritime structures. Guide to the design and construction of breakwaters*

##### Canadian standards

Canadian Standards Association, Rexdale, Ont

CSA-S471-04 (2004). *Design, construction and installation of fixed offshore structures. Part I: general requirements, design criteria, the environment, and loads*

##### European standards

Eurocode 7 – see EN 1997-1:2004 and EN 1997-2

Eurocode 8 – see EN 1998-1:2004 and EN 1998-5:2004

EN 1997-1:2004. Eurocode 7. *Geotechnical design. General rules*

EN 1997-2 *Geotechnical design. Ground investigations. Lab testing*

EN 1197-2 *Geotechnical design. Ground investigation and testing*

EN ISO 11058:1999. *Geotextiles and geotextile-related products. Determination of water permeability characteristics normal to the plane, without load*

EN ISO 12956:1999. *Geotextiles and geotextile-related products. Determination of the characteristic opening size*

EN 1998-1:2004 Eurocode 8. *Design of structures for earthquake resistance. General rules, seismic actions and rules for building*

EN 1998-5:2004 Eurocode 8. *Design of structures for earthquake resistance. Foundations, retaining structures and geotechnical aspects*

##### French standards

Association Française de Normalisation (AFNOR), La Plaine Saint-Denis

NF G38-061:1993. *Recommendations for the use of geotextiles and geotextile-related products. Determination of the hydraulic properties and installation of geotextiles and geotextile-related products in filtration and drainage systems*

**Box 6.1** Port 2000 project – Le Havre, France

The Port 2000 project (Figure 6.5) extends the port of Le Havre to provide facilities to cater for increased container vessel traffic. The extension is on the north shore of the Seine estuary and incorporates a 5 km-long breakwater parallel to the river.



**Figure 6.5** Port 2000 Le Havre, France (courtesy Port du Havre)

Three principal sites were considered during the preliminary studies: the existing port at Le Havre, the Antifer terminal to the north and the Seine estuary. A public debate – the first in France on a major infrastructure project of this kind – took place throughout Normandy.

The port authorities put forward a long-term solution comprising investment outside the perimeter of the present port in the Seine estuary and a development scheme within the port (Figure 6.6), together with engineering works designed to provide environmental enhancement of the mudflats in the estuary.

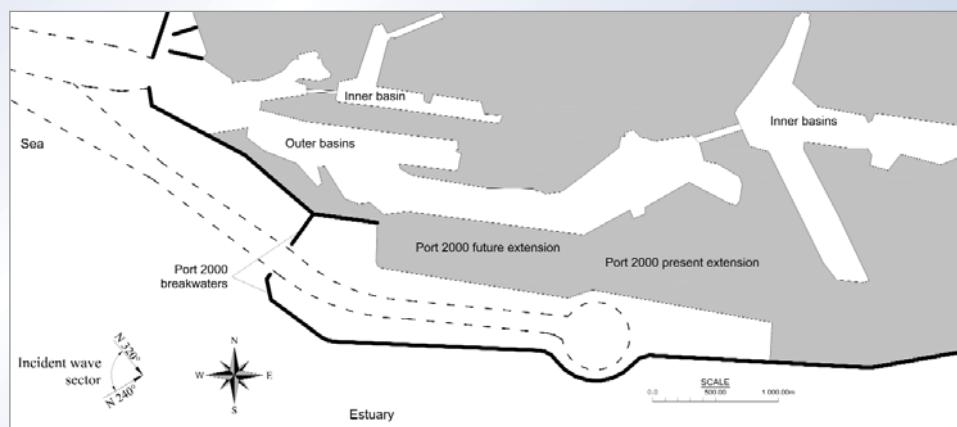


**Figure 6.6** Port 2000 layout (Le Havre, France)

The main advantages of this site were:

- the possibility of building a straight quay potentially 4200 m in length, representing 12 berths, with a 500 m-wide area of adjacent port land
- the possibility of dredging a short access channel that links with the present fairway 1 km west of the present entrance channel
- hydrosedimentological impacts on the estuary were minimised.

The information in Sections 6.1.4 to 6.1.7 is really only adequate for preliminary design purposes, so the detailed design for major breakwater projects should ideally be checked in a hydraulic physical model (see Section 5.3.2), making use of state-of-the-art techniques. Alternatively, uncertainties in the design formulae may be translated into (increased) safety factors, but even for small breakwaters this generally leads to substantial cost increases. In most cases model tests are cost-effective and lead to optimisation of the preliminary design.

### 6.1.3.2 Data collection and boundary conditions

The main environmental conditions serving as input parameters for the design formulae and mathematical or physical models are given in Table 6.1 below.

**Table 6.1** Main environmental input parameters for design formulae and models

Input parameters		Output	Tools
Environmental conditions	Water depth, tides and currents, long-term wave statistics	Design water levels, currents and wave statistics at the structure	Section 4.2.2: Marine water levels Section 4.2.3: Marine and estuarine currents Section 4.2.4: Wind waves and swell
	Seabed properties, bathymetry	Bearing capacity, geometry of the structure	Section 4.1.2: Bathymetry and morphology related to marine structures Section 4.4: Geotechnical investigations and data collection
Conditions during construction	Short-term wave statistics and seasonal variation, meteorological conditions	Construction methods and cost Design elevations	Section 4.2.4.8: Short-term or daily wave climate Section 9.3: Equipment
Environmental restrictions	Availability of construction material, infrastructure facilities Presence of protected fauna or flora	Construction costs Mitigation measures	Sections 3.2–3.11: Quarried rock Section 9.4: Transport
Present constraints	Availability of labour and equipment, local experience, safety of labour and public	Production costs and works duration	Sections 3.2–3.11: Quarried rock Section 9.5.2: Key hazards sources and their delivery
Future constraints	Facilities for future maintenance Durability of construction materials	Design details	Section 2.4.6: Maintenance and repair Section 2.4.7: Removal Chapter 10: Repair and replacement

### 6.1.3.3 Materials availability

The material for rock structures is supplied by quarries (see Section 3.9), the geological characteristics of which determine the maximum size and shape of the armour stones. Where a quarry is dedicated to a breakwater project, blasting to obtain the required design sizes of armourstone for a conventional rubble mound breakwater usually involves production of greater quantities of materials than are required by the design. This often results in an overproduction of certain gradations for which normally no other application can be found, even when that required for concrete aggregates has been used. This material is then effectively classified as waste. The design of a rock structure in this situation should therefore be tailored to the expected quarry yield as much as possible. This practice has been successfully adopted in Iceland and Norway.

Use of concrete armour units (see Sections 3.12 and 6.1.4) and berm breakwaters (see Section 6.1.6) are examples of design approaches that help achieve this kind of tailoring. Information

## 6.3 SHORELINE PROTECTION AND BEACH CONTROL STRUCTURES

Shoreline protection (or coastal defence) and beach control structures built of and/or armoured with stones have a number of benefits when compared with other materials and forms of construction. Table 6.4 below summarises both the advantages and disadvantages of using rock in such structures. The designer should appreciate the limitations of the form of structure that they are considering. This section aims to relate these limitations and considerations to the designer in the form of practical guidance.

**Table 6.4** *Advantages and disadvantages of rock structures for shoreline protection*

<b>Advantages</b>	
Durability	Rock from most sources withstands wear and attrition sufficiently and is ideally suited to the coastal environment.
Wave absorption	Porous and generally have gently sloping faces, so readily absorb wave energy and minimise adverse scour consequences caused by vertical reflective surfaces of seawalls and other structures.
Flexibility	Readily modified to take account of changing environmental conditions.
Cost effectiveness	Can be cost effective, eg using locally available materials.
Visual impact	Often considered visually attractive compared with other forms of sea defence, for example large seawalls or concrete stepped revetments.
Ease of construction	Even with limited equipment, resources and professional skills, structures can be built that function successfully.
Settlement	These are flexible structures that can adjust to settlements and are only damaged in a modest way if the design conditions are exceeded.
Maintenance	Repair works are relatively easy and generally do not require mobilisation of very specialised equipment. If properly designed, damage may be small and repairs may only involve resetting of displaced stones.
<b>Disadvantages</b>	
Safety	Concern over access to structures and risk to members of the public from falling into and being trapped in voids.
Navigation	Long rock groynes may cause problems for navigation of small leisure craft and fishing vessels. Groynes and breakwaters may need to be marked with appropriate lights or marker beacons. Submerged rock structures can be considered a navigation hazard if located near busy shipping lanes or areas of high amenity usage.
Footprint on foreshore	Rock revetments and rock groynes take up more foreshore than vertical seawalls and timber groynes respectively. This may be a consideration if the foreshore has environmental designations. Access limitations due to beach levels for maintenance may also mean that rock structures are not suitable at certain locations.

This section concentrates on the features and design considerations for seawalls, shoreline protection structures and beach control structures that differ from those of breakwaters. Cross-reference is made to Section 6.1 on breakwaters where appropriate. The section covers a range of structures, from revetments and anti-scour mats to structures designed to retain sand or gravel beaches, including conventional and fishtail groynes as well as offshore (or detached) breakwaters and sills.

Guidance on the selection of protection concept and layout, armouring systems and structural details is given. Cost, construction and maintenance issues that influence the design are also discussed, with cross-reference to the relevant sections of Chapters 9 and 10 where necessary.

The concept generation, selection and detailing of shoreline protection and beach control structures can be summarised by the flow chart in Figure 6.41. The numbers refer to the relevant parts of this section.

combinations should be investigated to assess scour depth and toe stability – the worst case conditions may occur at a low water level even though wave heights may be lower. Consideration should also be given to the full life of the structure, ie to take account of natural foreshore changes and potentially increased wave activity at the end of the service period. For most coastal structures, wave forces (downrush and breaking) present the critical conditions when determining stability of the toe. However, currents can become important, particularly in deeper water or more sheltered sites where wave activity is restricted.

In summary the important considerations in establishing the nature of toe protection required are:

- location of the structure (scour is most severe near the wave-break point)
- form of structure (wave forces produced as a result of reflectivity or downrush)
- nature of the bed (resistance to erosion and grain size)
- nature of structure, revetment, breakwater etc.

As a general rule, scour potential is greatest where the water depth at the toe is less than twice the height of the maximum unbroken wave.

Special attention should also be given to areas where scour may be intensified, such as changes in alignment, structure roundheads, channels and downdrift of groynes etc.

Design methods for scour and toe protection are presented in Section 5.2.2.9.

#### **Depth and form of toe detail**

The basic principle of flexible toe protection is to provide an extension of the armour face such that the foundation material is kept in place beneath the structure to the bottom of the maximum depth of scour. Caution should be exercised if a non-flexible toe protection is to be adopted as this will not accommodate any change in profile if scour is to occur, which may lead to brittle failure.

When placing stones in a situation where the toe is below low water the construction aspects covered in Section 9.7.1.2 should be considered. The use of geotextiles should be carefully considered prior to their inclusion in a design with respect to installation, also covered in Section 9.7.1.2. Consultation with experienced installers and manufacturers should help assess the feasibility and cost benefits of using them. Consideration should be given to whether suitable granular underlayers and filters can be used instead.

A range of toe details are presented in Figures 6.57 to 6.64 for the following ground conditions.

- 1 Rock foreshore.
- 2 Impermeable layer near foreshore level.
- 3 Sand/gravel foreshore.

Different construction scenarios are discussed below. The list of examples is not exhaustive and there may be situations where a combination of the examples shown may be applicable.

The toe details shown in Figures 6.59–6.64 indicate that a geotextile may be necessary where construction is to take place on a granular material, to prevent loss of bed material through the structure. The designer should check whether a geotextile is required to ensure interface stability criteria between adjacent granular layers are met (see Section 5.4.3.6). This applies to the transition between the bed material and the placed layers (core or underlayer) and also between adjacent layers within the structure, for example between the underlayer and the core.

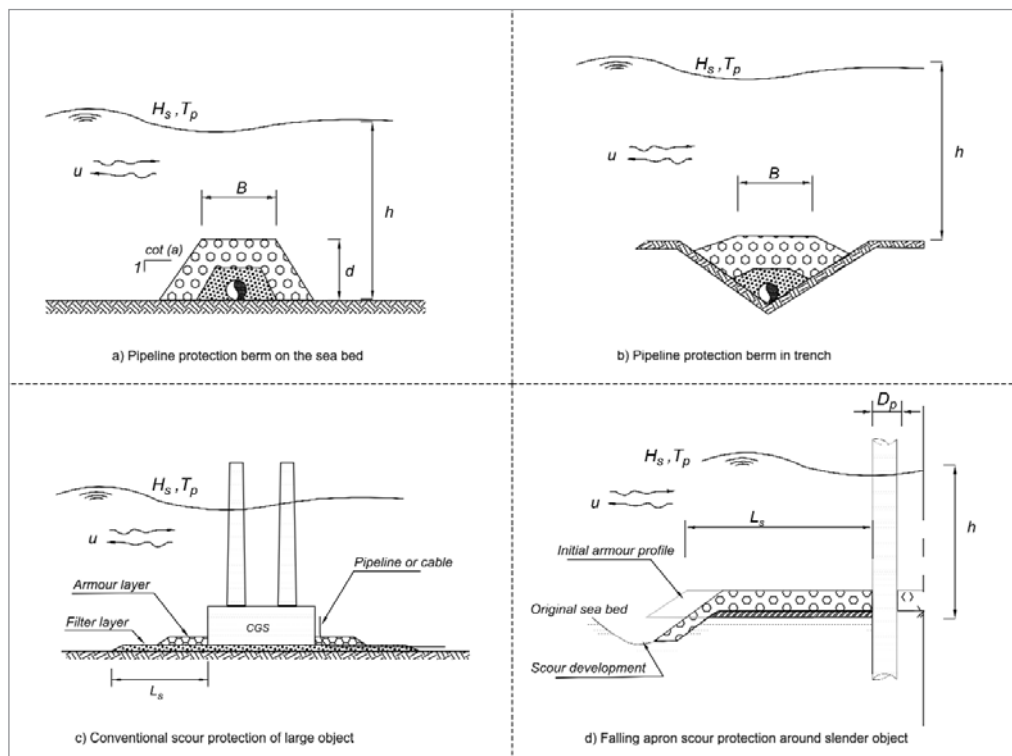


Figure 6.82 Schematic diagrams of offshore rock structures

#### 6.4.1.1

#### Pipelines and cables

It is often necessary to protect offshore pipelines and cables because an incident might result in:

- the release of the pipeline's contents, causing serious environmental damage
- high repair costs
- a loss of income in the period between the accident and the final repair
- reduced life expectancy for the structure.

During operation offshore pipelines can be subject to the following hazards:

- hydrodynamic forces from the action of waves and currents
- geotechnical instability of the berm or subsoil
- morphological changes (sandwaves)
- dropping or hooking by ship anchors
- hitting or hooking by fishing gear.

Additionally, pipelines can be at risk from the following hazards:

- dropped objects (containers, tools), especially near platforms
- overstressing and vibration of pipelines caused by freespan development. These freespans can be caused by scour of the sea bed or rapid morphological changes of the sea bed (sandwaves)
- buckling, caused by thermal expansion of pipelines
- waxing within pipelines as a result of a temperature drop along the pipeline
- increasing viscosity of the transported substances, caused by, among other factors, a temperature drop along a pipeline.

4.2.3). For steady-state conditions, the current may reach a magnitude of two to five per cent of the wind speed, whereas the effect on the water levels can usually be neglected, unless the fetch length is considerable (see Section 4.2.4.6).

#### Navigation, ship-induced currents and waves

The impacts of waves on the cross-sectional design should be considered in terms of the crest levels, slope angles and the extent of bed protection works. On rivers, the techniques of navigation vary considerably from those in a canal and should be considered accordingly in the design. Ship-induced hydraulic loadings acting on an inland waterway structure are:

- return current (see Section 4.3.4.1)
- water level depression and front wave (see Section 4.3.4.1)
- stern and secondary or interference waves (see Section 4.3.4.2).

As shown in Figure 8.21, an upbound vessel often navigates in the portion of channel where the stream velocity is lower, to save fuel and increase speed. By contrast, a vessel heading downstream generally navigates in the maximum flow. Several ship positions may need to be considered in the design. The designer should take into account local practices and regulations to establish the effect on channel and bank stability (see Section 8.3.5 for similar considerations for canals).

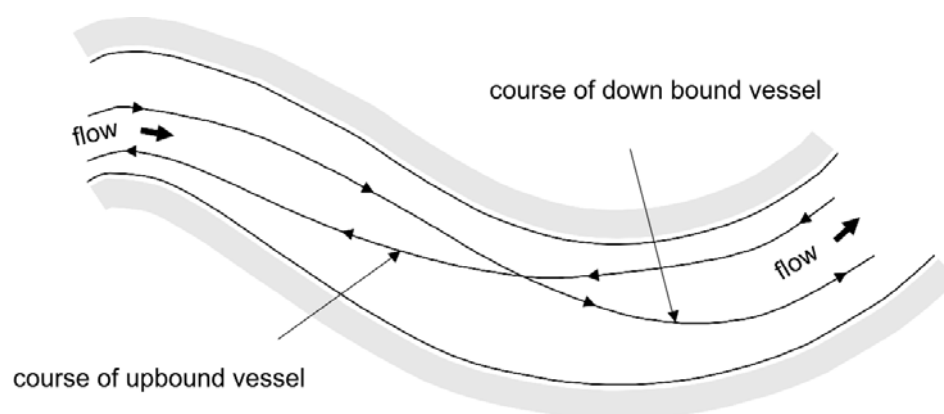


**Figure 8.21** Typical navigation courses

Table 8.2 indicates typical values for a number of hydraulic loads. These values should be used as a guide only. More accurate and site-specific data should be obtained for detailed design.

**Table 8.2** Typical values of hydraulic loads

Situation	Return ( $U_r$ ) or natural current	Water level depression		Secondary waves		Wind waves	
	Velocity (m/s)	Height $\Delta h$ (m)	Period $T$ (s)	Height $H_1$ (m)	Period $T$ (s)	Height $H$ (m)	Period $T$ (s)
Small river and restricted navigable channel	1.0–2.0 *	0.5–0.75	20–60	0.5	2–5	0.5	2
Large navigable channel	2.0	1.0	20–60	1.0	2–5	1.0	3–4
Large river and estuary	3.0–4.0	1.0	20–60	1.0	2–5	1.5–2.0	5–6

#### Note

\* Natural current velocities in steep upper reaches of rivers can be as much as 4 m/s.

## Ice loads

The resistance of river training works against the forces exerted by ice is of particular importance, eg along the shores of lakes and large rivers in arctic areas. The specific problems that have to be solved in such conditions are highlighted here. Ice riding up the embankment slope may damage the armour layer and in some instances the horizontal forces may become so large that the top part of a guide bund or dike is pushed backwards – inducing *decapitation*.

### NOTE: Considerations for design with ice loads

In fact, ice has both beneficial and detrimental effects. On one hand the presence of ice limits the wave climate and erosion. On the other hand, ice can damage slope protection, and can ride up and damage surface facilities. Breakwaters designed to withstand wave attack are often able to withstand ice forces. However, there is a delicate balance between the smoothness required to encourage ice bending (to minimise the ice load and movement of individual stones) and the roughness required to dissipate wave energy.

Armourstone can be subject to normal and shear stresses along the surface. These stresses will introduce a rotation, dislodging the individual stones. It is therefore desirable that the surface of the armourstone is relatively smooth and the stone layer is well keyed. Angular stones tend to nest together and interlock. The friction coefficient of ice on rock slopes varies between 0.1 and 0.5. It is obvious that smoother stone surfaces reduce the shear stress. Another disadvantage of a rough slope with relatively large surfaces of individual stones is the possibility of rigidly frozen ice that can remove the armourstone and float it away from the site.

From experience with ice and armourstone in bank protection works several rules of thumb can be defined:

- widely graded armourstone (or rip-rap) should be avoided; standard heavy gradings are preferred (see Section 3.4.3)
- for about 0.7 m thick ice, a standard heavy grading of 300–1000 kg or greater should be used
- generally, when there are significant water level changes and concerns over plucking out of individual stones, the median nominal stone size,  $D_{n50}$  (m), should exceed the maximum ice thickness,  $t_{ice,max}$  (m)
- the slope of the armour layer should be less than 30° to minimise the shear stress
- slopes below the waterline should be less steep than slopes above the waterline to encourage rubbing and prevent ice ride-up.

Further reference is made to Section 5.2.4 and McDonald (1988), and Wuebben (1995).

Designing with the above rules of thumb in mind often implies that conflicts (of interest) arise: stability requirements lead to angular, relatively heavy stone as armouring of the revetment, whereas coping with the ice loading effects leads to a smooth surface. In that case alternative materials may be attractive, such as some types of concrete armour units (see Sections 3.12 and 5.2.2.3), concrete block or gabion mattresses, and grouted stone (see Section 3.15, 5.2.2.7 and 8.6.2).

- where the water level has the potential to fall rapidly after being high for some time. This can destabilise the bank because the ground mass is saturated
- where the risk of slip failure is important, eg where the foundation soils are loosely deposited or where mica is present.

When a gentle slope cannot be achieved, alternatives should be considered and use of gabions to form a retaining wall may be considered.

Where a revetment is constructed in two or more levels, usually separated by a berm (see Figure 8.10), different slopes and types of armouring can be adopted for each of the levels. For instance, in a river environment, the upper layers of the protected soil mass may be loosely packed and more vulnerable to liquefaction in the case of earthquakes than other lower layers. The situation can be remedied by introducing a gentler slope in the upper part of the revetment. Conversely, in situations where the riverbank comprises loose sandy material overlain by layers of clay, it may be necessary to have a less steep slope on the lower part of the revetment.

### Crest level

The crest level of a revetment is normally set above the design flood level with freeboard in the order of 0.3 to 0.5 m. Larger values can be adopted in very large rivers or where wave run-up is expected. In summary, the crest level of revetments and river dikes is determined by:

- **design water** (= flood) level, which should be based on the probabilistic approach of both the river run-off discharge, the highest tidal level (HWS) in estuaries, and the wind set-up in estuaries and lakes (see Sections 4.2 and 4.3)
- **wave run-up** for which the two per cent exceedance level is often applied; this level depends on slope angle, slope roughness, existence of a berm, permeability of the structure, wave height and – period, and the angle of wave attack (see Section 5.1.1.3)
- a margin to take into account the **effects of seiches** (see Section 4.2) and gust bumps (single waves) resulting from a sudden violent wind rush), which may vary from a few tens of centimetres to a few metres (for seiches)
- **a rise of the mean sea level due to climate changes** (see Section 4.2), which applies to estuaries and locations along rivers close to the sea
- **settlement** of the subsoil and the structure itself during its lifetime (see Section 5.4)

The combination of the above factors in a probabilistic approach defines the crest level; the freeboard,  $R_c$  (m), relative to the design water level depends on the last four of the five listed factors above.

There are circumstances where the crest level of the revetment does not need to be as high as the flood level, notably for some spur-dikes that are overtopped in floods (see Section 8.2.7.1). It is also possible for a revetment to have the critical hydraulic loading occurring at standard water levels due to currents or waves, whereas loading in flood conditions is less severe.

### Berm

A berm may be designed on the slope between the lower part and the upper part of the revetment (see Figure 8.10). A berm may be required to improve the overall stability of the works and as an alternative to flattening the face slope of the whole revetment. It may also form a transition between parts of the revetment using different types of materials or placing techniques. It may also be a means to reduce run-up when this is critical.

As soon as all of the calculations for the joint scour and its consequences have been verified and are to an acceptable probability of exceedance, the designer should decide what counter-measures are to be taken. There are three different solutions for the problem of scour at the toe:

**Case 1: No significant scour – no need for protection.** The revetment has its toe at the meeting point between the slope and the riverbed level and no appreciable scour, ie scour that endangers the stability of the revetment, is expected.

**Case 2: Significant scour – bed protection provided to resist scour.** The revetment has its toe at the meeting point between the slope and the riverbed level but appreciable scour is expected and appropriate protection measures should be taken on the bed.

**Case 3: Significant scour – toe of revetment is extended** into the bed in anticipation of future scour: the revetment toe is placed in a trench, excavated in the riverbed, flood plain or foreshore at the time of construction, to form a falling apron.

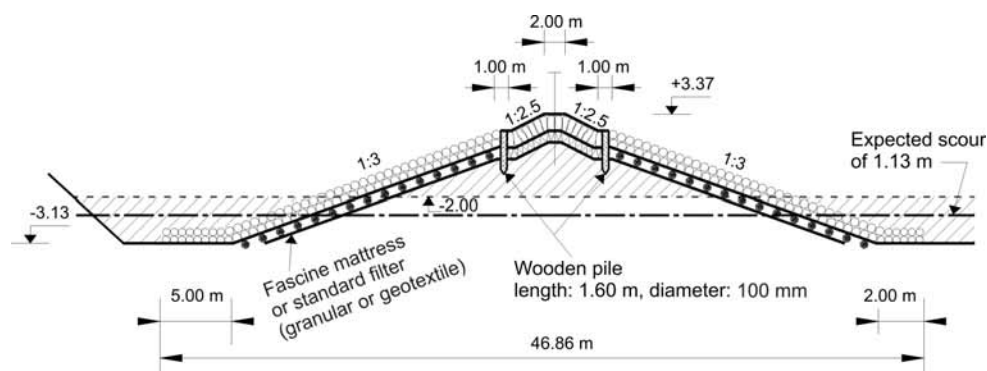


**Figure 8.26** Toe of spur-dike showing provision for scour

No appreciable scour can generally be found along inner bends of meandering rivers and along the stems of spur-dikes. Extension of the revetment cover layer over a few metres on the horizontal riverbed is usually sufficient. In many cases, this horizontal protection is already provided by the edge of the fascine mattress or the filter layer (see Figure 8.26). When there is a risk of erosion of soil through the cover layer, extension of the filter layer should be investigated.

When there is a risk of appreciable scour or if it is expected in front of the structure, suitable measures should be taken. The designer should start by assessing the future scour depth (Hoffmans and Verheij, 1997 and CIRIA, 2002). Depending on the outcome and the local circumstances, the designer should decide if the situation is case 2 or case 3 as defined above or a combination of both. In case 2, a falling apron may be recommended (see Section 8.2.7.4). In case 3, the revetment may be extended downward in an excavated trench (see Figure 8.27). In Figure 8.27, the lower part of the revetment and the falling apron have all been placed under water. When the geotextile filter is placed under water, fascines may be added to help the placing (see Section 9.7.1.2).

**Box 8.2** Recent laboratory research on falling aprons

A pilot study was performed on the behaviour of falling aprons by testing small-scale models in the flume (van der Hoeven, 2002). The falling aprons tested were designed for the guide banks of the Jamuna Bridge project (see Box 8.1). Figure 8.28 shows the expected behaviour of the falling apron in prototype and in the laboratory.

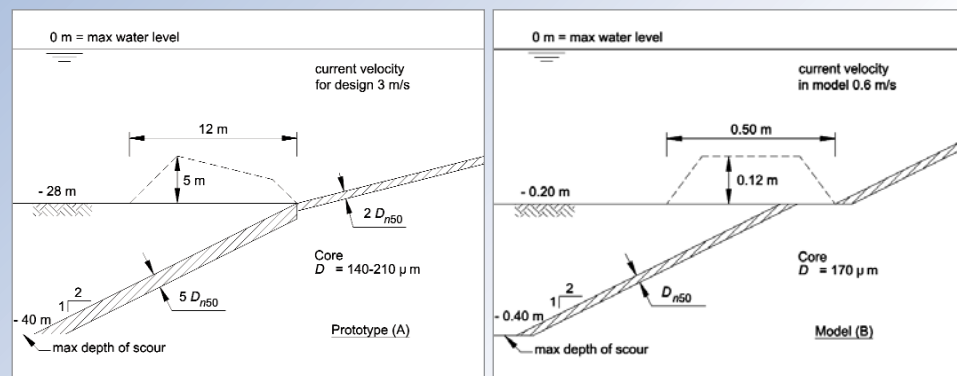


**Figure 8.28** Expected behaviour in prototype (A) and observed behaviour (B) in laboratory test

The purpose of the laboratory tests was to:

- 1 Obtain insight into the falling process and the successive phases.
- 2 Determine whether different configurations influence the final slope ie is special care during dumping necessary.
- 3 Determine how an apron with insufficient armourstone should be re-strengthened.
- 4 Determine whether the use of a falling apron can provide a durable protection against scour.

When designing a falling apron, the following aspects should be considered. As the apron will finally be formed in the model, it will be of a single armourstone layer on a steep slope 1:2. It should first of all be checked whether the armourstone size ( $D_{n50} = 0.20$  m in the prototype) is large enough on this steep slope. A verification of the slope stability (see Box 8.3) is done, not using the revetment angle but the apron slope angle,  $\alpha = 26.5^\circ$  (1:2 slope). Considering this apron angle and a value of  $\phi = 40^\circ$  for the angle of repose, the relevant slope reduction factor can be assessed using Equation 5.116 (Section 5.2.1.3):  $k_{sI} = 0.7$ . The appropriate size of the armourstone required for stability against current velocities up to  $U = 3$  m/s can be evaluated using the Pylarczyk formula, Equation 5.119 (Section 5.2.3). Values used for the various factors and parameters are: mobility parameter,  $\psi = 0.035$ ; relative buoyant density of the stones,  $\Delta = 1.65$ ; stability factor,  $\Phi_{sc} = 0.75$ ; velocity profile factor (for  $h = 30$  m),  $k_h = 0.68$ ; and turbulence factor,  $k_t^2 = 1.0$  (ie normal turbulence level). The armourstone size required is:  $D_{n50} = 0.19$  m, with a corresponding mass of  $M_{50} = 20$  kg. An armourstone grading of 5-40 kg ( $D_{n50} = 0.22$  m) is appropriate. A wide grading is intentionally selected to limit loss of fines from the underlying material, since a granular filter layer or geotextile under the apron is missing. An expected scour of 6 m implies a minimum volume of armourstone in the apron of  $0.22 \times 6.0 \times \sqrt{5} = 2.96$  m<sup>3</sup> per linear metre of revetment. The apron should be placed at a water depth of 15 m, necessitating high placement tolerances. The behaviour cannot be predicted in detail when a volume of 6 m<sup>3</sup> per linear metre of revetment is placed.

### 8.2.7.5 Flexible open revetment

The terminology *open revetment* is used to distinguish loose stones from fully or partly grouted armourstone. A practical design procedure for a flexible open revetment is presented here. It often takes place in successive steps described as follows:

- Step 1:** Assessment of the **erosion resistance of the non-protected** soil and determination of the area of slope to protect.
- Step 2:** **Sizing the cover layer** for stability against hydraulic loading, including wave attack above water and current attack under water.
- Step 3:** **Selection of the material** including size and durability.
- Step 4:** Design of the **filter system** and the **sub-layer**.
- Step 5:** Design of the **toe protection** and any **transitions**.

### Armourstone sizing against current attack

The loading considered here is the natural current. For the design of a revetment exposed to loadings due to ship-induced water movements the reader should refer to Section 8.3.6. The hydraulic stability of the cover layer is evaluated by means of deterministic calculations (see Section 2.3.3.3) based on a value of the design current. The water level during flooding is determined from Section 4.3.5. The current velocity and local current and shear are determined from Section 4.3.2.

The appropriate armourstone size may be determined using the widely used Izbash approach (see Section 5.2.1.4). More detailed or generalised equations are given in Section 5.2.3.1 from Pilarczyk (Equation 5.219), Escarameia and May (Equation 5.223) or Maynard (Equation 5.224). The results given by these three equations are compared in Box 5.24 indicating similar results for normal and more conservative results from Maynard and Escarameia and May for increased turbulence.

Box 8.3 discusses the differences of results for the design against current attack using these different methods.

### Armourstone sizing against wave attack

The dimensioning of the upper part of the revetment against wave attack may be performed using the design method presented in Section 5.2.2:

- for a straight slope of a non-overtopped structure, see Section 5.2.2.2
- for side slopes of low-crested structures, see Section 5.2.2.4
- for crest and rear-side of marginally overtopped structures, see Section 5.2.2.11.

In general a statically stable design is preferred. Note that using wide grading armourstone, eg rip-rap, tends to increase damage (see discussion in Section 5.2.2.2). In addition, in estuarine rivers the ocean wave at the structure may be significantly oblique which should be taken into account (see Section 5.2.2.2).

**NOTE:** Armourstone cover layers on structures in very shallow water and gently-sloping foreshores are more vulnerable to damage than those in deeper water because of wave shape changes while travelling towards the shore (see Section 5.2.2.2), when otherwise the same wave conditions at the toe of the structure apply. As a rule of thumb, the size of the stones required for stability of the armour layer is some 10 per cent larger than that in deeper water. As a guidance for the term *very shallow water* the following may be applied:  $h < 2 H_{s-toe}$  where  $h$  is the water depth in front of the structure relative to design water level (m) and  $H_{s-toe}$  is the significant wave height just in front of the toe of the structure (m). Note that deep water is defined as  $h > 3 H_{s-toe}$  (see Section 5.2.2.2):

Where smaller armourstone is preferred, grouting (see Section 8.6.1) or gabions (see Section 8.6.2) may be an appropriate response and their design is also discussed in 5.2.2.7.

The design methodology is illustrated in Box 8.5 for ship-induced waves, see Section 8.3.5.2.

### Step 3: Selection and specification of the cover layer material

The design value of  $D_{n50}$  being determined (see Step 2), the median mass required  $M_{50}$  can be determined by  $M_{50} = \rho_r D_{n50}^3$  (see Equation 3.9). The appropriate grading is selected from the standard grading requirements of EN 13383:2002 (see Section 3.4.3.2). It may be necessary to use a non-standard grading for specific cases or to fit local production (see

Section 3.4.3.9). The *simple* non-standard grading approach is usually sufficient, however, for specific requirements a detailed approach may be used.

Attention should be paid to durability of the armourstone used (see Section 3.6), notably with reference to weathering processes such as freeze and thaw (see Section 3.8.6).

**Box 8.3**      *Design of a revetment cover layer against current attack*

The reader should note that design equations are sensitive to the choice of input parameters. In particular, the depth-averaged velocity should be used for Pilarczyk's and Maynard's approaches while the near-bed velocity is to be used for Escarameia and May's approach. Standard values of the other input parameters are given in Section 5.2.3.1, however, more detailed values may be relevant. When using Pilarczyk's approach, the reader should refer to:

- Section 5.2.1.3 to determine the turbulence factor  $k_t$ . At a site where fairly high but not excessive turbulence is expected, a value of  $r = 0.20$  may be used (see Section 4.3.2.5).
- Section 5.2.1.8 to determine the depth factor  $\Lambda_n$  required to determine the velocity profile factor  $k_n$ .

When using Escarameia and May's approach, the reader should refer to Section 4.3.2.5 to determine the turbulence intensity required for calculation of the turbulence coefficient  $C_T$ .

The result is expressed as an armourstone size required for stability, including a safety coefficient for Maynard's approach. The reader should note that both Pilarczyk's and Escarameia and May's approaches provide a median size  $D_{n50}$  that can be easily converted into  $M_{50}$  and allow selection of a standard grading (see Step 3). However, Maynard's equation provides a median sieve size  $D_{50}$  with  $D_{n50} \cong 0.84 D_{50}$  (see Section 3.4.2 for further discussion on the relation between  $D_n$  and  $D$ ).

A standard double layer thickness is  $2k_t D_{n50}$  (see Section 3.5.1 for values of the layer thickness coefficient,  $k_t$  (-)). When small armourstone is required for weak currents, it may be practical to use a thicker layer to sink a geotextile and a fascine mattress. Conversely, assuming a minimum thickness of 0.5 m is required for construction purposes, ie  $D_{n50} = 0.203$  m, the hydraulic stability for this armourstone size may be checked to confirm if sufficient.

**Step 4: Design of the filter system and sublayer**

In principle, a granular filter could be used between the subsoil and the cover layer. In practice, geotextiles are increasingly used for this purpose. The filter criteria for both granular and geotextile filters are given in Section 5.4.3.6. Three different criteria should be satisfied by the filter system:

- functional requirement, ie meeting filter rule requirements
- construction requirement, notably when placing geotextile or granular filter underwater
- durability requirement, ie sufficient resistance during construction and the structure lifetime.

The option of a full multi-layered granular filter, placed in thin layers on a slope underwater, is rarely practicable in river engineering works, except for very large structures. A composite filter, consisting of a geotextile and a granular layer is more common. Often it is appropriate to place the armour layer directly onto a geotextile (without sublayer), or onto a gravel underlayer without geotextile.

In Box 8.4, the functional requirements are discussed for the specific case of a geotextile filter. These functional requirements concern the interface stability of the base soil with the geotextile filter fabric and the filter permeability. When the cover layer is directly applied onto the geotextile filter, specific attention should be paid to ensuring it is not damaged during construction (see Section 9.7.1).

### 8.2.10 Maintenance issues that influence design

Chapter 10 examines maintenance in detail. However, it is important to consider in the early stages of design how and when maintenance will take place, in particular with reference to the flood season. Maintenance should also be considered when selecting the appropriate type of cross-section for river training structures. It is also vital to determine who will be responsible and what equipment will be available for maintenance activities. Issues to consider in the various design stages in respect of river training works include:

- **durability** of the protection system, including the accepted reduction in stone size and acceptable damage during service, and the capacity of the owner to maintain the structure
- **size of stones** in view of manual or equipment handling
- **availability of local material** for repair and possibility to create stockpile of material for maintenance purposes
- **provision of a berm** to allow maintenance of the lower part of the revetment
- **wide crest**, eg of spur-dike, to allow access for large trucks.

An effectively designed structure should withstand the loads imposed by the river, but other causes of damage should also be considered in the design. Table 8.3, adapted from PIANC (1987b), gives an *aide-memoire* of design measures that can help to overcome or address causes of damage. The aim of these measures is to avoid degradation or to make maintenance easier.

**Table 8.3** Causes of damage to bank protection (after PIANC, 1987b)

Feature	Cause	Effect	Design measure
Abrasion	Ice floes and debris floating in the waterway	<ul style="list-style-type: none"> <li>● impact near waterline</li> <li>● displacement of armourstones</li> <li>● puncturing of membranes</li> </ul>	<ul style="list-style-type: none"> <li>● design for resistance to impact</li> <li>● allow for easy repair</li> <li>● deflect water flow, eg by groynes</li> </ul>
	Abrasive sediment in high velocity flow, such as sand, gravels, cobbles, boulders	Grinding action at toe wearing through exposed fabrics, gabion baskets	<ul style="list-style-type: none"> <li>● incorporate a sacrificial layer of armour</li> <li>● avoid use of gabions in cases of extreme abrasion</li> </ul>
	Pack ice	Shearing force on cover layer due to ice-sheets riding up the revetment	Provide cover layer able to withstand load, design procedures are available CRREL (1980) and see Section 5.2.4)
Biological	Livestock	Grazing and trampling leading to destruction of vegetative protection	<ul style="list-style-type: none"> <li>● fence-off revetment</li> <li>● use non-degradable reinforcement to soil</li> </ul>
	Vermin	Burrowing into bank Gnawing through geotextiles or cables	Pest control Provide an impenetrable top layer
	Plant growth	Roots alter geometry of top layer	Vegetation control if necessary
	Seaweed and algae	Surface damage to asphaltic top layers	Bituminous sprays
	Microbes	Attack some natural fibres	Use resistant materials unless degradation is a specific requirement
Chemical	Oils and hydro-carbons	Attack bituminous systems	Avoid contact
	Sulphates	Attack concrete	Use sulphate resisting cement
	Other aggressive salts	Corrosion of steel wire, cables, connections	<ul style="list-style-type: none"> <li>● protect by galvanising and/or pvc coating</li> <li>● use heavier wires and cables, or suitable stainless steel wires and cables</li> </ul>

## 8.7 REFERENCES

- BAW (Bundesanstalt für Wasserbau) (1990). *Code of practice – Use of Cement-bonded and Bitumen-bonded materials for grouting armourstone on Waterways*. MAV, Karlsruhe, Bundesanstalt für Wasserbau
- Bonasoundas, M (1973). *Stromungsvorgang und Kolkproblem am runden Brückenpfeiler [Flow structure and problems at circular bridge piers]*. PhD thesis / Report no. 28, Oskar V. Miller Institute, Technical University, Munich [in German]
- CRREL [Cold Regions Research and Engineering Laboratory] (1980) IAHR *Working group on ice forces on structures*. Carstens, T. Special report 80-26, June, 153 pp
- CUR/TAW (1991). *Guide for the design of riverdikes volume 1 – upper river area*. CUR, Gouda, pp 59-65
- Delft Hydraulics (1973). *Improvement of the navigability of the river-canal crossing near Wijk bij Duurstede, The Netherlands; morphological aspects*. Delft Hydraulics report M974-975 (in Dutch)
- Delft University (1983). *Hydraulic response to wind and ship induced waves for channel and coastal design*, Delft University Press, Delft
- Environment Agency (1999). *Waterway bank protection: a guide to erosion assessment and management*. R&D Publication 11, The Stationary Office, pp105
- Escarameia, M (1998). *Design manual on river and channel revetments*. Thomas Telford, London
- Hemphill, R W and Bramley, M E (1989). *Protection of river and canal banks*. CIRIA report, Butterworths, London
- Hjorth, P (1975). *Studies on the nature of local scour*. Bulletin Series A, No. 46, 1975. Dept. Water Resources Engineering, Lund Institute of Technology, University of Lund, Sweden
- Hoffmans, G J C M and Verheij, H C (1997). *Scour manual*. AA Balkema, Rotterdam, The Netherlands, 205 pp, ISBN 9054106735
- Jansen, P, Ph, Van Bendegom, L, Van Den Berg, M, De Vries, M and Zanen, A (1994). *Principles of river engineering; The non-tidal alluvial river*. Pitman, London, ISBN: 9040712808
- Larinier, M, Porcher, J P, Travade, F and Gosset, C (1994). *Passes à poisons, expertise, conception des ouvrages de franchissement collection mise au point*. Conseil Supérieur de la Pêche, 336 pp
- LCPC (1989). *Les enrochements*. Ministère de l'Équipement, Paris, 106 pp
- Mamak, D W (1958). *River regulation*. (translated and re-print of publication in Polish), Office of Technical Services, US Dep of Commerce, Washington
- May, R, Ackers, J and Kirby, A (2002). *Manual on scour at bridges and other hydraulic structures*. CIRIA, C551, London
- McDonald, G N (1988). "Riprap and armour stone". In: A C T Chen and C B Leidersdorf (eds), *Arctic coastal processes and slope protection design: a state of the practice report*. Technical Council on Cold Regions Engineering Monograph, ASCE, New York, pp 190–207
- PIANC (1987a). *Guidelines for the design and construction of flexible revetments incorporating geotextiles for inland waterways*. InCom Working Group 04, Supplement to PIANC Bulletin No 57, Brussels
- PIANC (1987b). *Risk consideration when determining bank protection requirements*. InCom Working Group 03, Supplement to PIANC Bulletin No 58, Brussels
- Pilarczyk, K W (1998). *Dikes and revetments: design, maintenance and safety assessment*. AA Balkema, Rotterdam
- Rajaratnam, N (1976). *Turbulent jets*. Elsevier Scientific Publishing Company, Amsterdam and New York, 304 pp
- Simons, D B (1984). *Hydraulic test to develop design criteria for the use of reno mattresses*. Water Resources Archive, Colorado State University, Fort Collins

scour may necessitate the use of larger quantities of core material but can be prevented by providing protection with a stone-dumping vessel before the core construction.

In a land-based operation, the scour protection, toe, berm and armour all demand cranes with sufficient reach. Excavators cannot be used, so rope-operated crawler cranes are necessary. The smaller armourstone in the berm and scour protection is placed using a skip or tray.

The capacity of a crane is determined by the maximum mass of stones plus container at the longest reach, ie *EUL* of the stone grading. Ultimately, the stones at the toe and the berm of the structure determine the type and size of crane required. For large breakwaters in deep water two cranes can be used. First a large crane can place the toe and the lowest part of the underlayer and armour layer, after which a smaller crane can follow to place the top part of the underlayer and the armour layer.

It is important to note that the mass of a grab for core and armour respectively used by these cranes is 30 per cent of the maximum payload. To avoid this loss of lifting capacity when handling large armour stones, eyebolts can be provided. Diligence is required to ensure that the eyebolts are adequately designed and certified for the task. If core material for bed protection is tray-placed, the mass of the container is about 15 per cent of the payload. The relationships between masses, reaches and hoist moments are discussed in Section 9.3.3.

The buoyancy of the stones can be used to extend the reach (see Figure 9.57). This figure illustrates the lifting capacity as a function of the horizontal distance to the crane axis. By keeping the element under water during the placing operation, the reach in this example can be extended by some 12 m.

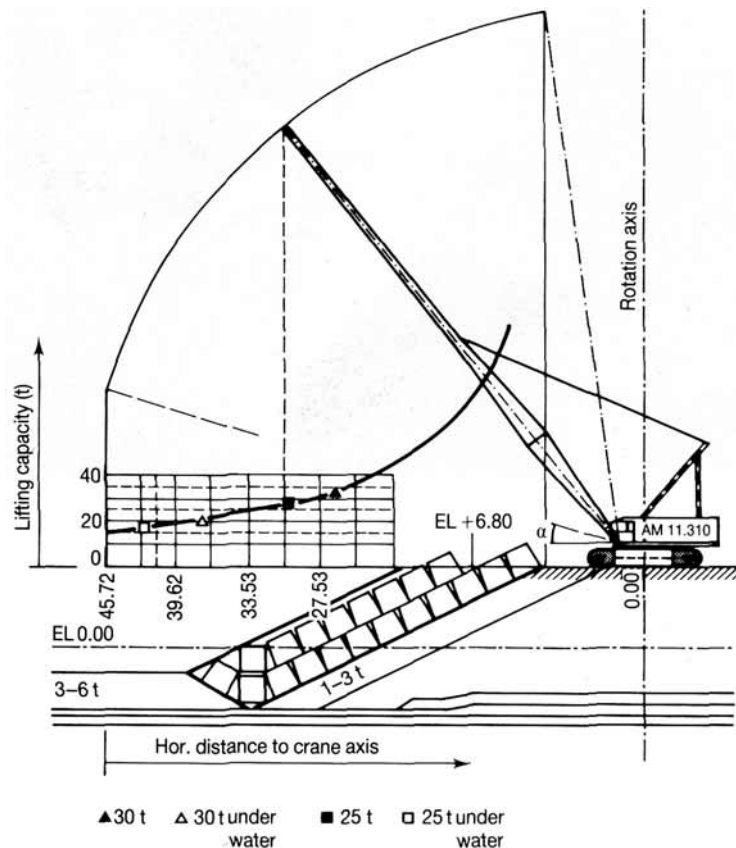


**Figure 9.57** Extending the crane reach by making use of buoyancy

The capacity, the lifting speed, the vertical movement of the boom and the swing speed are important properties of a crane suitable for placing armourstone. Typically, lifting cranes have one main drum for the lifting rope, which is usually reeved, plus a smaller drum for the

### 9.7.2.6 Placement of concrete armour units

Placing concrete armour units can be a time-consuming part of the breakwater construction because of the large number of units that should be placed and the constraints that exist on the placement procedures for slender and highly interlocking armour units. Placement rates typically range between three and 15 units per hour and may vary significantly with the environmental conditions (wave conditions, currents, visibility etc). Suitable and reliable equipment should be selected in order to achieve reasonable placement rates.

The breakwater slope should be properly profiled and, to facilitate placement, the median mass of the armourstone in the underlayer should not exceed 15 per cent of the armour unit mass (see Table 5.36 for details and see Section 5.4 for further discussion on filter requirements and sizing of underlayers). Deviations of the slope surface of the underlayer from design levels and slope should not exceed the nominal stone diameter  $D_{n50}$  of the underlayer. Tolerances are discussed further in Section 9.3.7 (Table 9.7).

Armour units are placed with a sling, which is equipped with a quick-release hook operated by a tag line (see Figure 9.61) and a guide line to locate the unit in the correct position, while a clamp is used to place cubes.



**Figure 9.61** Use of a quick-release hook (courtesy Interbeton)

Most concrete armour units are placed randomly in relation to the orientation of the units, but are located on a predefined grid. In order to place the units accurately on this grid, the crane should be equipped with a GPS antenna on the boom. Single-layer concrete armour units like Accropode, Core-loc and Xbloc are placed on a staggered grid (see Figure 9.62).

The placement of single-layer armour units starts at the breakwater trunk in a relatively sheltered area with the placing of a triangular section. Subsequently an armour unit is added to the first row, at the breakwater toe, to the second row resting on two units of the first row: the unit that has been placed before and the neighbouring unit, to the third row and so on. The placing of armour units proceeds with the construction progress of breakwater core and

It has been stressed that in the design process new guidance on layer thickness and as-placed density, especially of individually placed armour layers, as presented in Section 3.5.1, should be adopted in finalising design profiles. The mass of armourstone that the contractor has purchased and placed in the armour layer is then more likely to be close to the designer's estimate of required mass calculated from the design volume. The designer or client requires quality workmanship without liability for paying for fluids when rock was wanted, and without liability for paying for overly tight armourstone when less material was intended. The contractor wants speedy execution and full recouping of the cost outlay on materials. It is important to recognise a balance between the two parties' legitimate concerns. This requires that the designer's assumption for the armour layer porosity,  $n_v$ , applicable to the spherical probe survey method, is known, and that the validity of this assumption is checked during approval of the test panel.

It is recommended that the client declares in the contract:

- the payment rate for the mass of armourstone placed in each class of armourstone
- the assumed armour layer porosity,  $n_v$ , in each class of armourstone
- the assumed design layer thickness coefficient,  $k_t$ , for armour layers.

The test panel should form part of a larger completed section within realistic boundaries. Blocks falling on the boundaries of the panel are treated appropriately so as not to bias results. Particular care should be taken to ensure the test panel armourstone is representative of the specified grading. If necessary, adjustments to the trial panel are made until:

- grading is within specification
- final survey heights are within tolerance limits of the design drawing heights. Any serious difficulty in meeting these tolerances suggests that stone shape characteristics have not been accounted for and/or that inappropriate estimates of the  $k_t$  factor were assumed in the design. These problems can be resolved by rebuilding, resetting the design drawing surface levels or resetting tolerances
- in the eyes of the engineer, the visual appearance reflects the designer's intention as implied by the placement methods referred to in the contract and classified as random, standard, dense or specific.

This trial panel is then termed visually accepted and is subject to further analysis.

Given the placement method referred to in the contract on the one hand, and the blend of on-site factors (materials characteristics, placement machinery, operator training and experience, working conditions, time constraints) on the other, the trial panel exercise may point to a need to revise the most appropriate layer (or volumetric) porosity assumption for use in the payment calculation if payment is on a basis of armourstone tonnages deduced from surveyed volumes and target layer porosity.

Data obtained from the visually accepted test panel include:

- individual masses of all blocks in the panel. This provides further on-site control of heavy gradings. Individual weighing is preferred to the alternative of mass estimation from density and volume assessment using suitable block dimensions and shape factors. The total mass of armour in the panel is divided by apparent rock density,  $\rho_{app}$  ( $\text{kg/m}^3$ ), to give the volume of armourstone in the panel,  $V_r$  ( $\text{m}^3$ )
- the surveyed armour layer volume,  $V_{bs}$ , corrected to spherical end  $0.5D_{n50}$  probe method. The chainage length is multiplied by the average area enclosed between the upper and lower surveyed surface of the armour layer (see Equation 3.24,  $V_{bs} = A_{cs}L$ ). Normally it should be sufficient to have four profile lines surveyed across the structure at 2.5 m intervals, making sure the end points of the survey line are included

- the number of blocks placed in the armour layer per unit of slope area covered. This should be presented both for the visible upper layer of blocks and for the total number of blocks.

Equation 9.9 gives the relation between the armour layer porosity (expressed as a fraction) of the visually accepted test panel and the relevant armour layer volumes.

$$n_{vp} = (1 - V_r / V_{bs}) \quad (9.9)$$

If there is less than a 2 per cent difference in value between  $n_{vp}$  and  $n_v$  assumed in the design (ideally also indicated in the contract), the panel is in every way acceptable as a construction benchmark to be followed for the contract.

If the difference is more than 2 per cent, another attempt might be made to construct nearer to the design armour layer porosity, without an unreasonably onerous burden being placed on the rate of build, given the classified placement method originally specified.

If after this rebuild the new surfaces surveyed fulfil tolerances and are visually accepted, but the test panel still has more than a 2 per cent difference, the contractor and engineer should agree that this panel becomes the benchmark for acceptable construction practices.

For those contracts where payment is based on a tonnage placed calculated from volume surveys, it is also an opportunity to validate and if necessary, revise the armour layer porosity assumption. If the contract states a pay rate for tonnage of armourstone placed in the works to be a tonnage calculated from surveyed bulk volume, assumed armour layer porosity and apparent rock density, then an appropriate basis for payment of the panel (see Equation 3.26,  $V_r = V_b (1 - n_v)$ ) is given by Equation 9.10, an expression for the total mass of the armour,  $M_t$ .

$$M_t = \rho_{app} \cdot V_{bs} (1 - n_{vp}) \quad (9.10)$$

Placement workmanship at sample areas throughout the structure may be compared with the test panel(s) on visual criteria and also by comparing the number of blocks per unit area with results from the test panel(s). Major variations in block count results should be explained and removed by reworking if necessary. As the finished profiles of the entire works are normally checked for tolerances, the bulk-placed volumes of the entire armour layer in the completed structure can be similarly computed and bills for placed tonnages prepared accordingly. Precisely worded clauses usually exist to exclude liability for the client having to pay for armourstone determined by survey to be on average above an upper tolerance line.

Alternative simple schemes for payment based directly on tonnages placed exist. For example, contract payment for armour materials may be based on a rate per tonne delivered to site given satisfactory criteria for proof of delivery to site.

## 9.9 SURVEY AND MEASUREMENT TECHNIQUES

Because of the direct relationship between survey techniques and payments, all parties to a works contract should ensure that an accurate, fair and pragmatic approach to surveying is adopted that will lead to the correct method of payment for the work done. To suit the requirements of the works, tolerance levels should be practical, sensible, achievable and affordable. The various definitions of the term *tolerance* are set out in Section 9.3.7.

In addition to discussing the various survey techniques, this section also provides tables with information on achievable vertical tolerances for land-based and marine equipment, for both bulk and individually placed armourstone and concrete armour units.

$D_s$	Size of the equivalent volume sphere	(m)
$D_z$	Block size corresponding to sieve size $z$	(m)
$D_{50}$	Sieve diameter, diameter of stone that exceeds the 50% value of sieve curve	(m)
$D_{85}$	85% value of sieve curve	(m)
$D_{15}$	15% value of sieve curve	(m)
$D_{63.2}$	Location parameter in the Rosin-Rammler equation for sieve size distribution	(m)
$D_*$	Non-dimensional sediment grain diameter, $D_* = D_{50}(g\Delta/v^2)^{1/3}$	(-)
$d$	Structure (crest) height relative to bed level (breakwaters, dams etc)	(m)
$d$	Thickness or minimum axial breadth (given by the minimum distance between two parallel straight lines between which an armour block can just pass)	(m)
$d_c$	Crown wall height	(m)
$d_{ca}$	Difference of level between crown wall and armour crest, $d_{ca} = R_c - R_{ca}$	(m)
$E$	Young's Modulus	(N/m <sup>2</sup> )
$E$	Estuary number	(-)
$E_c$	Impact energy absorbance capacity	(kJNm)
$E_D$	Total degradation energy applied to the material	(J)
$E_i$	Incident wave energy	(N/m)
$E_r$	Reflected wave energy	(N/m)
$E_t$	Transmitted wave energy	(N/m)
$E_{\eta\eta}$	Energy density of a wave spectrum	(m <sup>2</sup> s)
$E_{i;d}$	Design value of the effect of actions	(Unit of $E$ )
$E_{i;k}$	Characteristic value of the effect of actions	(Unit of $E$ )
$e$	Void ratio, $e = n_v/(1 - n_v)$	(-)
$e_{sp}$	Spur ratio, defined as the ratio of the head loss in a river between two successive spur-dikes, $U^2 S_{sp}/(C^2 h)$ , and the velocity head, $U^2/(2g)$	(m)
$F$	Fetch length	(m)
$F$	Factor of safety (geotechnical), defined as ultimate resistance/required resistance	(-)
$F^*$	Non-dimensional freeboard parameter, $F^* = (R_c/H_s)^2 (s_{om}/2\pi)$	(-)
$Fr$	Froude number, $Fr = U/(gh)^{1/2}$	(-)
$F_H$	Horizontal force (on caisson or crown wall element)	(N/m)
$F_U$	Uplift force (on caisson or crown wall element)	(N/m)
$F_{j;d}$	Design value of an action or force	(N/m)
$F_{j;k}$	Characteristic value of an action or force	(N/m)
$F_q$	Discharge factor, ratio of critical discharge for bed protection and that of closure dam, $q_{cr-b}/q_{cr-d}$	(-)
$F_o$	Parameter expressing the amount of fines after minor breakage	(%)
$F_s$	Shape factor (of armour stone)	(-)
$f$	Friction factor	(-)
$f$	Frequency of waves, $f = 1/T$	(1/s)
$f$	Lacey's silt factor	(-)
$f_c$	Friction factor for currents	(-)
$f_i$	Stability increase factor for armourlayers with stepped or bermed slopes	(-)
$f_p$	Peak frequency of wave spectrum	(1/s)
$f_w$	Friction factor for waves	(-)
$G$	Shear modulus	(N/m <sup>2</sup> )
$g$	Gravitational acceleration	(m/s <sup>2</sup> )
$H$	Wave height, from trough to crest	(m)
$H$	Water level upstream of a dam or sill, relative to dam crest	(m)
$H_{1/10}$	Mean height of highest 1/10 fraction of waves	(m)
$H_{1/3}$	Significant wave height based on time domain analysis, average of highest 1/3 of all wave heights	(m)
$H_{2\%}$	Wave height exceeded by 2% of waves	(m)
$H_o$	Stability number, $H_o = N_s = H_s/(\Delta D_{n50})$	(-)
$H_o T_o$	Dynamic stability number, $H_o T_o = N_{sd} = N_s T_m (g/D_{n50})^{1/2}$	(-)
$H_d$	Drop height	(m)